# Interaction of *Staphylococcus aureus* with Skin Epithelia

A thesis submitted to The University of Manchester for the degree of Doctor of Philosophy in the Faculty of Biology, Medicine and Health

2019

**Arwa Nasr Al Kindi**

School of Biological Sciences Infection, Immunity and Respiratory Medicine

# Contents

**Word count: 27401**

# List of Figures

# List of Tables

# List of Abbreviations

| | |
|---|---|
| AD | Atiopic dermatitis |
| ADAM10 | A disintegrin and metalloproteinase domain 10 |
| AMP | Antimicrobial peptides |
| AV | Annixin V |
| CA-MRSA | Community-acquired methicillin-resistant *S. aureus* |
| CFU | Colony forming unit |
| CoN | Coagulase negative staphylococci |
| CWA | Cell wall anchored proteins |
| CXCL | Chemokine |
| DCs | Dendritic cells |
| $dH_2O$ | distilled water |
| DNA | Deoxyribonucleic acid |
| DLD | Dihydrolipoyl dehydrogenase |
| DTT | Dithiothreitol |
| EDTA | Ethylene Dimethyl Tetra Acetic acid |
| EGFR | epidermal growth factor receptor |
| ELISA | Enzyme-linked immunesorbant assay |
| EV | Extracellular vesicles |
| FACS | Fluorescence-activated cell sorter |
| FiTC | Fluorescein isothiocyanate |
| FLG | Filaggrin |
| FnBPs | Fibronectin-binding proteins |
| FPLC | Fast-protein liquid chromatography |
| FSA | Filtered supernatant from *S. aureus* |
| FSE | Filtered supernatant from *S. epidirmidis* |
| GM | Keratinocytes growth media |
| GFP | Green fluorescent protein |
| GST | Glutathione S-transferase |
| HaCaT | Human aneuploid immortalised keratinocytes |
| His | Histidine |
| HKSA | Heat killed *Staphylococcus aureus* |

| | |
|---|---|
| HyD | Hybrid detector |
| IgG | Immunoglobulin G |
| IL | Interleukin |
| ILCs | Innate lymphoid cells |
| ILK | integrin-linked kinase |
| IPTG | Isopropyl-β-D-galactopyranoside lysine |
| kbp | kilo base pair(s) |
| kDa | kilo Dalton |
| KGF | keratinocyte growth factor |
| KLK | Kallikrein |
| LAP-3 | Leucine aminopeptidase 3 |
| *lac* | lactose operon |
| LB | Luria-Bertani |
| LCs | Langerhans cells |
| LiSA | Live *Staphylococcus aureus* |
| LiSE | Live *Staphylococcus epidermidis* |
| M | Molar or moles per litre |
| MCS | Multi Cloning Sites |
| mg | milligram ($10^{-}3$ g) |
| MHC | Major histocompatibility complex |
| ml | millilitre ($10^{-}3$ L) |
| mM | millimolar ($10^{-}3$ M) |
| NA | Nutrient agar |
| $Na_2CO_3$ | Sodium carbonate |
| $Na_2HPO_4$ | Disodium phosphate |
| $NaCl_2$ | Sodium chloride |
| NaOH | Sodium hydroxide |
| NB | Nutrient broth |
| ng | nanogram |
| NHEK | Juvenile primary Normal Human Epidermal Keratinocytes |
| nm | nanometer |
| $^{o}C$ | degree Celsius |
| OD | Optical density |

| | |
|---|---|
| Ori | Origin of replication |
| PAMPs | Pathogen-associated molecular pattern |
| PARs | Protease-activated receptors |
| PBS | Phosphate buffered saline |
| PCR | Polymerase Chain Reaction |
| PDHa | Pyruvate dehydrogenase alpha subunit |
| PDHC | Pyruvate dehydrogenase complex |
| PFA | Paraformaldehyde |
| PFT | Pore forming toxins |
| PRR | Pattern recognition receptor |
| PSMs | Phenol-soluble modulins |
| PVL | Panton-Valentine leukocidin |
| RT | Room temperature |
| rpm | revolutions per minute |
| *S. aureus* | *Staphylococcus aureus* |
| Sbi | *S. aureus* second IgG binding protein |
| SCID | severe combined immunodeficiency |
| SDS | Sodium Dodecyl Sulfate |
| SDS-PAGE | Sodium Dodecyl Sulfate Polyacrylamide Gel Electrophoresis |
| SEM | Standard Error of Mean |
| *S. epidermidis* | *Staphylococcus epidermidis* |
| SFM | Serum free media |
| SpA | *S. aureus* protein A |
| Spls | Serine protease-like proteins |
| SplD | Serine protease-like D |
| SSSS | Staphylococcal Scalded-Skin Syndrome |
| ST2 | Suppressor of tumorigenicity-2 |
| SSTI | Skin and soft tissue infections |
| TAE | Tris acid-EDTA |
| Th | T helper |
| TLR | Toll-like receptor |
| TNF-α | Tumour necrosis factor-alpha |

| | |
|---|---|
| TSLP | Thymic stromal lymphopoitin |
| TSST | Toxic shock syndrome toxin |
| UV | Ultraviolet |
| vWbp | Willebrand factor binding protein |
| WT | Wild-type |
| WTA | Wall teichoic acid |
| α | Alpha |
| β | Beta |
| Δ | deletion |
| µg | microgram |
| µl | microliter |
| µm | micrometre |

# Abstract

**Background** *Staphylococcus aureus* is a major trigger of atopic dermatitis (AD) and causes the majority of skin and soft tissue infections. The precise staphylococcal factor that promotes type 2 inflammation in the skin, and the reason why recurrent skin infections are common despite seemingly adequate antibiotic treatment are currently unclear.

**Aims** The aims of this study were to:

1. purify and identify *S. aureus* bioactive factor(s) that drive type 2 inflammation by primary human keratinocytes (NHEK).
2. to determine the ability of antibiotics to eliminate *S. aureus* internalised by NHEK.

**Methods** Release of IL-33 and TSLP from NHEK by *S. aureus* and its filtered supernatant (FSA) were assessed by ELISA. Purification of the active factor was achieved by FPLC and confirmed by mass spectroscopy. Internalisation of *S. aureus* and *S. epidermidis* by NHEK were assessed by flow cytometry and confocal microscopy. Viability of intracellular *S. aureus* was determined by growth on nutrient agar plates after lysis of keratinocytes by physical disruption.

**Results** *S. aureus* Second IgG binding protein (Sbi) was identified as the unique type 2 promoting biofactor. Confocal microscopy and flow cytometry showed that *S. aureus*, but not other staphylococci, was rapidly internalised into NHEK and could survive for 24 hours without inducing cytotoxicity or release of alarmins. The antimicrobials flucloxacillin, clindamycin, linezolid, and teicoplanin failed to eliminate intracellular *S. aureus* even at concentrations 20X MIC. Only rifampicin was effective at eradicating intracellular *S. aureus*.

**Conclusions** Sbi was identified as the unique factor that induced type 2 promoting cytokine release by NHEK. The exact mechanism by which Sbi mediates inflammation still need to be determined. Many anti-staphylococcal antibiotics used to treat *S. aureus* infections have little effect on internalised microbes, possibly explaining recurrent reinfection. Rifampicin is the only antibiotic to effectively kill internalised *S. aureus* in our *in vitro* experiments.

# Declaration

No portion of the work referred to in the thesis has been submitted in support of an application for another degree or qualification of any other university or other institute of learning.

# Copyright statement



iii. The ownership of certain Copyright, patents, designs, trademarks and other intellectual property (the "Intellectual Property") and any reproductions of copyright works in the thesis, for example graphs and tables ("Reproductions"), which may be described in this thesis, may not be owned by the author and may be owned by third parties. Such Intellectual Property and Reproductions cannot and must not be made available for use without the prior written permission of the owner(s) of the relevant Intellectual Property and/or Reproductions.

iv. Further information on the conditions under which disclosure, publication and commercialisation of this thesis, the Copyright and any Intellectual Property and/or Reproductions described in it may take place is available in the University IP Policy (see http://documents.manchester.ac.uk/DocuInfo.aspx?DocID=487), in any relevant Thesis restriction declarations deposited in the University Library, The University Library's regulations (see http://www.manchester.ac.uk/library/aboutus/regulations) and in The University's policy on Presentation of Theses

# Acknowledgments

I would like to express my deepest gratitude to my supervisors; Dr Peter Arkwright, Dr Joanne Pennock and Professor Catherine O'Neill for their continues support and professional guidance throughout this project. Their knowledge, advice and valuable critique helped me greatly in this research work.

I would like to thank my colleagues in Joanne's Lab; Abdullah Alkahtani, Helen Williams, Charis Saville, Yasmine Alshammari, Basmah Eldakhakhny, Adefunke Ogunkanbi, and members of Catherine's Lab; Carol Ward, Cecile El-Chami and Muna Alhubail for without their kind assistance I would not have been able to finish my project.

I sincerely appreciate the valuable cooperation and support of Gareth Howell from the Flow Cytometry Core Facility and Hayley Bennett from Gene Editing Unit.

I wish to express my deepest appreciation to the Sultan Qaboos University for generously granting me with a scholarship to pursue my PhD studies.

I would like to also thank Munirah and Hafida for their unforgettable friendship.

I am extremely grateful to my family; my parents for their love, care and inspiration in life, my sisters and brothers for their encouragement, and my husband Nasser for his unmatched patience, endless support and persistent encouragement throughout this experience especially when times get rough. Also, to my wonderful children; Ahmed and Aseela, I would like to thank you for inspiring me and enduring the hardship of living away from your beloved extended family and relatives during this time.

Finally, I would like to dedicate this thesis to my beloved grandmother, Thuraya, whose memory will forever stay with me and enlighten my life.

# Chapter 1 : Introduction

## 1.1 Foreword

*Staphylococcus aureus* is a major cause of sepsis as well as skin and soft tissue infections (SSTI). It is also commonly associated with flares in atopic dermatitis. The molecular mechanism by which *S. aureus* causes inflammation in the skin is not fully understood. This chapter will review *S. aureus*, its virulence factors and its association with disease. Also, a brief description of skin structure and the mode of interaction of *S. aureus* with skin cells will also be highlighted.

## 1.2 Staphylococci

In 1882, Sir Alexander Ogston first described *Staphylococcus* as a group of *Micrococci* that caused disease. He showed that when pus containing these bacteria was injected into mice, they developed similar symptoms to those seen in the patients from which the sample was taken. In 1884, Rosenbach grew *Staphylococcus* in culture and studied their physical and biochemical characteristics. It was however only in 1957 that *Staphylococcus* was acknowledged as a separate genus, when Evans demonstrated that *Staphylococcus* can grow anaerobically and ferments glucose. In the 1960s, staphylococci were differentiated from micrococci by DNA analysis (Götz *et al.*, 2006). In 1974, Baird-Parker identified three species of the genus: *S. aureus, S. epidermidis,* and *S. saprophyticus*. Today, 36 species and subspecies have been identified using DNA technology (Götz *et al.*, 2006).

Staphylococci are Gram-positive, facultative anaerobes that grow in irregular grape-like clusters and are positive for catalase and benzidine (Götz *et al.*, 2006; Baird-Parker, 1990). Staphylococcal species are divided into two groups based on coagulase activity. They have adapted to inhabit different environments and typically inhabit skin and mucous membranes. *Staphylococcus epidermidis* is a skin commensal (Kloos & Schleifer, 1975), but it and other coagulase negative staphylococci (CoNs) can become opportunistic pathogens, particularly in patients with medical devices such as premature infants in neonatal intensive care units, as well as in immunocompromised individuals (Huebner & Goldmann, 1999; Jean-Baptiste *et al.*, 2011).

### *1.3 Staphylococcus aureus*

*Staphylococcus aureus* is a Gram positive and coagulase positive bacteria. It is the most common cause of SSTIs (Tong *et al.*, 2012). This bacterium is increasingly resistant to antibiotics e.g. methicillin (MRSA) (Götz *et al.*, 2006; Lacey *et al.*, 2016).

*S. aureus* colonises nasal mucosa in 20 % of people without causing any symptoms (Mulcahy & McLoughlin, 2016). People colonised with *S. aureus* are at higher risk of developing infection with the colonising strain (von Eiff *et al.*, 2001; Wertheim *et al.*, 2004). Why some individuals develop overt infections rather than just being asymptomatic colonisers of *S. aureus* is not fully understood, but it is thought to be due to the ability of *S. aureus* to manipulate host immune response and facilitate anti-inflammatory responses (Mulcahy & McLoughlin, 2016). The severity of the infection depends on host factors such as barrier dysfunction and immune responses to *S. aureus* (Zecconi & Scali, 2013).

## 1.4 *Staphylococcus. aureus* and Skin and Soft Tissue Infections (SSTI)

*S. aureus* causes a range of diseases including SSTIs, pneumonia, endocarditis, bacteraemia and sepsis (Flick *et al.*, 2013). SSTIs are caused when bacteria colonising the epithelial surface infiltrate to deeper tissue layers. This occurs after a breach in the skin caused by scratching or injury (Lacey *et al.*, 2016). 80-90% of all skin and soft tissues infection are due to *S. aureus.* Each year in the United States, more than 10 million cases of SSTIs caused by *S. aureus* and around half a million patients are admitted to hospital with these infections (Hersh *et al.*, 2008). *S. aureus* virulence factors that predispose to infection are introduced in the next section.

## 1.5 Virulence factors facilitating *S. aureus* infection

*S. aureus* expresses a wide range of virulence factors that facilitate its attachment to host cells and evasion of host immunity. Studies investigating *S. aureus* during the colonisation phase and after disease progression found increased expression of surface proteins and toxins that facilitate adhesion to the host cell and evasion of immune responses (Kusch & Engelmann, 2014; Jenkins *et al.*, 2015).

### 1.5.1 Cell-wall anchored proteins

*S. aureus* expresses 25 Cell-Wall Anchored (CWA) proteins. They are mainly encoded by the bacterial core genome and are highly conserved in all *S. aureus* strains (Chua *et al.*, 2013). These proteins contain "sorting signals" in their C-terminal (LPXTG motifs) recognised by sortase A, that help to determine which cellular compartment the proteins are destined for. Sortase A is a transpeptidase that cleaves the amide group between glycine and threonine, allowing protein attachment to the N-terminal of peptidoglycan of the cell wall (Lacey *et al*., 2016; Foster *et al*., 2014). Fibronectin-binding proteins (FnBP) A and B also facilitate *S. aureus* adherence to host cells and enable its internalisation via α5β1-integrin expressed on host cells (Lacey *et al.*, 2016).

Various CWA also promote abscess formation (Kwiecinski *et al.*, 2014). Clumping factor A (ClfA) inhibits neutrophil phagocytosis of *S. aureus* (Kwiecinski *et al*, 2014; Higgins *et al*., 2006), as does protein A (SpA), which binds to IgG, TNF receptor 1 (TNFR1) and von Willebrand factor (vWF) (Lacey *et al.*, 2016). Binding of SpA to TNFR1 on keratinocytes initiates pro-inflammatory responses (Classen *et al.*, 2011). SpA also acts as a "B-cell superantigen", inducing B-cell apoptosis through interaction with $V_H$ region on the B-cell receptors (BCR) (Goodyear & Silverman, 2003).

### 1.5.2 Secreted toxins

*S. aureus* toxins play an important role in inflammation and immune evasion. Although few are conserved and encoded by core genomic island (Liu, 2014), most are encoded by mobile genetic elements (MGEs) explaining the variability in pathogenicity levels between *S. aureus* strains. *S. aureus* toxins are classified into three different types (Oliveira *et al.*, 2018):

- Pore-Forming Toxins (PFTs)
- Exfoliative Toxins (ETs)
- Superantigens (SAgs)

#### 1.5.2.1 Pore-Forming Toxins (PFTs)

These proteins punch holes in host cell membranes leading to cell lysis and an inflammatory response which damages the skin (Lacey *et al.*, 2016). They induce pain in subcutaneous skin infection in mice (Blake *et al.*, 2018). PFTs can be grouped into:

1. haemolysins such as; α-haemolysin (Hla) (also called α- toxin) which is a heptameric β-barrel forming toxin (Hla) causing "dermonecrosis". It is released as a monomer that then bind to ADAM10 on the host cells which lead to formation of the transmembrane channel causing cell lysis (Oliveira *et al.*, 2018) (Fig. 1.1 A).

2. leukocidins (Panton Valentine Leukocidin (PVL), LukGH, LukED), which consist of two subunits F and S that lead to the formation of β-barrel pores in the lipid bilayer (Lacey *et al.*, 2016) (Fig. 1.1B).
3. Phenol-Soluble Modulins (PSMs), which are amphipathic α-helical peptide that are classified to α- and β-types based on their length. Unlike most toxins, PSM-α is encoded by core genomic island and is highly conserved in all *S. aureus* strains (Chua *et al*., 2013; Oliveira *et al.*, 2018). They cause human neutrophil lysis, enabling the bacteria to evade the immune system defense mechanisms (Wang *et al.*, 2007) and induce biofilm formation, preventing disassociation by host enzymes (Bleem *et al.*, 2017). PSMs thought to cause lysis by first non-specific binding to the cytoplasmic membrane which then initiate the formation of a transient pore in the cytoplasmic membrane (Fig. 1.2).

The role of *S. aureus* PFTs toxins in SSTs is summarised in Table1.1

**Table 1.1 *S. aureus* toxins involved in skin and soft tissues infections**

| Toxin | Abbreviation | Function | Reference |
|---|---|---|---|
| Panton Valentine Leukocidin | PVL | β-barrel forming neutrophil lysis | (Spaan *et al.*, 2013) |
| Bi-component leukocidins | LukGH, LukED | β-barrel forming neutrophil lysis | (Malachowa *et al.*, 2012) |
| α-hemolysin | Hla | β-barrel forming keratinocytes lysis via interaction with a disintegrin and metalloprotease 10 (ADAM10) receptor | (Wilke & Bubeck Wardenburg, 2010; Walev *et al.*, 1993) |
| Phenol-soluble Modulins | PSMs | neutrophil lysis after phagocytosis | (Surewaard *et al.*, 2013) |

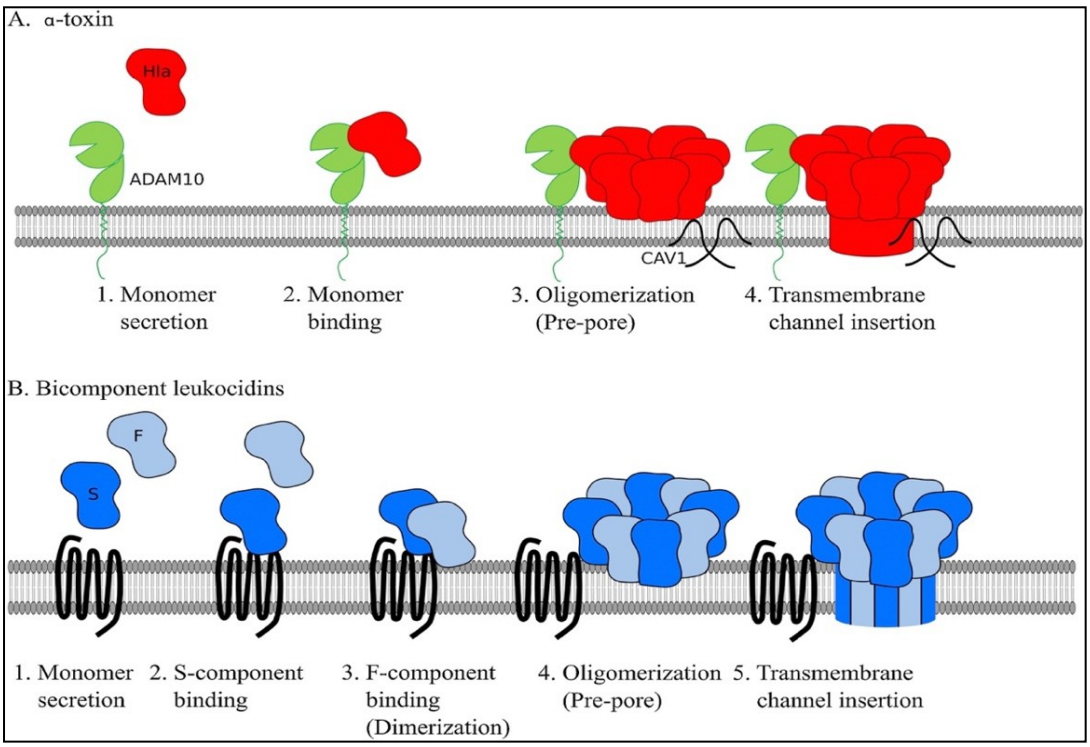


**Fig. 1.1: Schematic model of *S. aureus* PTFs pore- formation on target cells adapted from Seilie et al., 2017.**

A. 1. secreted monomer of α-toxin bind to ADAM10 receptor on target cell. 2. Binding to the receptor initiate oligomerisation into heptamer to form the pre-pore structure 3. The scaffolding protein Caveolin-1(CAV1) interact with Hla to stabilize the pre-pore. 4.Then the stem domain is inserted into the membrane bilayer to form the β-barrel transmembrane channel. B. 1. Secreted monomers (F and S) of bicomponent leukocidins. 2. S- component bind to a receptor on the target cell. 3. F- component then bind to the S- component to form a heterodimer. 4. Dimers then oligomerize forming a pre-pore . Followed by development of transmembrane channel.

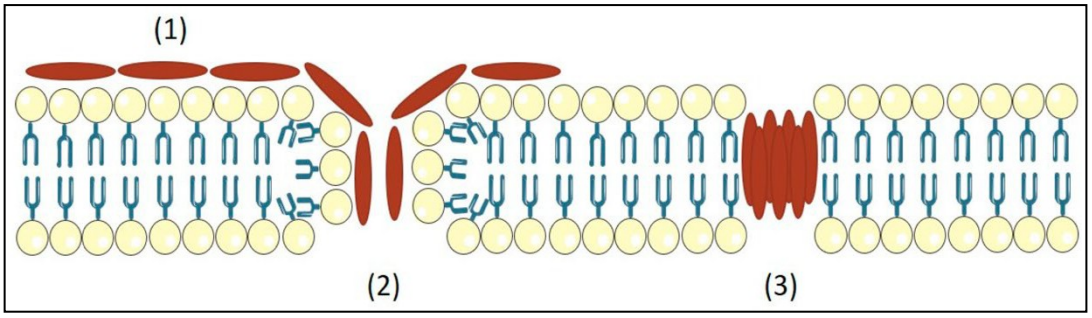


**Fig. 1.2 Schematic model of *S. aureus* PSMs pore-formation mechanisms adapted from Oliveira et al., 2018.**

1. PSMs peptides attach to cytoplasmic membrane without requirement of receptor. 2 attachments can lead to membrane disintegration. 3. PSMs peptides oligomerise forming a transient pore.

Moreover, PSM-α induces extracellular membrane vesicles (EVs) formation derived from cytoplasmic membranes (Wang *et al.*, 2018). EVs are bilayer membranes first observed in Gram negative bacteria (Knox *et al.*, 1966) and subsequently found in Gram positive bacteria and fungi (Rivera *et al.*, 2010; Olaya-Abril *et al.*, 2014; Resch *et al.*, 2016; Brown *et al.*, 2015). EVs main function is to transport proteins, polysaccharides, toxins into host cells and they therefore play an important role in host-pathogen interaction (Brown *et al.*, 2015).

#### 1.5.2.2 Exfoliative Toxins (ETs)

*S. aureus* ETs cause Staphylococcal Scalded-Skin Syndrome (SSSS), which mainly affects children (Oliveira *et al.*, 2018). ETs amino acid sequences share similarity with serine protease that cleave Desmoglein 1 (Dsg1) in the epidermis, causing loss of adhesion between keratinocytes and superficial skin layer peeling and blistering (Yamaguchi *et al.*, 2002; Nishifuji *et al.*, 2008).

#### 1.5.2.3 Superantigens (SAgs)

*S. aureus* SAgs cause sudden and excessive activation of T-cells, leading to a cytokine storms via direct binding to Major Histocompatibility Complex class II antigens (MHC II) on T-cells (Proft & Fraser, 2003). SAgs induce toxic shock syndrome (TSST-1) and food poisoning (enterotoxins) (Oliveira *et al.*, 2018). Enterotoxin SEB causes skin inflammation in human- SCID mouse model and atopic dermatitis (Herz *et al.*, 1998).

### 1.5.3 Enzymes and other secreted proteins

Coagulation and fibrinolytic pathways protect *S. aureus* from host immunity (Peetermans *et al.*, 2015a). *S. aureus* produce two coagulases: staphylocoagulase and von Willebrand binding protein (vWbp) (Bjerketorp *et al.*, 2002; Bjerketorp *et al.*, 2004). Both coagulases activate prothrombin, producing a structure called staphylothrombin that is not suppressed by classical coagulation inhibitors (Fig. 1.3). Staphylothrombin shields *S. aureus* from the immune system through the formation of "*S. aureus*-fibrin-platelet microaggregates" (Peetermans *et al.*, 2015b). Therefore, inhibition of staphylothrombin or *S. aureus* coagulases result in increased leukocyte activation and more effective elimination of *S. aureus* (Vanassche *et al.*, 2011). As *S. aureus* proliferate within the clot, Staphylokinase (Sak) activate host plasminogen, resulting in fibrin degradation and dissemination of the bacteria (Peetermans *et al.*, 2015a). *S. aureus* strains that produce larger amounts of Sak are less virulent because Sak interferes with the fibrin formation induced by *S. aureus* coagulase (Peetermans *et al.*, 2015a).

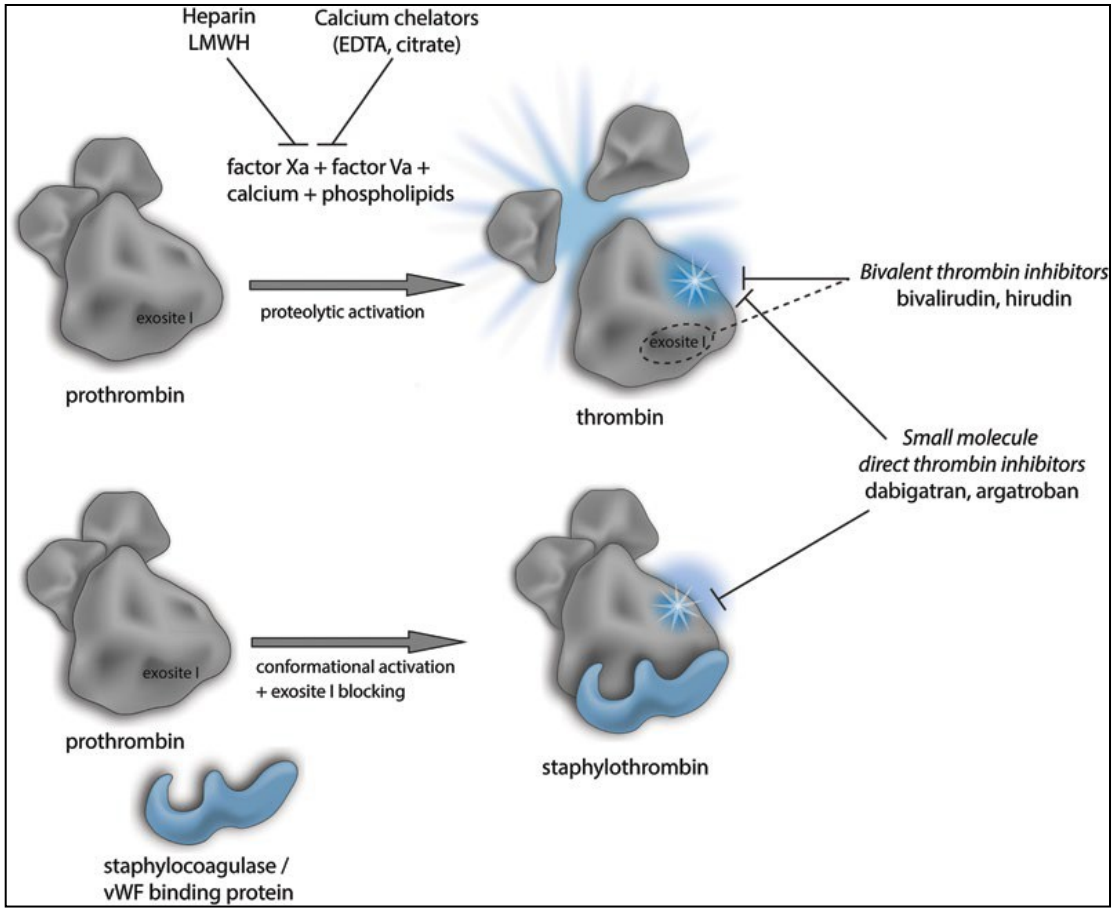


**Fig. 1.3 Summary of prothrombin activation mechanisms by coagulase adapted from Peetermans et al., 2015.**
*S. aureus* coagulases bind to prothrombin forming an active staphylothrombin complex. As exosite I is blocked by staph coagulases, common bivalent thrombin inhibitors are not effective against staphylothrombin. Only small molecule direct thrombin inhibitors can inhibit staphylothrombin

*S. aureus* also secretes extracellular proteases such as serine protease A (SspA), metallopretase Aureolysin (Aur) and cysteine proteases staphopain (ScpA and SspB). *SspA* also called V8 protease causes epidermal barrier dysfunction and initiates inflammation in the skin in both mice models and human keratinocytes (Wang *et al.*, 2016; Hirasawa *et al.*, 2010). Moreover, V8 and staphopains have inhibitory effect on biofilm formation (Mootz *et al.*, 2013). SspB can also mediate *S. aureus* infection by inducing cytoskeletal changes in neutrophil and monocytes leading to their apoptosis (Smagur *et al.*, 2009). On the other hand, Aur is an important immune evasion factor that facilitate *S. aureus* survival in macrophages (Kubica *et al.*, 2008) and also interfere with complement system pathway by inactivating C3, an essential factor in the activation of the complement reactions cascade (Laarman *et al.*, 2011). The complement system was long thought to be part of innate immunity, however it is now considered to be a bridge between innate and adaptive immunity (Dunkelberger & Song, 2010). The complement system is an essential cascade of proteolysis that produce anaphylatoxins to mediate inflammation, opsonin to

mediate phagocytosis and components initiating membrane attack to facilitate immune responses against pathogens or damaged cells. It can be activated by three main pathways; classical, lectin and alternative pathways summarised in Fig. 1.4.

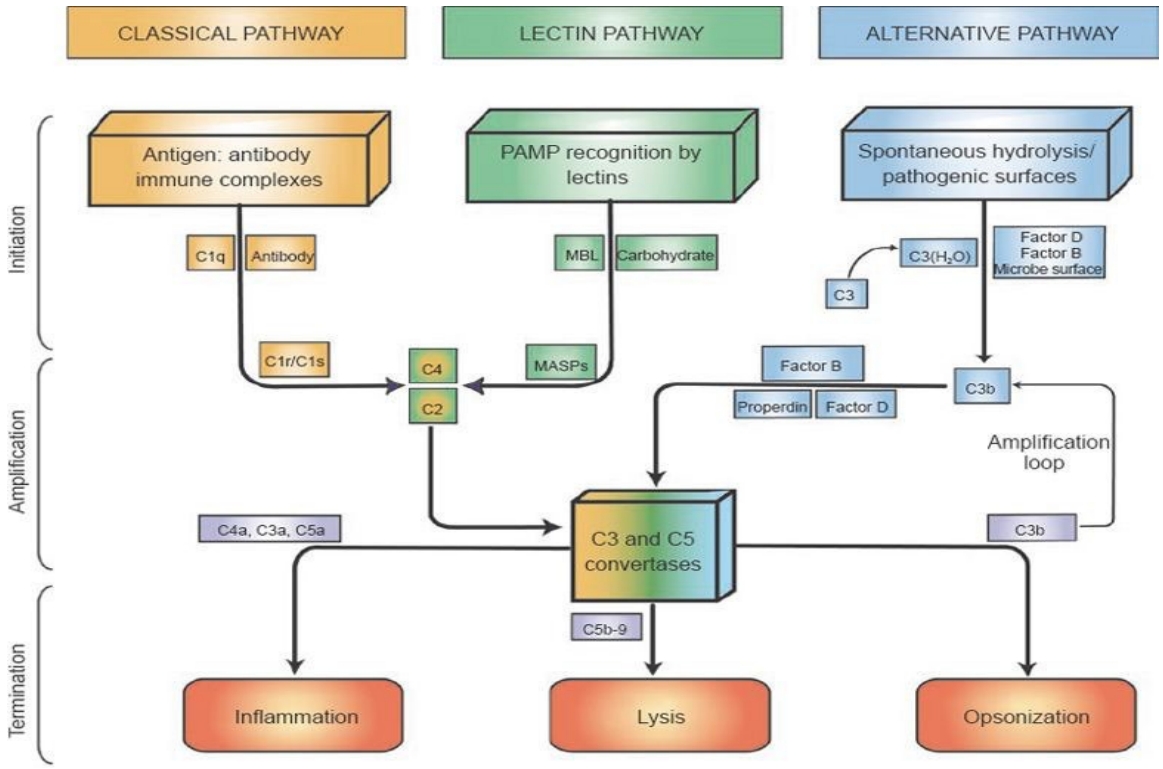


**Fig. 1.4 Schematic diagram of the complement system pathways adapted from Dunkelberger & Song, 2010.**
Classical and Lectin pathways require the presence of antigen to be activated whereas the alternative pathway is constantly active in fluid phase. In all pathways C3 is a central factor in the cascade of reactions leading to the termination part in which the anaphylatoxins (C4a, C3a and C5a) mediate inflammation, C5 convertase initiate of MAC for cell lysis and the opsonin C3b mediate phagocytosis. Details about each pathway discussed in the text.

In the classical pathway, antigen-antibody complex is required for initiation of this pathway. It starts when C1q bind to Fc region of IgG or IgM that have been attached to a pathogen. This activates serine proteases C1r and C1s to cleave two other components C4 and C2 into C4 a, b and C2 a, b. C4bC2a then form a complex, C3 convertase, which cleaves C3 into C3a and C3b. C3a is an anaphylatoxin i.e. cause degranulation of mast cells and basophils and an inflammatory mediator whereas C3b is an opsonin that can coat pathogens to facilitate phagocytosis and pathogen clearance. In the terminal loop of this pathway; C3b can also bind to C5 component which causes conformational changes that attracts the C5

convertase (C4bC2a) to cleave C5 component into C5a and C5b. C5a act as chemotactic and a strong proinflammatory protein. C5b stimulates the formation of membrane attack complex (MAC) forming a transmembrane channel facilitating the lysis of pathogens by osmotic flux (Dunkelberger & Song, 2010; Merle *et al.*, 2015).

The lectin pathway is also activated by the presence of antigen but it is antibody independent, it recognises mannose-binding lectin (MBL) and ficolins which will then bind to MBL- associated serine proteases (MASPs1 and 2). These proteases cleave C2 and C4to form C3 convertase activating phagocytosis, inflammation and terminal part of the complement system same way as discussed earlier in classical pathway (Dunkelberger & Song, 2010).

Unlike the classical and lectin pathways, the alternative pathway is always active to sense for pathogens and does not require the presence of antigen for its initiation. In this pathway C3 can be cleaved spontaneously to C3($H_2O$) which can recruit factor B that forms C3 convertase C3($H_2O$)Bb, containing an activated thioester bond (TED). On healthy cells, C3($H_2O$)Bb bind to inhibitory receptors or proteins on cell surface which in turn activate its degradation and recycling. On a pathogen, C3b bind to a protein called Factor B forming a complex that will then be cleaved by a serine protease (factor D) to form C3b-Bb complex which act as C3 convertase cleaving C3 to C3a acting in the amplification loop and C3b-Bb-c3b complex that will activate C5 facilitating MAC. This pathway is controlled by Factor I and it cofactor, Factor H that facilitate C3 degradation into inactive iC3b and C3dg which inactivate the alternative cascade (Zipfel *et al.*, 1999).

Moreover, *S. aureus* also secretes extracellular serine like proteases of which SplD was found to induce Th2 mediated allergic reactions in mouse asthma model (Stentzel *et al.*, 2017). Although the pathway of which SplD causes inflammation is not yet fully understood but it is mediated by IL-33 release in airway epithelium (Teufelberger *et al.*, 2018) as summarised in (Fig. 1.5).

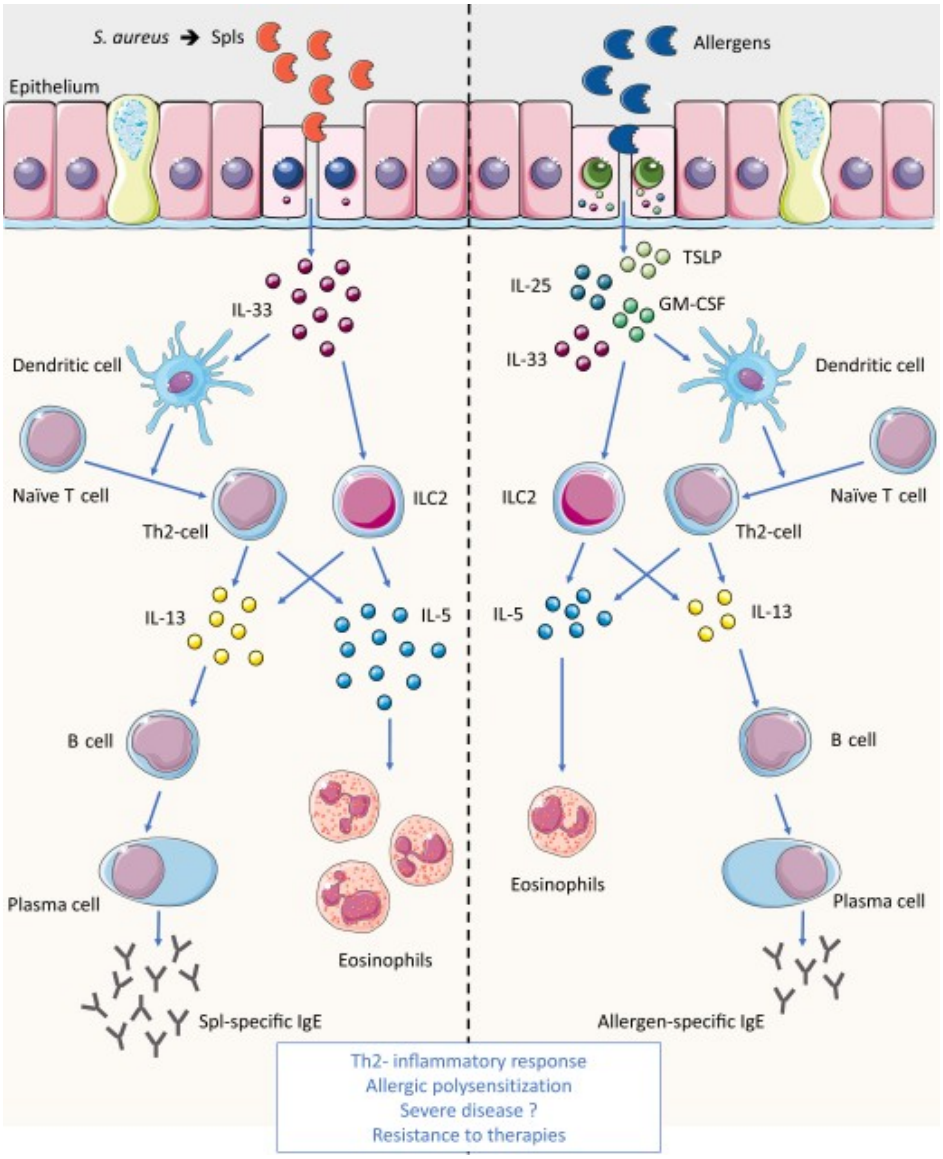


**Fig. 1.5 allergic immune reactions in response to Serine-like protease D (SplD) in the airway adapted from Krysko et al, 2019.**
SplD exposure can cause synergetic effects in "allergic sensitisation" leading to aggressive airway inflammation. SplD induce the release of IL-33 which activate innate lymphoid cells type2 (ILC2), T helper cells type 2 (Th2) and Dendritic cells via ST2 receptor. This leads to amplification of adaptive immune responses producing type 2 cytokines which reduces the adaptive tolerance to allergens resulting in aggressive airway inflammation. Exposure to allergens induces the release of epithelial damage associated cytokines such as IL-33, TSLP. Recurrent exposure to SplD or allergens result in production of specific immunoglobulin E (IgE).

## 1.6 Unique interaction between *S. aureus* and the skin

The skin provides an external interface with the environment. It is colonised by a wide range of commensal micro-organisms. These micro-organisms work in synergy with the skin to form the first line of protection from harmful bacterial pathogens. If this homeostasis is disrupted, opportunistic bacteria invade deeper into the skin and infection occur. To understand the interaction between skin and *S. aureus* and what causes infections, features of the skin that facilitate its important role as a physical, chemical and immunological barrier are discussed below.

### 1.6.1 Structure of the skin

The skin consists of three layers, the epidermis, dermis and subcutaneous tissue (Kupper & Fuhlbrigge, 2004) (Fig. 1.6). The epidermis consists of keratinocytes that differentiate from the basal layer as they progress through the spinous, granular and finally to the stratum corneum layers (Krishna & Miller, 2012; Grice & Segre, 2011). Deep to the epidermis is the dermis which is divided into two sublayers of connective tissues, the more superficial papillary dermis and the deeper reticular dermis (Krishna & Miller, 2012). The papillary dermis is so called because it has protrusions into the epidermis (Krishna & Miller, 2012). The deepest layer of the skin is the subcutaneous tissue, which contains capillaries that express endothelial adhesion molecules (E-selectin), intercellular adhesion molecule 1 (ICAM1) and other adhesion molecules that aid in the recruitment of cutaneous lymphocyte antigen (CLA) specific T-cells (Kupper & Fuhlbrigge, 2004). $CLA^+$ T-cells bind to T-cell receptors (TCR) specific to the pathogen that causes the inflammation (Kupper & Fuhlbrigge, 2004). Protruding through the skin layers are skin appendages, including sweat glands, hair follicles and sebaceous glands (Krishna & Miller, 2012; Grice & Segre, 2011). Sweat glands function as thermal and pH regulators. Sebaceous glands secrete oily substance called sebum that functions as a lubricant and antibacterial agent (Grice & Segre, 2011). Studies have shown that sebaceous glands promote colonisation of *Propinobacterium acenes,* a facultative anaerobic commensal (Brüggemann *et al.*, 2004). *P. acenes* produces lipases that degrades skin sebum into fatty acids promoting an acidic skin pH. Acidic skin pH inhibits the growth of pathogenic bacteria such as *S. aureus* (Grice & Segre, 2011). Keratinocytes also control skin pH via their sodium-proton exchanger (NHE1) (Behne *et al.*, 2002) and by degrading filaggrin into urocanic acid and pyrrolidone carbolic acid during keratinocyte differentiation. Urocanic acid and pyrrolidone carboxylic acid not only reduce skin pH but also inhibit the ability of *S. aureus* to express clumping factor B (ClfB) and fibronectin-binding protein A (FnBP A) that are considered important for *S. aureus* colonisation (Krishna & Miller, 2012).

The skin is also considered as an immunological barrier because of the presence Langerhans cells (skin Dendritic Cells), mast cells, T- and B-cells (Krishna & Miller, 2012; Kupper & Fuhlbrigge, 2004). In addition, keratinocytes express pattern recognition receptors (PRRs) such as TLRs and NOD-like receptors. These act synergistically with immune cells to stimulate innate immune responses when skin barrier is compromised (Krishna & Miller, 2012; Kupper & Fuhlbrigge, 2004).

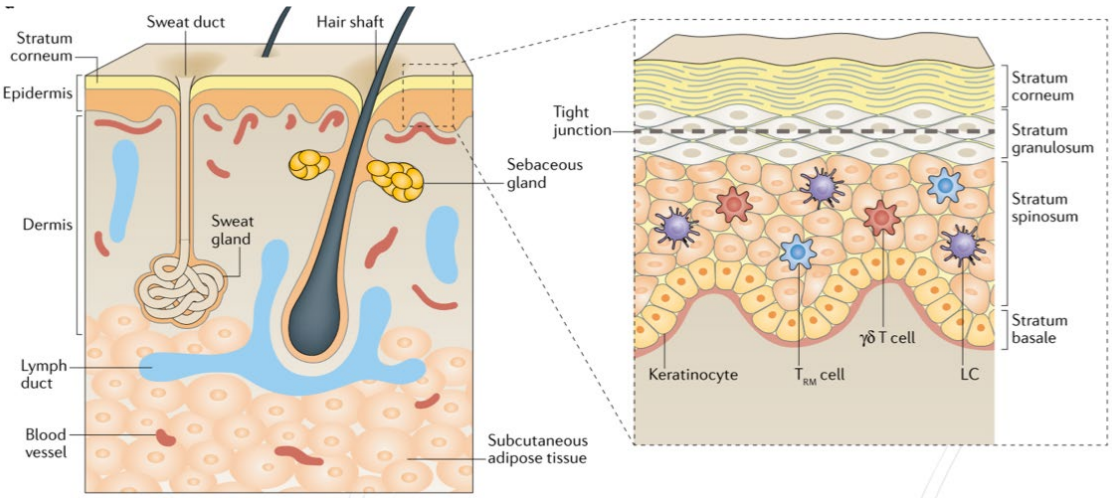


**Fig. 1.6 Structure of the skin Adapted from (Kabashima *et al.*, 2019)**
The skin consist of the epidermis, dermis and subcutaneous tissue. The epidermis composed of four layers of keratinocytes in which immune cell population reside ( Langerhans cells (LCs), γδ T cells and resident memory T (TRM) cells. Skin appendages (hair follicle, sweat gland and sebaceous gland) protrude through skin layers lacking stratum corneum.

## 1.6.2 Commensal skin microorganisms

Microorganisms colonising the skin vary with age of the individual, topography, gender and environmental factors such as personal hygiene and exposure to UV (Grice & Segre, 2011). Newborn skin microbiota is derived from either mother's birth canal microbiota (*Lactobacillus*, *Prevotella* and *Sneathia* species) or skin. After Caesarean section, babies are colonised largely by staphylococci and propionibacteria (Dominguez-Bello *et al.*, 2010). In 1969, a study on changes of microflora with age found that beside the predominance of CoNs and micrococci, infant's skin is inhabited by streptococci. Children have diverse micro-organism communities including Sarcina, diphtheroids and spore forming bacilli (Somerville, 1969). Adult skin contains largely non-pathogenic diphtheroids. Whereas, older people's skin is inhabited by diphtheroids and streptococci (Somerville, 1969).

Hormonal changes at puberty modify sebum secretion, leading to further changes in microbial diversity, with some differences between males and females (Grice & Segre, 2011;

Powers et al., 2015). Growth of lipophilic bacteria such as Propionibacterium species are promoted, particularly on the face, back and chest (Grice & Segre, 2011). Skin microbiota also varies depending on location, with different niches enhancing the colonisation of specific microorganisms (Fig. 1.7). For example, skin with higher temperature and humidity such as the groin and axilla are colonised with Gram negative bacilli, corynebacteria and *S. aureus*. In contrast, areas with higher density of sebaceous glands promotes colonisation of lipophilic microorganisms. Dry skin areas with greater temperature fluctuations e.g. legs and arms have less bacteria. Cosmetics, soaps and detergents can all affect microbiota (Grice & Segre, 2011). While UV exposure and frequent use of antibiotics can also affect the quantity and diversity of microbial community because of their "bactericidal properties" (Kong *et al*., 2012; Grice & Segre, 2011).

Skin commensals directly inhibit the colonisation of pathogens and synergise with the host immunity to suppress pathogens (Grice & Segre, 2011; Powers *et al*., 2015; Cogen *et al*., 2010). A good example is *S. epidermidis*, a skin commensal that stimulates keratinocytes to release AntiMicrobial Peptides (AMP) such as β-defensin and Phenol Soluble Modulins (PSMs) γ and δ , which suppress *S. aureus* colonisation and biofilm formation (Grice & Segre, 2011; Cogen *et al*., 2010). This defence mechanism is specific in that it kills pathogenic skin bacteria without affecting survival of commensal bacteria (Cogen *et al.*, 2010). *S. lugdunensis* produces an AMP called lugdunin that inhibits *S. aureus* colonisation in a mouse model (Zipperer *et al.*, 2016). Interestingly introducing antimicrobial producing staphyloccocal CoN strains including *S. epidermidis* and *S. hominis* onto skin of atopic dermatis patients reduced colonisation of *S. aureus* (Nakatsuji *et al.*, 2017).

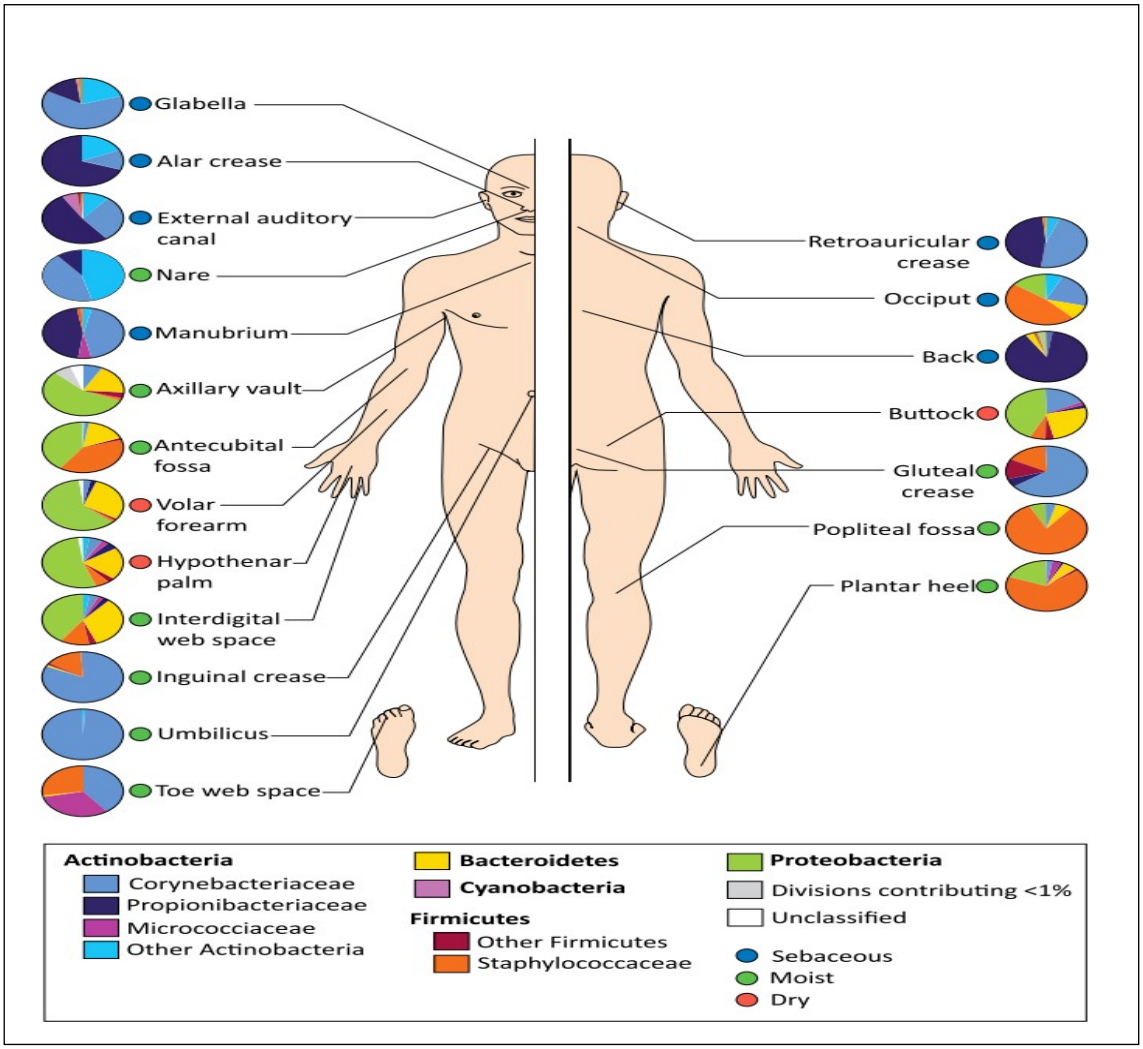


**Fig. 1.7 Micro-organism distribution varies with skin topography. Adapted from (Grice & Segre, 2011)**

### 1.6.3 Interaction of *S. aureus* with host cells

*S. aureus* is classically considered an extracellular pathogen, interacting with skin keratinocytes, fibroblast, endothelial cells and immune cells via surface proteins. However, some studies have shown that *S. aureus* can be internalised by a number of skin cells, including keratinocytes, fibroblasts, and endothelial cells (Rocha-de-Souza *et al.*, 2008; Giese *et al.*, 2011; Abel *et al.*, 2011). Interaction of *S. aureus* with keratinocytes and some immune cells will be discussed below.

#### 1.6.3.1 Interaction of *S. aureus* with keratinocytes

Stratum corneum is the first line of defence against *S. aureus.* The bacteria are recognised by TLR and other pattern recognition receptors (PRR) on keratinocytes.

TLR-1, TLR-2 and TLR-6 are the most important PRR expressed on keratinocytes that recognises *S. aureus* cell-wall components; lipopeptides, lipoteichoic acid and peptidoglycan, initiating innate immune response against *S. aureus* (Shukla *et al.*, 2015).

Protease activated receptors (PARs) are also expressed in keratinocytes (Adams *et al.*, 2011). These are transmembrane G-coupled receptors that can be activated by endogenous and exogenous proteases such as thrombin, trypsin, allergens with protease activities and bacterial proteases (Ramachandran et al, 2012). From the four types of PARs; PAR2 is thought to play an important role in skin inflammation that is not yet well understood. PAR2 is activated by endogenous and exogenous serine proteases. Activation occurs by cleavage of its N-terminus exposing endogenous "tethered ligands" allowing binding to the receptor pocket (Ramachandran *et al.*, 2012). The epidermal serine protease Kallikrein-5 was found to activate PAR2 leading to increased thymic stromal lymphopoietin (TSLP) release in skin of mice models (Jang *et al*., 2015; Rothmeier & Ruf, 2012).

*S. aureus* can be internalised by keratinocytes, surviving within these cells to avoid the host immune response and subsequently shed to cause reinfection. The molecular pathways involved in this process are not fully understood. *S. aureus* internalisation into primary keratinocytes is facilitated by FnBP-dependent and independent pathways, whereas in immortalised keratinocytes it is largely through FnBP-α5β1-integrin (Kintarak *et al.*, 2004a; Borisova *et al.*, 2013; Kintarak *et al.*, 2004). Internalisation may also occur via αβ1 integrin-linked kinase (ILK)-Rac1 pathway (Fig. 1.8). Interestingly, ILK facilitated internalisation of *S. aureus* is not followed by a TLR2 immune response (Sayedyahossein *et al.*, 2015). Clumping factor B (ClfB) has also been found to have a role in facilitating the attachment of *S. aureus* to keratinocytes, but it does not seem to be involved in internalisation (Kintarak *et al.*, 2004a).

Keratinocytes not only internalise bacteria but also internalise particles such as melanosomes in a process called melanosome transfer, which leads to epidermal pigmentation (Sayedyahossein *et al.*, 2012; Sharlow *et al.*, 2000). Keratinocyte internalisation of particles is regulated by keratinocyte growth factor (KGE) and PAR2 (Fig. 1.8) (Sayedyahossein *et al.*, 2012; Sharlow *et al.*, 2000). Activation of PAR2 mediates cytoskeleton rearrangement and morphological changes in the keratinocytes cell surface, resulting in enhanced phagocytosis. Moreover, PAR2 activation also leads to increased release of active serine protease which activates PAR2 through a positive feedback loop. Serine proteases inhibitors inhibit this pathway and therefore inhibit internalisation of bacteria by keratinocytes (Sharlow *et al.*, 2000).

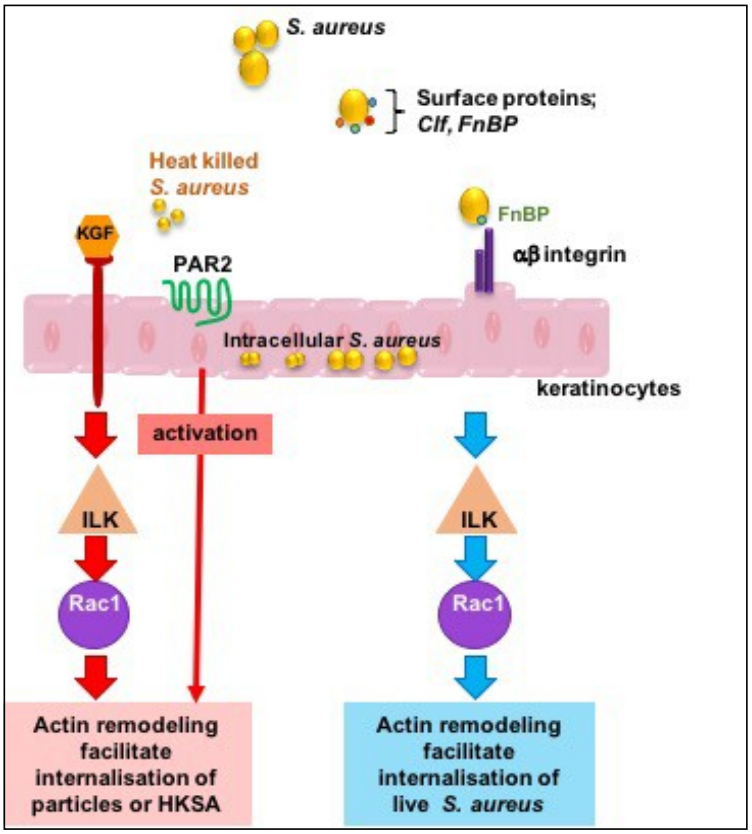


**Fig. 1.8 Proposed mechanism of *S. aureus* internalisation into keratinocytes.**
Internalisation of heat killed *S. aureus* is mediated by PAR2 and keratinocyte growth factor (KGF), while internalisation of live *S. aureus* is facilitated by FnBP-integrin/ILK-Rac1 pathways. They all activate actin remodelling. Depicted using information from figures in Shukla *et al.*, 2015 and Sayedyahossein *et al.*, 2012.

### 1.6.3.2 Interaction between *S. aureus* and immune cells

Mast cells have an essential role in stimulating innate immune responses. Studies have shown that mast cells can interact with *S. aureus* in two ways, producing an "extracellular trap" and secreting AMPs that kill *S. aureus*. In addition, mast cells release TNFα, which enhances the recruitment of phagocytes to clear *S. aureus*. However, *in vitro* studies have shown that *S. aureus* can escape from the mast cell defence mechanisms after internalisation (Abel *et al.*, 2011). *S. aureus* uptake by mast cells is thought to involve α5β1-integrin on host cells and fibronectin-binding proteins FnBP A & B (Abel *et al.*, 2011). Anti-β1 integrin antibodies inhibit *S. aureus* internalisation, but do not eliminate it completely suggesting that there are other pathways involved in the process (Rocha-de-Souza *et al.*, 2008). A study by Rocha-de-Souza *et al* found that CD48 and TLR2 signalling enhance internalisation of *S.*

*aureus* into cord blood mast cells (Rocha-de-Souza *et al.*, 2008). Once internalised, *S. aureus* produces α-hemolysin that enhances survival (Abel *et al.*, 2011). Moreover, in mast cell, *S. aureus* encounters several forms of stress, specifically cell wall stress stimulation (CWSS), that stimulates thickening of its cell wall. This is thought to be a defence mechanism that *S. aureus* uses to shield itself from intracellular AMPs and from antibiotics (Abel *et al.*, 2011). CWSS is regulated by vancomycin resistance-associated sensor/regulator (vraSR), which stimulates the production of cell wall peptidoglycan and contributes to its resistance to β-lactam and glycopeptides (Kuroda *et al.*, 2003). Intracellular *S. aureus* cell wall thickening is part of a "transcriptional adaptation" to the harsh environment inside the mast cell which drives increased expression of genes responsible for cell wall synthesis (Garzoni *et al.*, 2007). Internalised *S. aureus* are a threat not only because the bacteria can escape from antibiotic treatment and immune responses, but also because it leads to an "infection reservoir", which may help to explain recurrent infections seen in patients with for example atopic dermatitis (AD) (Liu *et al.*, 2011).

## 1.7 Antibiotic treatment of *S. aureus* infections

Community-acquired methicillin-sensitive *S. aureus* (CA-MSSA) causes approximately 90% of all SSTIs. There is therefore an urgent need to develop other methods of preventing *S. aureus* infections. However, the molecular mechanisms and exact immune response pathways that contribute to the elimination of *S. aureus* are not clearly understood (Lacey *et al.*, 2016). In addition, *S. aureus* can be internalised protecting them from antibiotic action. A study has shown that antibiotics such as vancomycin, daptomycin and linezolid fail to eliminate internalised MRSA. In addition, vancomycin fails to clear bacteraemia in a mouse model. Further investigations suggested that this could be due to *S. aureus* being internalised into host neutrophils (Lehar *et al.*, 2015). The same study developed an Antibody-Antibiotic Conjugate system (AAC) in order to effectively eliminate internalised *S. aureus* from phagosomes. The AAC system consist of antibody (anti-Wall Teichoic Acids (anti-WTA), a protease sensitive linker and an antibiotic (rifalogue in this study found to be more effective). This system with the cleavable linker released the antibiotic inside the internalised cells to eliminate the intracellular *S. aureus* (Fig. 1.9). In comparison to vancomycin or rifalogue treatment, a single dose of ACC was more effective in killing internalised *S. aureus* (Lehar *et al.*, 2015). Moreover, a study on mouse keratinocytes and fibroblast infected with *S. aureus* suggested that treatment with antibiotics such as linezolid, clindamycin and azithromycin reduced the cytotoxicity of infected cells but did not inhibit the viability of intracellular *S. aureus*. In contrast, rifampicin was effective in the elimination of intracellular

*S. aureus* within three days of infection (Krut *et al.*, 2004). However, in an *in vivo* mouse peritonitis model, rifampicin was found to be more effective in eliminating extracellular *S. aureus* and oxacillin was effective in the elimination of intracellular *S. aureus* only at high doses (Sandberg *et al.*, 2009). A combination of two antibiotics (florfenicol and thiamphenicol) having synergistic effects against *S. aureus* infections may be more effective than using just one (Wei *et al.*, 2016).

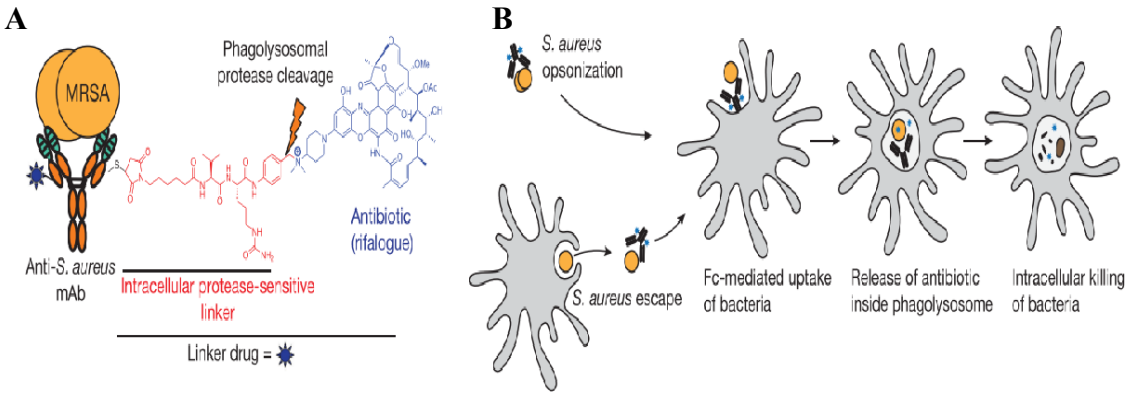


**Fig. 1.9 Antibody-Antibiotc Conjugate system (AAC) design adapted from (Lehar *et al.*, 2015).** A Model of AAC. B. Mechanism AAC action.

## 1.8 Atopic Dermatitis

*S. aureus* is the most common cause of infection in atopic dermatitis (AD) patients which mainly occurs in childhood. Clinical symptoms are itchy erythematous skin rash, particularly in the flexures (Kupper & Fuhlbrigge, 2004; Peng & Novak, 2015a; Jang *et al.*, 2015). Skin of AD patients is infiltrated with immune cells such as T-cells, DCs, macrophages, mast cells and eosinophils which produce cytokines and chemokines mediating inflammation (Kupper & Fuhlbrigge, 2004; Peng & Novak, 2015a). The factors that make AD patients more susceptible to *S. aureus* infections and immune pathways involved in the pathogenesis of AD are discussed here.

### *1.8.1* AD patients are more susceptible to infection with *S. aureus*

AD patients in Northern Europe and Eastern Asia are more likely than individuals from other parts of the world to express mutations in the filaggrin gene (*FLG*). Filaggrin controls skin pH and it is also important in keratin filaments organisation in the epidermis (Peng & Novak, 2015a). Mutations in *FLG* lead to abnormal skin barrier function and contribute to the pathogenesis of AD by allowing ingress of environmental allergens, which initiate inflammatory responses and flares of AD (Peng & Novak, 2015a). Mutations in *FLG* lead to changes in skin pH and hydration levels. Because the pH of AD skin is higher than normal skin, it enhances colonisation with *S. aureus,* that secrete virulence factors, exotoxins and superantigens. These enhance bacterial attachment to skin cells and induce inflammatory responses without triggering secretion of AMPs (Kupper & Fuhlbrigge, 2004; Peng & Novak, 2015b; Benenson *et al.*, 2005).

Increased pH activates serine proteases which disrupt corneodesmosomes, directly induce Th2 inflammatory responses and increase the permeability of skin allowing uptake of allergens (Peng & Novak, 2015a). Studies have shown that AD patients express high levels of proteases and PAR2 (Lee *et al.*, 2010). Increased expression of PAR2 had been associated with induction of skin disease (Frateschi *et al.*, 2011) and increased TSLP release (Jang *et al*., 2015; Rothmeier & Ruf, 2012).

### 1.8.2 Role of the immune response in the pathogenesis of acute and chronic AD

Studies had shown that acute AD is mainly associated with Th2 response, while in chronic AD is driven by mixed Th1, Th2, Th17 and Th22 responses (Peng & Novak, 2015b; Weidinger *et al.*, 2018) (Fig. 1.10). In acute AD, scratching disrupts the skin barrier and allows allergens to stimulate antigen-presenting cells such as DC and mast cells (MCs). They release inflammatory mediators such as, IL-6, IL-8 and TNFα initiating Th2 response (Peng & Novak, 2015b;Weidinger *et al.*, 2018). AD patients have elevated levels of IL-33, IL-25 and TSLP in their skin (Brandt & Sivaprasad, 2011). TSLP released by damaged keratinocytes is an important trigger of Th2 immune responses in AD patients (Omori & Ziegler, 2007; Kim *et al.*, 2013). Overexpression of TSLP in mice lead to AD-like symptoms (Kim *et al.*, 2013; Li *et al.*, 2008). IL-33 released by keratinocytes and immune cells also play an important role in the pathogenesis of acute AD by stimulating Th2 inflammation ( Neill *et al.*, 2010; Cevikbas & Steinhoff, 2012). Both IL-33 and TLSP interact with cutaneous sensory neuron leading to pruritus (Weidinger *et al.*, 2018). There is a positive feedback loop with TNFα inducing keratinocyte apoptosis and leading to disruption of tight junctions, which enhances Th2 responses by stimulating epithelial cells to increase the expression of TSLP (Peng & Novak, 2015a).

In chronic AD, Langerhans cells (LCs) release IL-12 and IL-18, which induce a Th1-response. This activates keratinocytes apoptosis. In addition, Th22 response is responsible for AD skin thickening (Peng & Novak, 2015b).

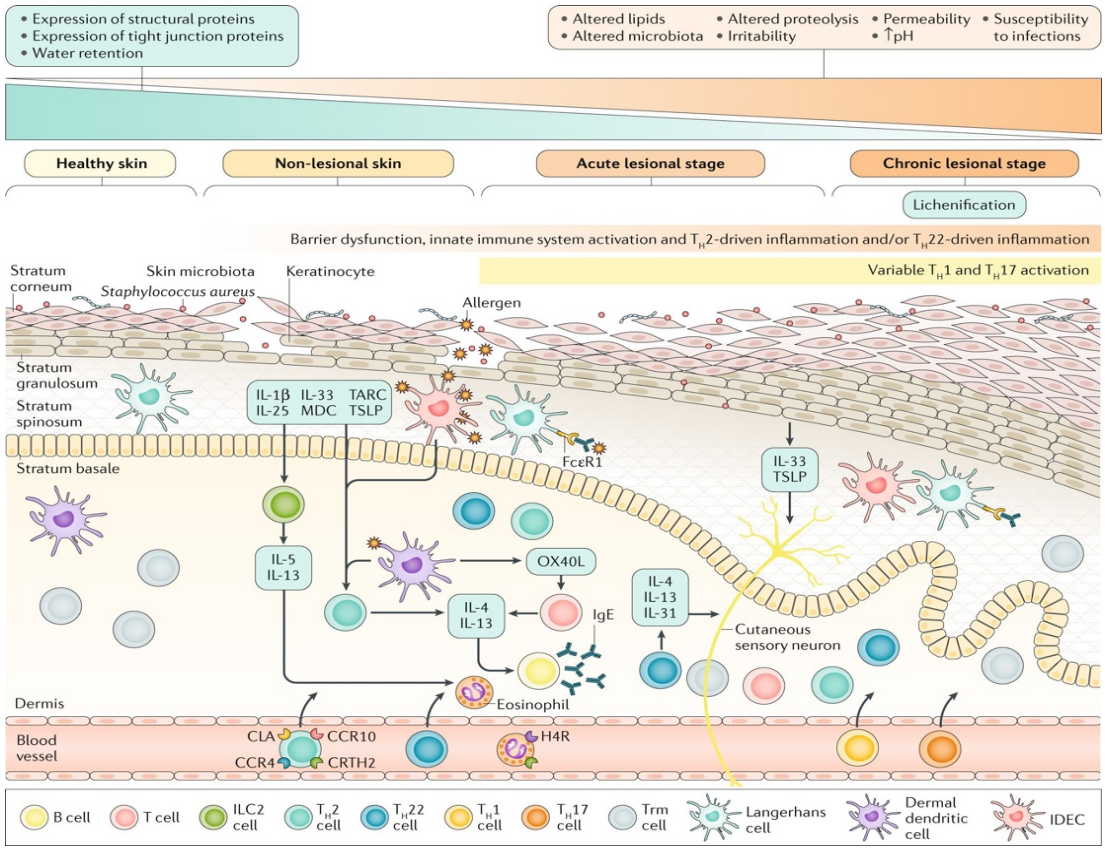


**Fig. 1.10 Immunological mechanisms involved in the pathogenicity of acute and chronic AD. Adapted from (Weidinger et al., 2018)**

## 1.9 Summary

The skin is a defence barrier that inhibits pathogens colonisation via the collaborative roles of commensal micro-organisms, skin cells and resident immune cell (Grice & Segre,2011). The defence mechanisms of the skin barrier sometimes fail and pathogens enter the body and cause infection. *S. aureus* is unique in its predominance as the key bacterial pathogen causing serious infection of skin, soft tissues and deeper structures. Questions raised here are: what makes *S. aureus* a unique inducer of inflammation in atopic dermatitis? Andwhat are the real-life implications of its ability to be internalised into keratinocytes of the epidermis? Although *S. aureus* cell wall proteins and secreted toxins facilitate its pathogenicity, the properties of this bacteria that make it such a successful skin pathogen are not fully understood. Studies by Saydahossein *et al.* showed that *S. aureus* invasion into keratinocytes is linked to ILK, Rac1 and β1-integrin (Sayedyahossein *et al.*, 2015). However, mutants lacking these genes have a significant but not complete suppression of internalisation suggesting that there could be other molecular mechanisms involved which can be studied.

Most published reports suggest that *S. aureus* cell wall proteins are essential to induce inflammation via TLRs (Rocha-de-Souza *et al.*, 2008; Olaru & Jensen, 2010; Vu *et al.*, 2010; Zecconi & Scali, 2013; Takai *et al.*, 2014; Shukla *et al.*, 2015). However experimental data from our laboratory has found that *S. aureus* as well as its sterile filtered supernatant can induce IL-33 and TSLP in mouse fibroblasts and adult human keratinocyte cell line. This effect seems to be TLRs independent, since anti-TLR2,4 and 6 antibodies did not inhibit the inflammatory response. Whereas, protease inhibitors reduced the induction of IL-33 and TSLP release from mouse fibroblasts and adult primary keratinocytes in response to *S. aureus*. The mechanism of this and molecular pathways involved are still to be elucidated.

## 1.10 Hypothesis

IL-33 and TSLP are considered as biomarkers of AD. Although these two cytokines can be released by keratinocytes, their role in mediating skin infection is not well discussed in the literature. On the other hand, *S. aureus* ability to evade host immune cells and persist intracellularly raise a question about how might this explain recurrent infections in AD patients. Based on this; two key hypotheses are examined in this PhD project:

1. *S. aureus* secretes unique bioactive factor(s) that specifically induce skin inflammation. Inhibition of this pathway may provide new therapeutic targets for *S. aureus* treatment.
2. Internalisation of *S. aureus* by human keratinocytes enables the bacteria to not only escape host immunity, but also prevent antibiotics, this forming an intracellular reservoir for frequent infection.

## 1.11 Aims

PART I

Identify the bioactive factor(s) produced by the *S. aureus* secretome (filtered supernatant (FSA)) that induce inflammation in human primary keratinocytes via IL-33 and TSLP release.

PART 2

Assess the ability of regularly used anti-staphylococcal antibiotics to kill *S. aureus* that have been internalised by human skin keratinocytes. Prior to this, the ability of keratinocytes to internalise *S. aureus* will be assessed.

# Chapter 2 : Materials and Methods

**Table 2.1 List of materials and reagents used in the study**

| REAGENT or RESOURCE | SOURCE | IDENTIFIER |
|---|---|---|
| **Bacterial strains** | | |
| Clin1-SA | A. McBain, University of Manchester, UK | N/A |
| Clin2-SA-NC2669 | Public Health England | NCTC 2669 |
| RN4220 wt | G. Xia, University of Manchester, Manchester, United Kingdom | N/A |
| RN4220;ΔtagO | | N/A |
| RN4220;Δspa | | N/A |
| Lab1-SA-SH1000 and its isogenic fnbA fnbB mutant | Joan Geoghegan, University of Dublin, Ireland | 8325-4 |
| Lab2-SA-GFP | Professor A. Horswill, University of Colorado, USA | AH2547 |
| *S. epidermidis* | Dr G. Xia, University of Manchester, UK | N/A |
| *E. coli* DH5α | Professor Ian Roberts, University of Manchester | N/A |
| *E. coli* NEB® 5-alpha | New England BioLabs, UK | C2987H |
| *E. coli* BL21(DE3) | New England BioLabs, UK | C2527H |
| *E. coli* ArcticExpress (DE3) | Agilent Technologies, USA | 230192 |
| **NHEK culture** | | |
| Primary Normal Human Epidermal Keratinocytes (NHEKs) | PromoCell, Heidelberg, Germany | C-12002 |
| DetachKit2 Trypsin, Trypsin neutralizing solution | PromoCell, Heidelberg, Germany | C-41212 |
| **Antibiotics** | | |
| Etest- RIFAMPICIN | bioMérieuxLtd,Basingstoke,UK | 412450 |
| Etest- LINEZOLID | bioMérieuxLtd,Basingstoke,UK | 412396 |
| Etest- CLINDAMYCIN | bioMérieuxLtd,Basingstoke,UK | 412315 |
| Etest- OXACILLIN | bioMérieuxLtd,Basingstoke,UK | 412432 |
| Etest- TEICOPLANIN | bioMérieuxLtd,Basingstoke,UK | 412461 |

**Table 2.2 cont. List of materials and reagents used in the study**

| REAGENT or RESOURCE | SOURCE | IDENTIFIER |
|---|---|---|
| **Antibiotics** | | |
| Rifampicin | Sigma-Aldrich, UK | R3501 |
| Linezolid | Sigma-Aldrich, UK | PZ0014 |
| Clindamycin | Sigma Aldrich, UK | C2250000 |
| Flucloxacillin | Wockhardt Ltd, UK | 10427812 |
| Teicoplanin | Sigma-Aldrich, UK | Y0001102 |
| Penicillin (100U/ml) & streptomycin (0.1mg/ml) | Sigma Aldrich, UK | P4333 |
| **Antibodies and fluorescent labelling** | | |
| FITC isomer | Sigma-Aldrich, UK | F7250 |
| Alexa Fluor® 647 Mouse Anti-Human Cytokeratin 14/15/16/19 (clone KA4) | BD Bioscience, UK | 563648 |
| Claudin-I (Rabbit, polyclonal, MH25) | Thermo Fisher Scientific, UK | 71-7800 |
| Texas red goat anti-rabbit antibody | Life Technologies, USA | T-2767 |
| **Plasmids** | | |
| pGEM-T easy vector | Promega, UK | A3600 |
| pGEM-T;*SplD* | This study | - |
| pQE30 | Qiagen, Crawley, UK | - |
| pQE30;*SplD* | This study | |
| pGEX-6P-1 | Sigma Aldrich, UK | GE28-9546-48 |
| pGEX*;pdhA* | This study | - |
| pGEX*;pdhD* | This study | - |
| pGEX*;Sbi* | This study | - |
| | | |

## 2.1 Bacterial Species and Strains

*Staphylococcus aureus* (Clin1-SA) was isolated from a chronic leg wound (courtesy of Professor A. McBain, University of Manchester, United Kingdom). Lab strain of *S. aureus* SH1000 (Lab1-SA-SH1000) and its isogenic *fnbA fnbB* mutant were kindly provided by Professor J. Geoghegan, University of Dublin, Ireland. *S. aureus* NCTC 2669 was purchased from Public Health England (Clin2-SA- NC2669). *S. aureus*-Lab2-SA-GFP (Green Fluorescent Protein), chloramphenicol-resistant strain was provided by Professor A. Horswill, University of Colorado, United States of America. *S. epidermidis* and other *S. aureus* strains (RN4220 wt and its mutant strains deficient in staphylococcal protein A (RN4220Δspa), wall teichoic acid (WTA) (RN4220ΔtagO) were a gift from Dr. G. Xia, University of Manchester, United Kingdom.

For cloning and plasmid propagation, the following competent *E. coli* strains were used; DH5α (Woodcock *et al.,* 1989), NEB® 5-alpha , BL21 (DE3) (New England BioLabs, UK ) and Arctic Express (DE3) (Agilent Technologies, USA).

## 2.2 Bacterial growth conditions and calibration curve

All bacterial strains except Lab2-SA-GFP, were grown in Nutrient broth (NB) or agar (NA) (0.5% peptone, 0.1% beef extract and 0.2% yeast extract) at 37ºC for 18-24 h. Lab2-SA-GFP was grown in Luria-Bertani (LB) broth (1% tryptone, 0.5% yeast extract and 1% NaCl) or agar (LB agar) with 10µg/ml chloramphenicol (Sigma Alderich). Bacterial stocks were prepared in Microbank$^{TM}$ (Pro-Lab Diagnostics) beads according to manufacturer instructions and also in 50 % glycerol and stored at -80 ºC. The bacterial calibration curve was plotted using measurement of bacterial OD at 600 nm and viable bacterial count by miles and misra. Miles and Misra is a standard way to determine bacterial CFU. It was done by inoculating one bead from Microbank$^{TM}$ stock in 13 ml NB or LB chloramphenicol for 18-24 h at 37 °C. Then a 10-fold serial dilution was made up to $10^{-8}$, 50 µl of each dilution was spread on NA or LB chloramphenicol agar plates with a sterile spreader and incubated at 37 °C for 18-24 h. Colonies were then counted. Plates containing less than 30 or more than 300 colonies were discounted. Then the CFU was determined using the following formula:

$$\text{Bacterial CFU/ml} = \frac{\text{number of colonies}}{\text{cultured volume}} \times \text{dilution factor}$$

The optical density of overnight culture was measured at 600 nm by spectrophotometer. The following dilutions of overnight culture were then prepared (1:2, 1:4, 1:8 and 1:16), $OD_{600}$ was measured and bacterial count was calculated based on overnight culture CFU/ml. Correlation between $OD_{600}$ and CFU/ml was plotted and the calibration curve equation was used for estimation of bacterial CFU/ml for future experiments.

## *2.3* Preparation and Fluorescent Labelling of *S. aureus* and *S. epidermidis*

Overnight cultures of bacterial strains were prepared. Next, the bacterial count was assessed using a calibration curve. 10 ml of the overnight culture was washed in phosphate buffered saline (PBS), centrifuged (1600 x*g*, 5 min), and re-suspended in 10 ml of 0.1 M carbonate buffer (pH 9) containing 100 mg/l FITC isomer (Sigma–Aldrich, United Kingdom) for 1 h at room temperature, according to manufacturer instructions. Bacterial cultures were centrifuged at 1600 x*g* for 5 min, washed with PBS, re-suspended in 1% glycerol, and stored at -80ºC until needed.

## 2.4 Preparation of bacterial filtered supernatant

One bead of *S. aureus* or *S. epidermidis* was inoculated in 13 ml NB in a 50 ml falcon tube and grown overnight at 37°C. Then the bacterial culture was washed with PBS, centrifuged at 1600 xg for 5 minutes and the pellet was re-suspended in 10 ml of keratinocyte growth media (GM). In a 50 ml tube; 5 ml of the bacterial culture mix was added to 15 ml of GM and then incubated at 37°C for 6 h in a shaking incubator. After 6 h the tubes were centrifuged at 1600 xg for 5 min. Then the supernatant was filtered using Millipore filters of a pore size of 0.2 µm (PALL, USA) and stored at -80 °C.

## 2.5 Fractionation of *S. aureus* filtered supernatant

Filtered *S. aureus* supernatant (FSA) was prepared as mentioned in 2.4. It was then fractionated by two methods. First by size exclusion centrifugal filter columns; FSA was fractionated via Amicon® Ultra-15 Centrifugal Filter Units (Mereck, UK) with 50kDa or 100kDa cut-off membrane, centrifuged at 3000 xg for 8-10 minutes at 4 °C. Retained and filtrate fractions were collected and used for the stimulation experiment. Second fractionation was to fractionate FSA 100kDa retained fraction by AKTA Purifier Fast Protein Liquid Chromatography (FPLC) using Superdex 200 and Superpose 6 size exclusion chromatography column in collaboration with Biomolecular Analysis core facility, University of Manchester. For this a larger volume of FSA was required to provide more

concentrated starting sample as the fractionation results in sample dilution. Multiple aliquots of 100 kDa retained fractions were pooled together (1 ml) and fractionated further by FPLC using a Superdex 200 column; small – scale size exclusion chromatography column with fractionation size range of 10-600 kDa or Superose 6 column which has wider fractionation size range (5 - 5000 kDa). Forty-eight fractions of 0.5 ml were collected for NHEK stimulation.

## 2.6 Primary Normal Human Epidermal Keratinocytes (NHEKs) Culture

NHEKs (PromoCell, Heidelberg, Germany) were grown until 80% confluent before passage in keratinocyte complete growth media (with supplements) (PromoCell, Heidelberg, Germany) at 37 °C, 5% $CO_2$. Cells were detached using 0.025% trypsin / 0.01% EDTA (PromoCell) for 5 min at 37°C, 5% $CO_2$ followed by trypsin neutralisation (0.05% Trypsin Inhibitor from soybean and 0.1% Bovine Serum Albumin). Cells were reseeded at $10^6$ cells in a T-75 cm / 25 cm flask or at $10^5$/well in 24 well plates and incubated at 37 °C, 5% $CO_2$. The media was changed twice a week until cells were 70-90% confluent. Primary cells were used between passage one and five before disposal.

## 2.7 NHEK-bacterial co-culture

NHEKs were cultured in 24-well tissue culture plates at a density of $10^5$ cells/ well. Once confluent they were used for experiments. All stimulations were for 6 h at 37 °C and 5% $CO_2$ unless stated otherwise. NHEK/bacterial co-culture was with $10^7$ CFU/ml of *S. aureus* strains, $10^7$ CFU/ml of *S. epidermidis*, Heat Killed *S. aureus* (HKSA, $10^6$ CFU /ml) was purchased from BioScience, Nottingham, UK. Where stated, NHEKs were stimulated with *S. aureus* filtered supernatant (FSA), *S. epidermidis* filtered supernatant (FSE), FSA fractions and other proteins as shown in chapter 4. After stimulation, supernatants were collected, centrifuged (12,000 *xg*, 15 min) and stored at -20°C prior to analysis.

## 2.8 Human IL-33 and TSLP ELISA

IL-33 and TSLP DuoSet® ELISA (R&D Systems) were used to analyse cytokine production. ELISA was performed according to the manufacturer's instructions. Briefly, 96-well flat bottom ELISA plates (Dynatech) were coated with anti-human specific capture antibody. After washing and blocking, detection antibody was added and the colour developed using Streptavidin-horseradish peroxidase and tetramethylbenzidine (R&D System). Optical density was measured using a Dynex MRX11 microplate Reader (Dynex Technologies, Berlin, Germany).

## 2.9 SDS-PAGE

Sodium dodecyl sulphate polyacrylamide gel electrophoresis (SDS-PAGE) was used to analyse protein content of FSA fractions. Precast 4-12 % Bis-Tris protein gradient gels (NuPAGE, Thermo Fisher scientific) were used. Then 12 µl of each sample to be analysed was reduced with 3 µl of a stock solution of 40 mM dithiothreitol (DTT) in RunBlue LDS sample buffer (4 x concentrate) for 7-10 minutes at 95°C. 10 µl of reduced sample was loaded onto precast gels run at 200 V for 30 minutes in a running buffer (NuPage® 1x MES running buffer (Novex by Life Technologies, UK). Gels were then stained either by Instant Blue Coomassie-based gel stain (1 h staining followed by 1 h de- staining with $dH_2O$) or by silver staining. SDS-PAGE was also for verification of gene expression and protein purification.

## 2.10 Silver staining

SDS-PAGE gel was fixed for 2 h in fixation buffer (50% methanol (MeOH), 12% acetic acid (HAc), 0.05% formalin) then washed three times with 35% ethanol (EtOH) for 20 mins. Next, the gel was sensitised in 0.02% $Na_2S_2O_3$ for 2 mins, washed three times with $dH_2O$ for 5 mins followed by staining for 20 min with silver nitrate (0.2% $AgNO_3$, 0.076% formalin). After that the gel was washed for 2 mins in $dH_2O$. A developer buffer (6% $Na_2CO_3$, 0.05% formalin, 0.0004% $Na_2S_2O_3$) was added to the gel and visualised on a white light dock until the bands were clear. Immediately, the reaction was stopped by stop solution (50% MeOH, 12% HAc) for 5 mins.

## 2.11 Western Blot

The expression of *pdhD* using pHis;*pdhD* plasmid was verified by western blotting. Samples of induced and non-induced bacterial cultures were thawed on ice and 10 µl of 1 mg protein was prepared in deionised water. Then they were reduced in NuPage® LDL sample buffer at 95 °C for 10 min. 20 µl of each sample was loaded on 10% precast gel and gel electrophoresis was performed. Proteins were then transferred from the gel into 0.45 µm Invitrolon™ PVDF membrane (Invitrogen by Life Technologies, UK). Briefly, the membrane was activated for 30 seconds in 100% methanol and then rinsed in deionised water. The membrane, filter paper and blotting pads were then equilibrated for 5 min in transfer buffer (50 ml 1x NuPage® transfer buffer (Novex by Life Technologies,UK): 100 ml Methanol :850 ml deionised water). After electrophoresis, the gel was separated from the cassette and the blot "sandwich" was assembled in the module. The blot module was then

filled with transfer buffer until the gel/membrane sandwich was covered. The outer chamber was filled with ~ 650 ml deionised water and the transfer was run for 1 h at 30 V.

To block non-specific binding of antibodies, the membrane was incubated with 5% milk Tris-*buffered* saline, 0.1% Tween 20 (TBST) for 1 h at room temperature (RT) with shaking. This was followed by overnight incubation with primary antibody (Dihydrolipoamide Dehydrogenase (DLD) Antibody NBP1-31302 (NovusBiologicals, USA)) diluted to 1 µg/ml in 5% milk TBST at 4ºC. The membrane was washed 4-6 times in wash buffer (0.05% TBST). After that, HRP-conjugated antibody was diluted to 1 µg/ml in 0.05% TBST and incubated for 1 h at RT with shaking followed by extensive washing with wash buffer. A substrate working solution was then freshly prepared by mixing the two available reagents in Pierce™ ECL western blotting substrate at a ratio of 1:1, which was added to the blot and incubated for 1 min at RT. Excess reagent was discarded and the blot was covered in plastic wrap and an absorbent tissue was used to remove excess liquid and to press out any bubbles that might be present between the blot and the membrane protector. Finally, the protected membrane was placed in a film cassette with proteins side facing up. Then the X-ray film was placed on top of the membrane and exposed for of 60 secs-5 min and finally the film was developed.

## 2.12 Mass Spectrometry analysis

A gel-top of entire sample was prepared for mass spectrometry analysis. This was done by running the protein sample into the top 5mm of a high concentration non-gradient gel (10% , NuPAGE, Thermo Fisher Scientific) to ensure all proteins were packed in a single band. The gel was then stained with Instant Blue Coomassie-based gel stain and destained with $dH_2O$ and left at 4°C overnight to washout all contaminents. Then an in-gel digestion and tandem mass spectrometry (LC-MS/MS) analysis was done by Bio-MS core facility( https://sites.manchester.ac.uk/bioms/ ). The data was generated against known protein sequences in Swissprot TrEMBL database using Firmicutes phylum (which includes *S. aureus*) as the most optimal taxonomic level available in the database.

## 2.13 *SplD* amplification and Cloning

Serine protease–like protein D (SpID) DNA manipulation and protein purification was done in collaboration with Professor Ian Roberts, University of Manchester. *SplD* gene was synthesised and amplified from a single colony of Clin1-SA by colony Polymerase chain reaction (PCR) using *SplD* primers shown in Table 2.3. PCR mix and program as follows;

| **PCR Mix** | x1 µl |
|---|---|
| Primers | 2.5 each |
| 10 mM of dNTP | 1 |
| 5x Phusion Buffer | 10 |
| Phusion® enzyme | 0.5 |
| Autoclaved water | 33.5 |

**PCR Program**

| | | | |
|---|---|---|---|
| Initial denaturation | 95˚C | 30 sec | |
| Denaturation | 95˚C | 10 sec | |
| Annealing | 59˚C | 30 sec | 35 cycles |
| Extension | 72˚C | 15 sec | |
| Final extension | 72˚C | 10 min | |

Then 10 µl of PCR products were loaded on 1% agarose gel prepared in TAE buffer. The PCR product of a positive clone was cleaned using the QIAquick PCR purification kit (QIAGEN, UK) according to manufacturer instructions (QIAGEN, UK). 3 µl of cleaned PCR product was ligated to 1 µl of pGEM-T easy vector (Promega, UK) by 1 µl ligase enzyme at 4°C overnight. pGEM-T easy vector is a good system widely used to clone PCR products. Its multiple cloning site (MCS) is within a coding region of β-galactosidase which will allow Blue/White screening for colonies with inserts in the plasmid on a selection plate. The ligation mix (10 µl) was then transformed into 100 µl of chemically competent *E-coli* cells DH5α and cultured on LB ampicillin/X-Gal agar plates. Positive colonies were selected based on colour; white colonies were patched on LB ampicillin/X-Gal plates then screened by PCR using M13 primers (Table 2.3**)** (PCR mix and program below) to confirm the presence of *SplD* fragment (720bp).

| **PCR Mix** | x1 µl |
|---|---|
| Primer F: 1:10 M13 | 2 |
| Primer R: 1:10 M13 | 2 |
| My Taq mix | 25 |
| Autoclaved water | 21 |

**PCR Program**

| | | | |
|---|---|---|---|
| Initial denaturation | 95˚C | 1 min | |
| Denaturation | 95˚C | 30 sec | |
| Annealing | 53˚C | 30 sec | 35 cycles |
| Extension | 72˚C | 30 sec | |
| Final extension | 72˚C | 10 min | |

Four clones with the correct fragment size were inoculated in LB ampicillin (100µg/ml) and grown overnight for plasmid DNA extraction and DNA verification by restriction enzymes HindIII and BamHI. Positive clones were sequenced using M13 primers to select a clone with no missense mutation before expressing the *SplD* gene. From the DNA sequence, the protein sequence was predicted by translate tool Expasy (https://web.expasy.org/translate/) and alignment of protein sequences was done by BLAST tool (https://blast.ncbi.nlm.nih.gov/) (data shown in appendix A). A positive clone was selected to use for sub-cloning the *SplD* gene into an expression vector pQE30 which is used to express N-terminally his-tagged proteins. Plasmid DNA was purified from the selected clone by QIAprep miniprep kit (QIAGEN, UK) to manufacturer's instruction. Then digested with HindIII and BamHI for 90 minutes at 37°C. *SplD* fragment was then gel purified by QIAquick gel extraction kit (QIAGEN, UK) and cloned into pQE30. Then the pQE30; *SplD* plasmid was transformed into DH5α and culture on LB amp plates. Colonies on LB amp were selected and screened by colony PCR using pQE30 primers (Table 2.3**).**

## 2.14 *SplD* expression and protein purification

This was done by Dr Charis Saville (a PDRA in our research group) in collaboration with Prof Ian Roberts. A clone with accurate SpID amino acid sequence was inoculated in LB ampicillin (100 µg/ml) broth and grown overnight at 37 °C. Next day the overnight culture was diluted 1:100 in LB ampicillin broth and grown until reached mid log phase OD 0.4-0.6. Expression of *SplD* was then induced by 0.1 mM Isopropyl β- D-1-ThioGalactopyranoside (IPTG) for 4 h and the cell pellet was collected. Cells were lysed by BugBuster® (Sigma Aldrich, UK) following manual instruction and purified by HisTrap™ –HP nickel column (GE healthcare life sciences) following the manufacturer instructions.

## 2.15 *pdhD*, *pdhA* and *Sbi* cloning and expression

Sequences of *S. aureus* DLD (gene; *pdhD*), PDHa (gene; *pdhA*) and Sbi (gene;*Sbi*) were acquired from KEGG website (https://www.genome.jp/kegg/). Then they were cloned by GeneArt, Thermofisher, UK into expression vector pHis (provided kindly by Edward Mckenzie protein expression unit, MIB). Unfortunately, the expression using this plasmid was leaky and several optimisation steps were performed to improve expression (details available in Appendix B). However, none of those optimisation attempts worked. Therefore, in collaboration with Dr Hayley Bennett from the Genome Editing Unit, University of Manchester, *pdhD*, *pdhA* and *Sbi* genes were subcloned into pGEX plasmid which produce N- terminally GST- tagged proteins using BamHI and EcoRI restriction enzymes. Ligation of *pdhD*, *pdhA* and *Sbi* to pGEX vector done overnight by T4 DNA ligase at 4°C. The

constructed plasmids were transformed into NEB® 5-alpha competent *E. coli* cells (New England BioLabs, UK) following manufacturer's instruction. Colonies were screened by colony PCR using pGEX forward and reverse primers (Table 2.3**)** and PCR cycle parameters as following;

**PCR program**

| | | | |
|---|---|---|---|
| Initial denaturation | 95˚C | 8min | |
| Denaturation | 95˚C | 20sec | |
| Annealing | 53˚C | 20 sec | 40 cycles |
| Extension | 72˚C | 1.5 min | |
| Final extension | 72˚C | 5min | |

Positive clones were selected, single colonies were inoculated into LB ampicillin broth and incubated overnight at 37°C. Plasmids were then purified using Isolate Plasmid Mini kit (Bioline,UK) and sequenced using pGEX primers (Table 2.3). Once the sequences were confirmed, *pdhD*, *pdhA* and *Sbi* were expressed in BL21 (DE3) *E-coli* cells (New England BioLabs, UK) for 3 h at 37°C or in Arctic Express *E-coli* cells (Agilent Technologies, USA) for 24 h at 12°C. After expression, cell cultures were centrifuged at 3500 xg for 20 min at 4°C. Supernatant was discarded and cell pellets were frozen in liquid nitrogen then at -80°C until used for protein purification.

**Table 2.3 Sequences of primers used in this study**

| Oligonucleotide | Sequence (5'-3') | Purpose |
|---|---|---|
| **SplD BamH1 F** | CCTGTAGGATCCATGAATAAAAATATAATCATCAAAAGTATTGCGG | Used to amplify *SplD* from Clin1-SA for cloning using BamHI-EcoRI sites of pGEM-T |
| **SplD HindIII R** | GCGCGATAAGCTTTTATTATTTATCTAAATTATCTGCAATAAATTTCTTAAT | |
| **M13 F** | CGCCAGGGTTTTCCCAGTCACGAC | Used to sequence *SplD* insert in pGEM-T vector |
| **M13 R** | AGCGGATAACAATTTCACACAGGA | |
| **PQE30 F** | AAGTGCCACCTGACGTCTAAG | Used to sequence *SplD* insert in pQE30 vector |
| **PQE30 R** | GGAGTTCTGAGGTCATTACTG | |
| **pGEX F** | GGGCTGGCAAGCCACGTTTGGTG | Used to screen for inserts *(pdA, pdhD and Sbi)* cloned in pGEX |
| **pGEX R** | CCGGGAGCTGCATGTGTGTCAGAGG | |

## 2.16 Protein purification by Glutathione Sepharose 4B beads

First a binding buffer [Tris $_{(20mM)}$ $NaCl_{(150mM)}$ $H_2O$, pH 8] was prepared and used cold in the purification procedure. Then 2 ml of Glutathione Sepharose 4B beads (GE healthcare life sciences, USA) were added to a 15 ml falcon tube, washed with Milli-Q water and then a further three times with binding buffer to remove the ethanol that was used for storage. In each of the washing steps, the mix was centrifuged at 355 x*g* for 5 min and supernatant was discarded gently to avoid losing the beads. From this a 50% slurry was prepared which consisted of 1.5 ml of washed beads and 1.5 ml of binding buffer. Once the slurry was prepared it was stored at 4 °C until required.

To prepare the lysate, the frozen cell pellet was first weighed. Then to 1 g of pellet, 10 ml of lysis buffer (Binding buffer + 1 mg/ml lysozyme + 1 mM DTT) was added. Cells were lysed by 2-3 freeze –thaw cycles until the sample appeared to be viscous indicating the release of nucleic acid. Then 0.5 µL of Benzonase (mixture of DNase and RNase) (Merck, United Kingdom) was added and incubated for 10 min RT on a rocker until sample was no longer viscous.

To purify the proteins from the lysate, 1 ml aliquots of the lysate were prepared in 1.5 ml Eppendorf tubes and centrifuged at 20,000 *xg* for 5-10 min. The supernatant was transferred to Eppendorf tubes which contained 75 µL of 50% slurry and incubated for 1 h at RT on a rotor. Samples were then centrifuged at 400 *xg* for 1 min and the flow through was transferred into a 15 ml tube without touching the beads. To the beads, 1 ml of wash buffer (binding buffer +50 µL DTT of 1 mM) was added. Centrifuged at 300 *xg* for 1 min, and the supernatant was discarded. This washing step was repeated three times. After the final wash, supernatant was discarded from all tubes and 1 ml of wash buffer was added to the first tube, and transferred to the next tube. Mixed gently, and transferred to the next tube and so on. Tubes with traces of the beads were stored at 4°C to use for SDS-PAGE analysis. To elute the proteins from the beads, 10 µL of PreScission protease (GE healthcare life sciences, USA) was added to the tube and incubated at 4 °C overnight on a rotor. Next day, the samples were centrifuged at 400 *xg* for 1 min and the supernatant was collected. Gradient SDS-PAGE (4-12 %) was used to verify the purification process and to check the product.

For the gel, 5 µl of each of following was loaded;

- Insoluble fraction: 1 ml wash buffer added to the cell pellet.
- µl of this sample + 2.5 µl water + 1.25 µl SDS-sample buffer
- Soluble fraction; the lysate centrifuged at 20,000 x*g* for 30 sec. 10 µl of the supernatant transferred into new tube (5 µl +1.25 µl SDS-sample buffer)
- Flow through from the first washing step after incubation with the beads (5 µl +1.25 µl SDS-sample buffer)
- Beads from last washing step (5 µl SDS-sample buffer was added the beads)
- Beads after elution step: 1 ml of wash buffer added, mixed and transferred. 5 µl of this sample + 1.25 µl SDS-sample buffer
- Purified protein 5 µl + 1.25 µl SDS-sample buffer
- Protein standard pre-stained ladder

## 2.17 Assessment of Bacterial Internalisation

### 2.17.1 Cell Culture

Normal Human Epidermal Keratinocytes were seeded in 24-well plates (1 x $10^6$ cells/ml) and incubated with $10^7$ CFU/ml of either FITC- or GFP-labeled bacteria in complete keratinocyte growth media for 1 h (37°C, 5% $CO_2$). 2% penicillin/streptomycin were then added to each well and left for 30 min to kill extracellular bacteria. Cells were analysed between 1 and 24 h post-internalisation. For both flow cytometry and Amnis® experiments, NHEKs were washed with PBS and detached using 0.025% trypsin/0.01% EDTA (PromoCell, Heidelberg, Germany) for 5 min at 37°C, 5% $CO_2$ followed by trypsin neutralisation (0.05% trypsin inhibitor from soybean and 0.1% bovine serum albumin).

### 2.17.2 Flow Cytometry

Initially, internalisation of bacteria by NHEKs was studied by standard flow cytometry (BD FACS Canto II, BD Biosciences, United Kingdom) and analysed using FlowJo software (Tree Star V10). Cells were prepared as described above. NHEKs inherent autofluorescence was excluded using a (PerCP)-Cy5$^{+}$ /FITC$^{+}$ gate as described in Figure 2.1. Single FITC$^{+}$ cells representing green florescent protein (GFP)-*S. aureus* positive NHEK were taken forward for analysis (gate labelled as SA+ in Fig. 2.1).

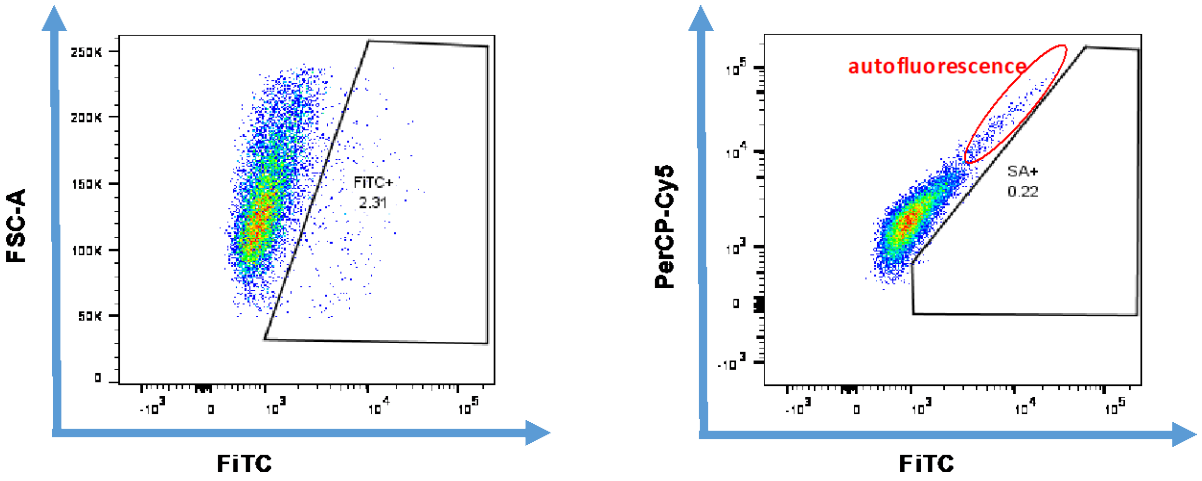


**Fig. 2.1 Gating setting for assessment of *S. aureus* internalisation into NHEK by flow cytometry**

Annexin V and DAPI were used to assess cell death. Annexin V detects apoptotic cells due to its ability to bind to the translocated phosphatidylserine on the cell membrane. Whereas DAPI (4′,6-diamidino-2-phenylindole) assess necrosis as it binds to DNA. Cells were incubated with Annexin V-APC (eBioscience, United Kingdom) in cell staining buffer (Biolegend, United Kingdom) for 20 min. Cells were then washed and DAPI (New England Biolabs, United Kingdom) added to a final concentration of 0.25 µg/ml prior to flow cytometry analysis. Internalisation was also assessed using Amnis® (ImageStream® MarkII Imaging FlowCytometer, Merck, United Kingdom), which allows microscopic visualisation of flow cytometry gated cells. NHEKs were prepared as described above. After 2% penicillin / streptomycin treatment, cells were incubated in keratinocyte growth media for 4 h (37°C, 5% $CO_2$) then fixed with 4% paraformaldehyde (10 min, RT) and permeabilised (0.1% Triton-X, 10 min). NHEKs were re-suspended with 1 µg/ml of Alexa Fluor®647 mouse anti-human cytokeratin 14/15/16/19 (clone KA4, BD Bioscience, United Kingdom) in permeabilisation buffer to identify primary keratinocytes (20 min, RT in the dark), washed, and re-suspended. Cytokeratin 14/15/16/19$^{+}$/*S. aureus*-FITC$^{+}$ cells were gated and sorted for Amnis® analysis using IDEAS 6.2.

### 2.17.3 Confocal Microscopy

Confocal microscopy was also performed to confirm internalisation of Lab2-SA-GFP by NHEK. $1x10^6$ cells/ml were incubated with $10^7$CFU/ml Lab2-SA-GFP (1 h, 37°C, 5% $CO_2$) then washed, treated with 2% penicillin / streptomycin (30 min), and incubated in media for 4 h (37°C, 5% $CO_2$). NHEKs were fixed with 4% PFA and permeabilised using 0.1% Triton-X. Cells were stained with CellMask Deep Red stain according to manufacturer's instructions (Thermo Fisher Scientific, United Kingdom). Images were collected on a Leica TCS SP5 AOBS inverted confocal using a 100x/1.40 immersion oil objective and 4x confocal zoom. The confocal settings were as follows: pinhole 1 airy unit, scan speed 400 Hz bidirectional, format 512x512. Images were collected using HyD detectors with the following detection mirror settings; FITC 493-589 nm, Texas red 599- 615 nm using the 488nm (10%) and 594 nm (1%) laser lines, respectively. When it was not possible to eliminate cross-talk between channels, the images were collected sequentially. When acquiring 3D optical stacks, the confocal software was used to determine the optimal number of Z-sections. Only the maximum intensity projections of these 3D stacks are shown in chapter5. Imaris X64 9.2.1 (Bitplane, United Kingdom) image analysis software was used to analyse the data.

## 2.18 Inhibition of Internalisation

To assess inhibition of *S. aureus* internalisation, cells were prepared as described above. Media in each well was discarded and cells washed with PBS. Where detailed in the text, NHEK were pre-treated with anti- α5β1 integrin antibody (clone JBS5, Sigma–Aldrich, United Kingdom) for 30 min (37°C, 5% $CO_2$) in complete keratinocyte media. Pre-treated NHEKs were then infected with *S. aureus* ($10^7$ CFU/ml) in the presence of inhibitor for 1 h. Media containing *S. aureus* and inhibitors was discarded and cells were treated with 2% penicillin / streptomycin for 30 min. Cells were then washed with PBS and detached for flow cytometry analysis as described above.

## 2.19 Antibiotic MIC Determination

The bactericidal properties of flucloxacillin (Wockhardt Ltd., United Kingdom), clindamycin, teicoplanin, linezolid, and rifampicin (all Sigma–Aldrich, United Kingdom) were assessed. Minimum inhibitory concentration (MIC) for each antibiotic was determined by both Etest reagent strips (bioMérieux Ltd., Basingstoke, United Kingdom) and the Microtitre Broth Dilution Method (MBC).

### 2.19.1 Etest

An overnight bacterial culture was prepared as previously described in NB (2.1). The following day a sterile swab was soaked in the overnight culture and used to streak an entire Muller-Hinton agar (Sigma-Aldrich) plate. The plates were left to dry for 15-20 minutes. Once completely dry, Etest strips were placed carefully on the plates using sterile forceps. A single strip was added to the middle of each plate and three plates for each antibiotic were prepared.

### 2.19.2 Microtiter Broth Dilution

Using predicted MIC by Etest, eleven concentrations of antibiotics were selected to include; five concentrations higher than MIC, MIC and five concentrations lower than MIC. Five-fold serial dilutions of the antibiotics in Muller-Hinton broth 2 (Sigma-Aldrich, USA) were prepared. A control of Muller-Hinton (without antibiotic) was included as a negative control. Using a multichannel pipette, 100 µl of each antibiotic concentration and the negative control were transferred into a 96-well plate (each in a single well-arranged from 1-12). *S. aureus* overnight culture was diluted to ($OD_{600}$ of 0.08-0.1) in autoclaved $dH_2O$. Then, immediately 5 µl of the bacterial cell suspension was added to a 96-well plate. The plates were incubated at 37°C for 24 hours. At least three technical repeats for each concentration was performed.

## 2.20 In vitro Infection of NHEK with *S. aureus* and Antibiotics Assay

NHEKs were seeded in 24-well plates at a density of $5x10^4$ cells/ml. When confluent, cells were infected with $10^7$ CFU/ml *S. aureus* (diluted in keratinocyte growth media from overnight culture) for 1 h at 37° C followed by treatment with 2% penicillin / streptomycin for 1 h to eliminate extracellular *S. aureus*. Cells were washed with PBS and incubated in complete keratinocyte media for 4 h (37 °C, 5% $CO_2$). Media was then replaced with or without anti-staphylococcal antibiotics in complete media for a further 24 h, as outlined in the text. 50 µl of supernatant was cultured onto nutrient agar plates in order to quantify extracellular *S. aureus*. Cells were then washed three times with PBS, treated with 2% penicillin / streptomycin for 1 h, and lysed in 300 µl of PBS using mini-scrapers (VWR

International, United Kingdom) and vigorous vortexing. Cell lysates were cultured on NA using serial dilutions to assess the number of intracellular *S. aureus*. For quantification of CFU, at least three technical replicates were performed for each well.

## 2.21 Detection of cell death by trypan blue

This was done to check the viability of NHEK after 24 h incubation with different concentrations of antibiotics used in in the effectiveness assay (2.20). NHEKs were prepared in 24 well plates and were incubated for 24 h with 10X MIC and 20XMIC of flucloxacillin , clindamycin, teicoplanin, linezolid, and rifampicin. Cell were then washed and detached as described in (2.17.1). Aliquots from each condition were mixed with 0.4% of trypan blue (1:1) for 2 min and analysed immediately using hemocytometer on an upright microscope. Unstained cells were counted as viable and blue cells were counted as dead cells. The percentage of viable cells was then calculated using following formula:

$$\text{Percentage of viable cells} = \frac{\text{viable cells}}{\text{ttttttttt nnnnnnnnnnn ttoo ccnnttttcc}} \times 100$$

## 2.22 Ex vivo human skin organ culture and infection with GFP-*S. aureus*

Human skin was obtained following liposculpture procedures performed on healthy adult patients. The study was approved by the North West Research Ethics committee (REC ref. 14/NW/0185) and all of the patients gave written informed consent. A 4-mm diameter biopsy punch (Integra™ Miltex™, Fisher Scientific) was placed in a Thincert cell culture insert with a pore size of 0.4 µm (Greiner Bio-One, United Kingdom) and cultured in a six-well plate, creating an air–liquid interface. The culture medium consisted of William's E media (Thermo Fisher) supplemented with 1% (v/v) L-glutamine, 0.02% (v/v) hydrocortisone, and 0.1% (v/v) insulin. The surface of the biopsy was loaded with 3 µl of $10^7$ CFU/ml Lab2-SA-GFP and incubated at 37°C, 5% $CO_2$ for 3 h. After culture the biopsies were snap-frozen in liquid nitrogen and stored at 80°C until use.

## 2.23 Immunofluorescence Staining

Skin tissue blocks were cut to 5 µm depth (20ºC, OFT Cryostat; Bright Instruments, United Kingdom) in triplicate onto Superfrost™ Ultra Plus Adhesion slides (Thermo Fisher Scientific, United Kingdom). Sectioning procedure was done from dermis to epidermis to avoid any possibility of pulling the bacteria from the top to deeper in the tissue. Sections were labelled and stored at -80ºC until needed.

Frozen sections were air dried (10 min, RT), then fixed with methanol:acetone (50:50 v/v) for 20 min at 20ºC. Slides were washed in tris-buffered saline (TBS) three times (5 min each) then permeabilised with 0.1% Triton-X100 (5 min, RT). 10% normal goat serum (NGS, Vector Laboratories Inc., United States) was used as diluent and to block non-specific binding (1 h, RT). Sections were stained with Claudin-I (rabbit anti-human polyclonal, MH25, Thermo Fisher Scientific, United Kingdom) diluted 1:50 in diluent and incubated overnight at 4ºC. Sections were washed in TBS-0.05% Tween-20 and incubated with Texas™ red goat anti-rabbit antibody (Life Technologies Corporation, Thermo Fisher) diluted 1:100 in block and incubated in the dark for 1 h at RT before washing again. Finally, sections were mounted with VETASHIELD® HardSet™ mounting medium (Vector Laboratories Inc., United States).

## 2.24 Statistical Analysis

Statistical comparisons were made using one-way or two-ways ANOVA, with Dunnet's *post hoc* test using GraphPad Prism 7. $P < 0.05$ was considered statistically significant.

# Chapter 3 : *S. aureus* filtered supernatant induces Type 2 inflammation in human primary keratinocytes

## 3.1 Foreword

*S. aureus* significantly colonises skin of AD patients and is readily isolated from skin during flares (Geoghegan *et al.*, 2018). Many studies have addressed pathogenic *S. aureus* surface proteins, secreted toxins and proteases that are involved in barrier dysfunction, driving inflammatory responses most of which related to innate immunity (Zecconi & Scali, 2013; Ryu *et al.*, 2014; Peetermans *et al.*, 2015; Thammavongsa *et al.*, 2015). IL-33 and TSLP are Th2 associated cytokines released by non-hematopoietic cells such as keratinocytes and they are both highly expressed in AD skin (Hvid *et al.*, 2011; Omori & Ziegler, 2007). IL-33 acts as an "alarmin" cytokine in which its release from cells in barrier tissues; in response to tissue damage or exogenous proteases, activate innate lymphoid cells type 2 (ILC2) and other immune cells to initiate Th2 mediated immune responses (Cevikbas & Steinhoff, 2012; Savinko *et al.*, 2012; Cayrol *et al.*, 2018). Moreover, TSLP is a key mediator of Th2 inflammation in allergic diseases through its activation of Dendritic Cells (DCs) (Lund *et al.*, 2013; Omori & Ziegler, 2007). It is known to be highly expressed in lesioned skin of AD patients and in asthmatic airways (Li *et al.*, 2008; Shan *et al.*, 2010) and involved in the development of dermatitis in murine model (Jang *et al.*, 2015).

Previous data from our laboratory showed that live *S. aureus* causes significant release of IL-33 and TSLP from mouse fibroblasts and adult human keratinocytes which is TLRs independent (Alkahtani 2016). Details about how *S. aureus* causes the release of danger signals from epidermal cells, and whether this is caused by a cell-wall component or by a secreted factor are not yet fully understood.

This chapter investigates the ability of live *S. aureus* and its filtered supernatant (FSA) to induce the release of two danger signals and biomarkers of AD (IL-33 and TSLP) from juvenile primary human keratinocytes (NHEK). In addition, fractionation of *S. aureus* sterile filtered supernatant (FSA) by size has been done using different approaches in order to help purify the secreted *S. aureus* bioactive factor/s.

## 3.2 *S. aureus* but not *S. epidermidis* induces release of IL-33 and TSLP from primary human keratinocytes (NHEK)

Alkahtani (2016) showed that *S. aureus* but not other staphylococcal species induced the release of IL-33 and TSLP from mouse fibroblasts and human adult primary keratinocytes. To confirm the ability of *S. aureus*, compared to *S. epidermidis*, in inducing the release of Th2-promoting cytokines from NHEK, $10^7$ CFU/ml of bacterial species and *S. aureus* strains were co- cultured with NHEK for 6 h at 37 °C. Th2-promoting cytokines (IL-33 and TSLP) were measured in the supernatant by ELISA (Fig. 3.1). *S. aureus* strains used in this experiment included clinical (Clin1-SA) and lab (RN4220 and SH1000) strains, as well as three mutant strains deficient in staphylococcal cell wall surface proteins and components that are required for adhesion to host cell; protein (SpA) (RN4220;Δspa), wall teichoic acid (WTA) (RN4220;ΔtagO) and fibronectin binding protein A and B (SH1000;ΔFnBP). Also used a commercially available heat killed *S. aureus* (HKSA)which is known to induce innate immune responses through TLRs especially TLR2. The concentration of bacteria and time course of the stimulation experiment was previously optimised as discussed in details in (Alkahtani, 2016).

Despite the fact that SpA, WTA and FnBPs are important for *S. aureus* adhesion to host cells, they play a role in the pathogenesis of *S. aureus*. SpA can produce pro- inflammatory responses in the skin via its interaction with TNFR1 (Classen *et al.*, 2011) and FnBPs are involved in *S. aureus* systemic infections (Lacey *et al.*, 2016). WTA is a cell wall component recognised by TLR receptors in the skin and can initiate innate responses (Shukla *et al.*, 2015).

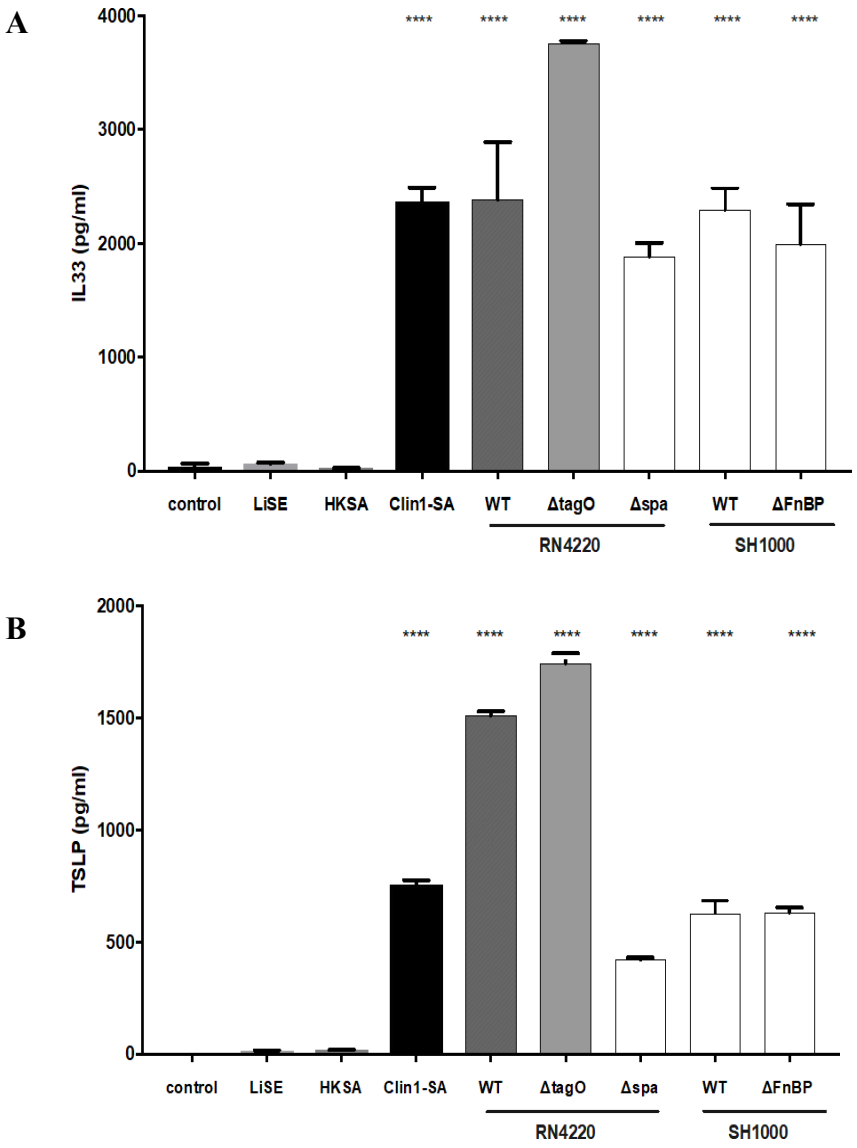


**Fig. 3.1 *S. aureus* strains but not *S. epidermidis* induced release of IL-33 and TSLP from NHEK.**
NHEK were stimulated with $10^7$ CFU/ml *S. epidermidis* (LiSE), $10^6$ CFU/ml HKSA, a clinical isolate of *S. aureus* $10^7$ CFU/ml (Clin1-SA), as well as *S. aureus* lab strains and their mutants (RN4220, RN4220;ΔtagO, RN4220;Δspa, SH1000, and SH1000;ΔFnBP) . Control is non infected NHEK. Supernatants were collected after 6 h. A. IL-33 and B. TSLP measured by ELISA. Data represent three independent experiments each performed in triplicate. P-values were determined in comparison with control by one-way ANOVA with Dunnett's post hoc test. Mean ± standard error of the mean. **** P<0.0001.

The results showed that all live *S. aureus* strains, but not *S. epidermidis* or HKSA, induced the release of both IL-33 and TSLP from primary human keratinocytes. Furthermore, surface molecules; WTA, FnBP and SpA were not required to induce release of these cytokines. This suggests that the *S. aureus* bioactive factor/s more likely to be in the secretome.

## 3.3 Sterile filtered *S. aureus* supernatant (FSA) induced release of IL-33 and TSLP from NHEK

From data presented in 3.2 the possibility that the factors responsible for the release of IL-33 and TSLP were secreted rather than cell wall bound was investigated. NHEK were stimulated for 6 h with sterile filtered *S. aureus* supernatant (FSA) or sterile filtered *S. epidermidis* supernatant (FSE). FSA was treated with 2% penicillin/streptomycin to ensure that effect on NHEK was not due to the presence of contaminating live bacteria. FSA was also heated at 95 °C to see if the factor is heat liable. IL-33 and TSLP were measured by ELISA (Fig. 3.2). Live *S. aureus* (LiSA) and *S. epidermidis* (LiSE) were used as positive and negative control respectively.

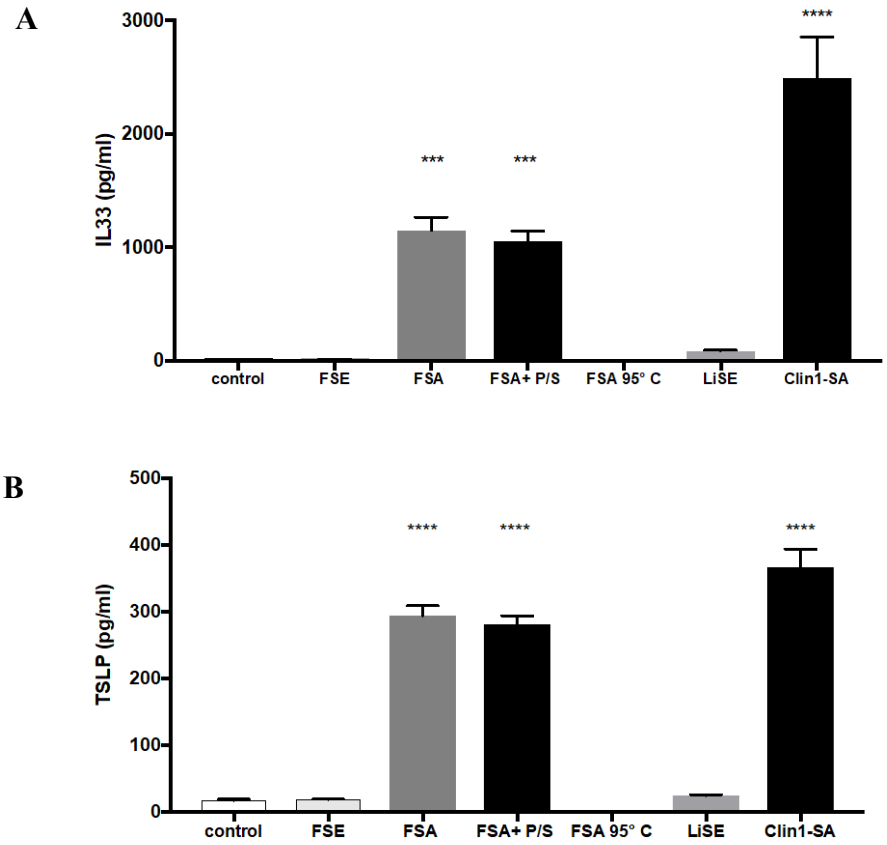


**Fig. 3.2 *S. aureus* filtered supernatant (FSA) induced release of IL-33 and TSLP from NHEK.**
Stimulation of NHEK with filtered *S. epidermidis* supernatant (FSE), filtered *S. aureus* supernatant FSA, FSA with 2% penicillin/streptomycin, FSA heated at 95 °C for 10 min, $10^7$ CFU/ml Clin1-SA and $10^7$ CFU/ml LiSE. Control is non infected NHEK. Supernatants were collected at 6h A. IL-33 and B. TSLP measured by ELISA. Data represent three independent experiments performed in triplicate. P-values were determined by one-way ANOVA with Dunnett's post hoc test. Mean ± standard error of the mean. ***P<0.0009, ****P=0.0001.

These data showed that FSA but not FSE induced release of IL-33 and TSLP from NHEK and that the factor responsible for this effect in FSA is heat liable.

## 3.4 Bioactive factor/s in filtered *S. aureus* supernatant (FSA) are ≥ 50kDa

*S. aureus* secretome (FSA) was fractionated by size exclusion centrifuge columns then by FPLC in order to purify the bioactive component/s. Summary of fractionation steps are highlighted in Fig. 3.3.

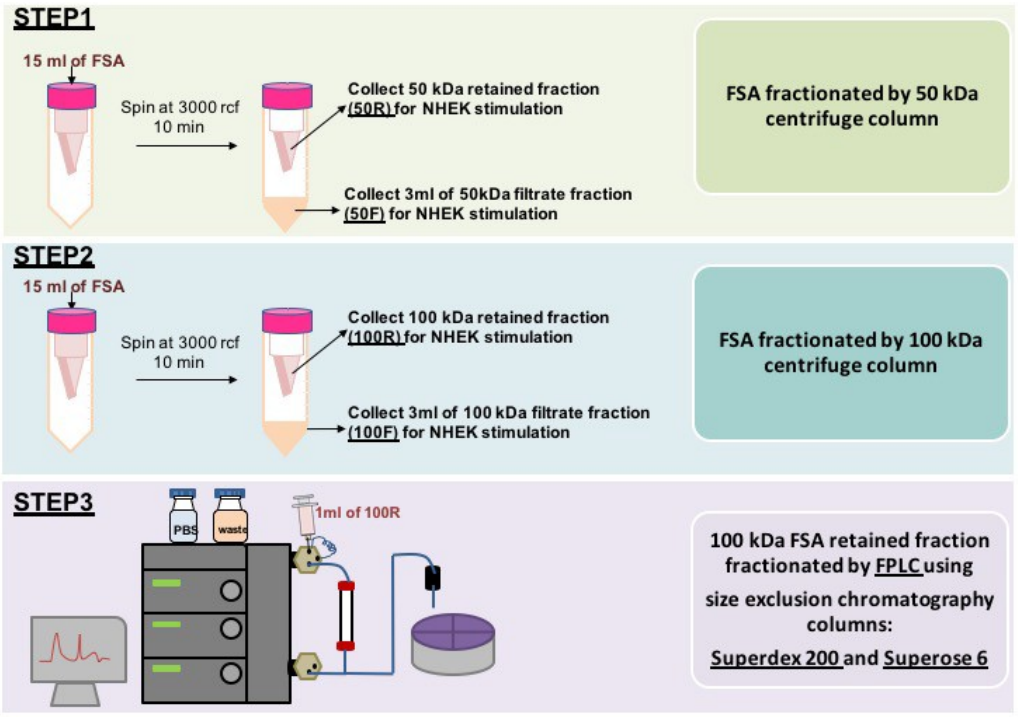


**Fig. 3.3 Summary of steps and methods used in fractionation of FSA to purify bioactive factor/s.**

First step: FSA was fractionated by 50 kDa centrifuge columns. Both retained and filtrate fractions were collected and used for NHEK 6 h stimulation. Second step was done to narrow down the range of protein sizes to help in the purification of bioactive factor/s . FSA was fractionated by 100 kDa centrifuge column and fractions were used in NHEK stimulation. Third step; larger volume of FSA used in the preperation of 100 kDa retained fraction. This was further fractionated by FPLC using Superdex 200 and Superose 6 chromatography columns.

In order to purify possible bioactive factor/s in FSA, fractionation of FSA by size was performed using Amicon-ultra 15 (Merck Millipore, Germany) with column size cut off of 50 kDa as summarised in Fig. 3.3. Retained and filtrate fractions were collected, used for NHEK 6 h stimulation and then levels of IL-33 and TSLP were measured in the supernatant by ELISA. Bioactivity of FSA was retained within the 50 kDa retention (50R) fraction (Fig. 3.4 A & B). SDS-PAGE silver stained showed two protein bands of sizes around 75 kDa and 50 kDa (Fig. 3.4 C). Therefore, a 100 kDa centrifuge column was used to narrow down the size range of proteins enabling better purification of bioactive factor/s.

Stimulation of NHEK with the 100 kDa retained and filtrate fractions shows that the bioactive factor/s were in the retained fraction (Fig. 3.5 A & B). SDS-PAGE silver stained showed that 100 kDa retained fraction contain a faint band of protein around 100 kDa and two smaller bands of sizes ≈ 75 kDa and 50 kDa similar to the bands appeared in the 50 kDa retained fraction (Fig. 3.5 C), suggesting that the bioactive factor might be part of a complex having total size of ≈ 100 kDa or greater. In other words, even though the bioactive factors did not pass through the membrane (100R fraction), they were dissociated in the reducing gel into smaller proteins' bands.

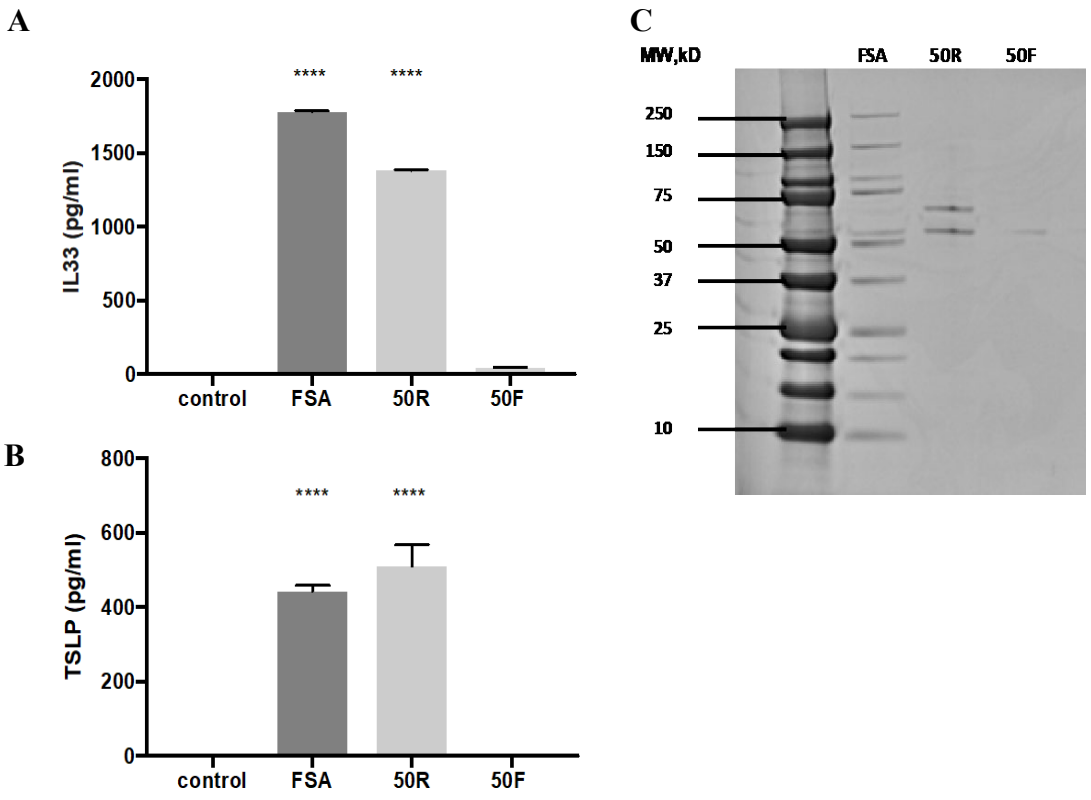


**Fig. 3.4 Bioactive factor/s in FSA ≥ 50 kDa.**
Stimulation of NHEK for 6 h with FSA fractionated by 50 kDa centrifuge column. A&B NHEK were stimulated with FSA and the 50 kDa retained fraction (50R), 50 kDa filtrate (50F), checked for activity using IL-33 and TSLP ELISA. Control is non infected NHEK. Data represent three independent experiments performed in triplicate. C. SDS-PAGE silver-stained of FSA and its fractions. All samples were diluted to 50 µg/ml and 12 µL loaded on the gel. P-values were determined by one-way ANOVA with Dunnett's post hoc test. Mean ± standard error of the mean. ****P=0.0001.

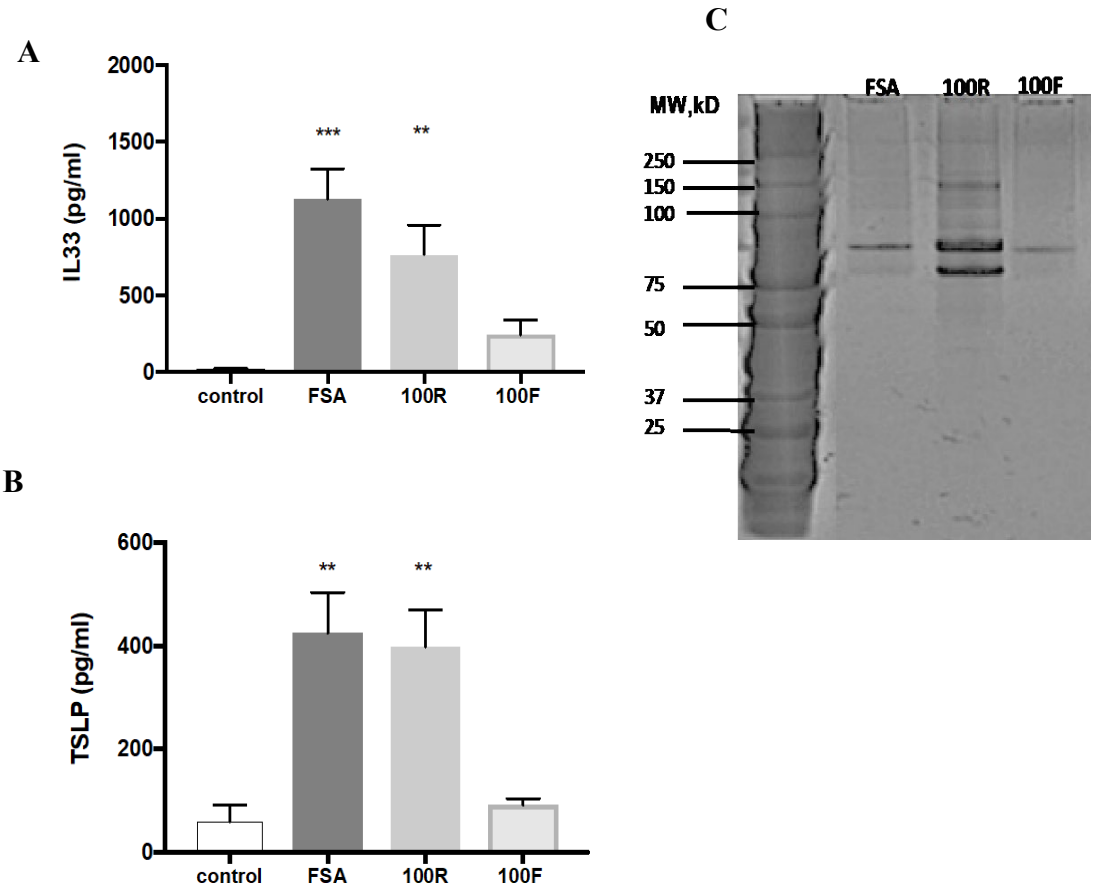


**Fig. 3.5 Bioactive factor/s in FSA were retained by the 100 kDa column.**
A&B: Stimulation of NHEK for 6h with FSA and its fractions, separated by a 100 kDa centrifugal filter. 100 kDa retained fraction (100R), 100 kDa filtrate (100F). Control is non infected NHEK. Supernatants were collected and IL-33 and TSLP measured by ELISA. C. silver-stained SDS-PAGE of FSA and its fractions. 100 kDa retained (100R), 100 kDa filtrate (100F). All samples were diluted to 50 µg/ml and 12 µL loaded on the gel. Data represent three independent experiments each performed in triplicate. P-values were determined by one-way ANOVA with Dunnett's post hoc test. Mean ± standard error of the mean. . **P= 0.0017 ***P=0.0001.

To identify the bioactive factor/s, 100 kDa retained fraction was analysed by mass spectrometry (Bio-MS core facility; https://sites.manchester.ac.uk/bioms/). Proteins (Table 3.1) were identified by comparison with known sequences in Swissprot TrEMBL database. Analysis of the identified proteins' functions according to data available in www.uniprot.org showed that around 80% were related to energy and nucleic acid metabolism (Fig. 3.6).

**Table 3.1 List of identified *S. aureus* proteins in 100 kDa retained fraction by mass spectrometry. Proteins identified against sequences in Swissprot TrEMBL database ranked by their relative abundance. Molecular weights acquired from www.uniprot.org**

| | Identified Protein | number of matched peptides | MW(Da) |
|---|---|---|---|
| 1 | Glyceraldehyde-3-phosphate dehydrogenase | 7 | 36,281 |
| 2 | Dihydrolipoyl dehydrogenase | 7 | 49,451 |
| 3 | DNA-directed RNA polymerase subunit beta | 7 | 135,409 |
| 4 | Pyruvate dehydrogenase E1 component alpha subunit | 6 | 41,383 |
| 5 | Transketolase | 6 | 72,317 |
| 6 | DNA-directed RNA polymerase subunit beta | 6 | 133,286 |
| 7 | Elongation factor Tu | 5 | 43,104 |
| 8 | Pyruvate carboxylase | 5 | 128,547 |
| 9 | 2-oxoisovalerate dehydrogenase | 4 | 35,246 |
| 10 | Immunoglobulin-binding protein Sbi | 4 | 50,070 |
| 11 | Inosine-5'-monophosphate dehydrogenase | 4 | 52,851 |
| 12 | Glycerol ester hydrolase 3B Lipase | 4 | 76,691 |
| 13 | Bifunctional autolysin | 4 | 136,868 |
| 14 | Chemotaxis inhibitory protein | 3 | 17,058 |
| 15 | 30S ribosomal protein S4 | 3 | 23,013 |
| 16 | 3-methyl-2-oxobutanoate hydroxymethyltransferase | 3 | 29,256 |
| 17 | Secretory antigen | 3 | 29,327 |
| 18 | Probable manganese-dependent inorganic pyrophosphatase | 3 | 34,069 |
| 19 | L-lactate dehydrogenase | 3 | 34,569 |
| 20 | 6-phosphogluconate dehydrogenase, decarboxylating | 3 | 51,803 |
| 21 | GMP synthase (glutamine-hydrolyzing) | 3 | 58,216 |
| 22 | Polyribonucleotide nucleotidyltransferase | 3 | 77,362 |
| 23 | Formate acetyltransferase | 3 | 84,862 |
| 24 | 50S ribosomal protein L21 | 2 | 13,135 |
| 25 | 30S ribosomal protein S13 | 2 | 13,719 |
| 26 | DNA-directed RNA polymerase subunit alpha | 2 | 35,012 |
| 27 | Alcohol dehydrogenase | 2 | 36,048 |
| 28 | 30S ribosomal protein S7 | 2 | 43,287 |
| 29 | Glucose-6-phosphate isomerase | 2 | 49,794 |
| 30 | Catalase | 2 | 58,612 |
| 31 | DNA gyrase subunit A | 2 | 99,621 |

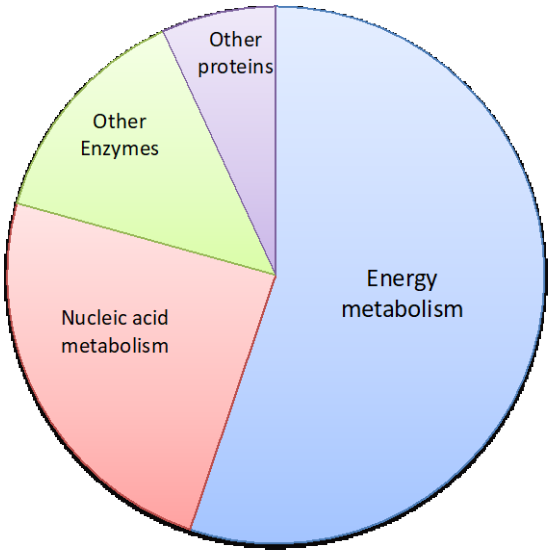


**Fig. 3.6 Majority of identified proteins in the 100 kDa retained fraction are related to energy and nucleic acid metabolism.**
Identified proteins in the 100 kDa retained fraction by mass spectrometry were divided into functional groups based on their known function. Information about proteins' functions acquired from https://www.uniprot.org.

## 3.5 Fractionation of 100 kDa retained fraction by FPLC and analysis of bioactive fractions by mass spectrometry

Because of the reasonably large number of proteins identified in the retention fraction, the bioactivity was further fractionated using Fast Protein Liquid Chromatography (FPLC). Fractions were collected, diluted in keratinocyte growth media (GM) (1:1) and used to stimulate NHEK for 6 h. Supernatant was then collected and IL-33 and TSLP was detected by ELISA. Four fractions B2 and B6-8 (indicated by stars) induced release of IL-33 and TSLP from NHEK (Fig. 3.8). Fractions B6-8 that had the highest bioactivity were pooled and protein content analysed by mass spectrometry (Table 3.2).

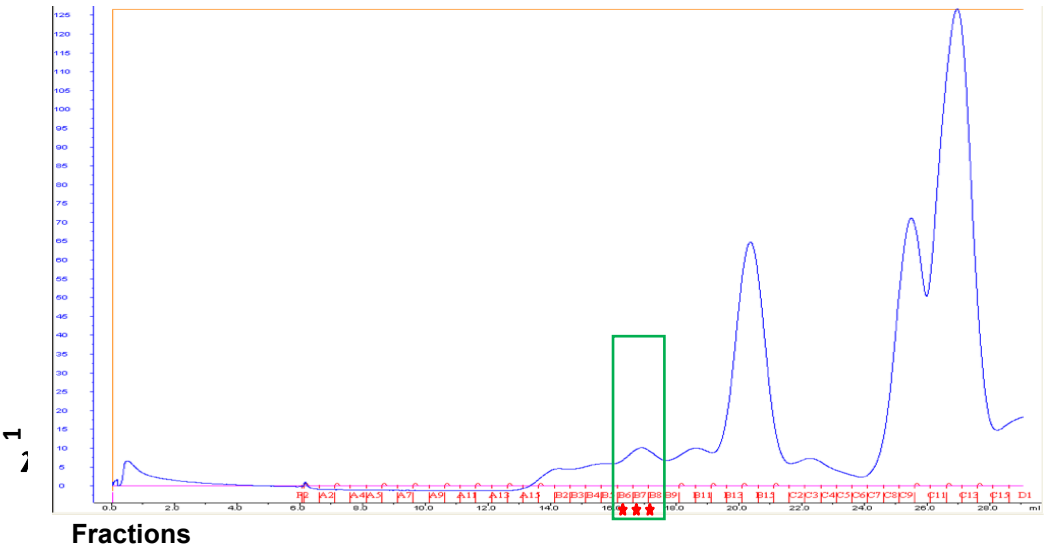


**Fig. 3.7 FPLC Superdex 200 chromatogram of 100 kDa retained fraction.**
90ml of FSA was used to prepare multiple aliquots of 100kDa retained fraction. All retained fractions were pooled for FPLC fractionation (total volume of 1ml) using a Superdex 200 column.

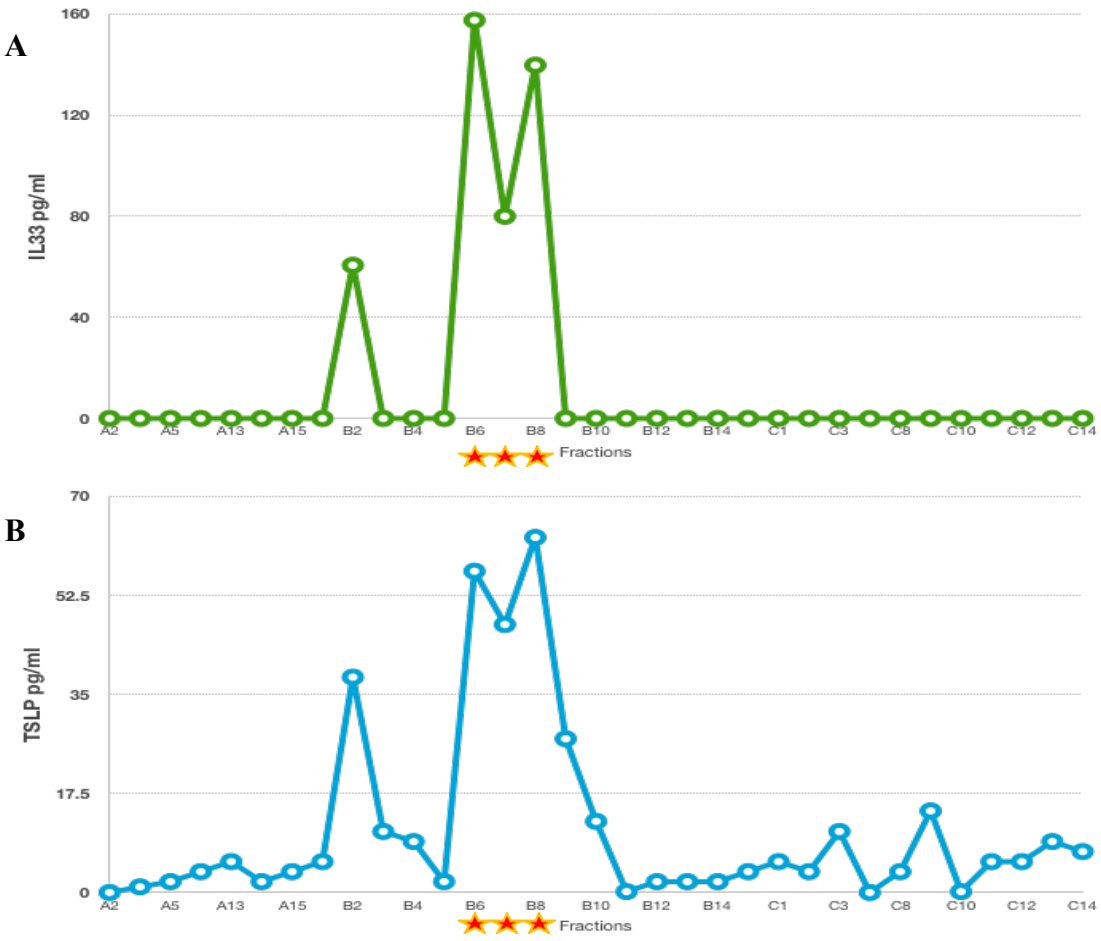


**Fig. 3.8 Bioactivity of FPLC Superdex 200 fractions.**
NHEK were stimulated with fractions from FPLC Superdex 200 fractionation A: IL-33 and B: TSLP released after 6 h stimulation measured by ELISA. Stars indicate B6-B8 fractions that had the highest bioactivity.

**Table 3.2 List of identified *Staphylococcus aureus*-derived protein in pooled bioactive fractions (B6-8) by mass spectrometry. Proteins identified against sequences in Swissprot TrEMBL database ranked by their relative abundance. Molecular weights acquired from www.uniprot.org.**

| | Identified Proteins | number of matched peptides | size Da |
|---|---|---|---|
| 1 | Enolase | 20 | 47,117 |
| 2 | Pyruvate carboxylase | 18 | 128,547 |
| 3 | DNA-directed RNA polymerase subunit beta | 16 | 135,409 |
| 4 | Phenylalanine-tRNA ligase beta subunit | 11 | 88,927 |
| 5 | ATP synthase beta chain | 10 | 54,584 |
| 6 | CTP synthase | 10 | 59,992 |
| 7 | Lipase | 9 | 76,675 |
| 8 | Polyribonucleotide nucleotidyltransferase | 9 | 77,362 |
| 9 | Pyruvate dehydrogenase E1 component beta subunit | 7 | 35,246 |
| 10 | Ornithine carbamoyltransferase | 6 | 37,534 |
| 11 | Inosine-5'-monophosphate dehydrogenase | 6 | 52,851 |
| 12 | Methionine--tRNA ligase | 6 | 74,902 |
| 13 | DNA-directed RNA polymerase subunit beta | 6 | 133,286 |
| 14 | 3-methyl-2-oxobutanoate hydroxymethyltransferase | 5 | 29,256 |
| 15 | Delta-aminolevulinic acid dehydratase | 5 | 36,583 |
| 16 | Dihydrolipoyl dehydrogenase | 5 | 54,272 |
| 17 | Leucine aminopeptidase 3, chloroplastic | 4 | 54,129 |
| 18 | Alanine dehydrogenase | 3 | 40,235 |
| 19 | Pyruvate dehydrogenase E1 component alpha subunit | 3 | 41,383 |
| 20 | Glutamate dehydrogenase | 3 | 45,760 |
| 21 | Formate acetyltransferase | 3 | 84,862 |
| 22 | 50S ribosomal protein L19 | 2 | 13,135 |
| 23 | HTH-type transcriptional regulator SarR | 2 | 13,669 |
| 24 | ATP synthase gamma chain | 2 | 32,106 |
| 25 | DNA gyrase subunit A | 2 | 99,621 |

As all bioactive fractions seemed to be eluted near the void volume (B6-8 marked on Fig. 3.7) therefore a Superose 6 column which has wider fractionation size range was used to ensure that bioactive proteins pass through the pores in the column's matrix and eluted in the elution. This allows better purification procedure of proteins in bioactive fraction. The

fractionation procedure was done with the help of Dr Charis Saville (a PDRA in our research group) and Dr Tom Jowitt from the Bio-molecular Analysis core facility, University of Manchester. In this case a larger volume (200 ml) of FSA was fractionated by 100 kDa column, and all retained fractions were pooled, then fractionated by FPLC Superose 6. The resulting FPLC chromatogram shown in (Fig. 3.9.A). Fractions were collected, mixed with GM (1:1) and used to stimulate NHEK for 6 h. Supernatant was collected and IL-33 and TSLP was detected by ELISA. Few fractions showed active release of IL-33 and TSLP (Fig. 3.9 B&C). Fraction 11(indicated by a star in Fig. 3.9) which had the highest activity was analysed by mass spectrometry and proteins were identified (Table 3.3).

**Table 3.3 List of *Staphylococcus aureus* identified proteins in bioactive fraction by mass spectrometry. Proteins identified against sequences in Swissprot TrEMBL database ranked by their relative abundance. Molecular weight acquired from www.uniprot.org.**

| | Identified Protein | number of matched peptides | MW Da |
|---|---|---|---|
| 1 | CHAP domain-containing protein | 8 | 16,915 |
| 2 | Immunoglobulin-binding protein Sbi | 8 | 50,070 |
| 3 | Dihydrolipoyl dehydrogenase | 8 | 51,112 |
| 4 | Triacylglycerol lipase | 8 | 76,418 |
| 5 | Clumping factor ClfB, fibrinogen binding protein | 7 | 97,262 |
| 6 | SpA IgG-binding domain protein | 5 | 26,011 |
| 7 | Pyruvate dehydrogenase E1 component alpha subunit | 4 | 41,383 |
| 8 | Fibrinogen-binding protein | 3 | 97,058 |
| 9 | Enolase | 2 | 47,117 |
| 10 | ATP synthase subunit beta | 2 | 51,400 |

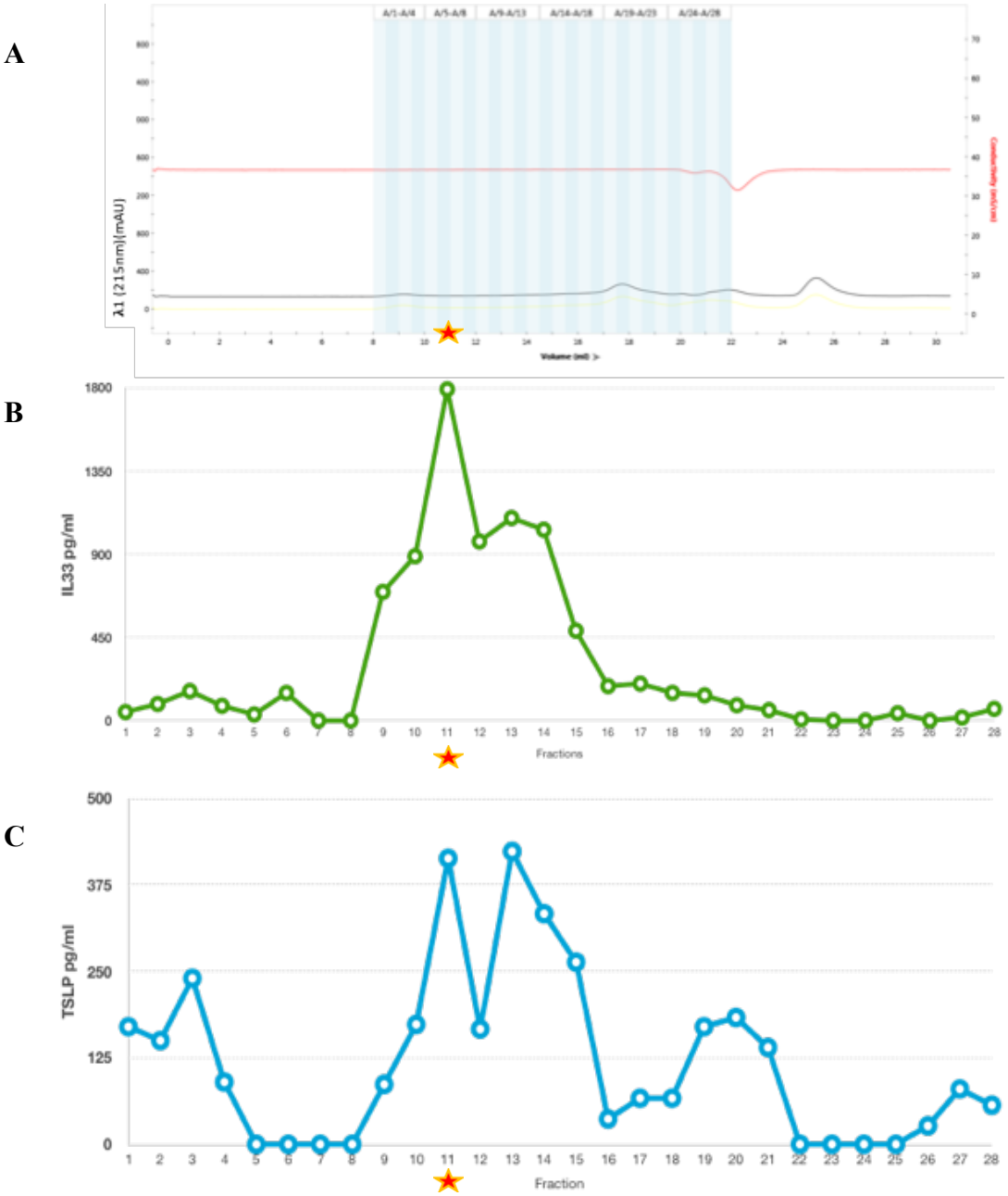


**Fig. 3.9 FPLC Superose 6 fractionation of FSA resulted in few bioactive fraction.**
200 ml of FSA was used in the preparation of a 100 kDa retained fractions which was pooled and run down the Superose 6 chromatography column. A. FPLC chromatogram. NHEK was stimulated with fractions and B. IL-33 and C. TSLP released after 6 h stimulation from NHEK measured by ELISA. The star represents fraction 11 that has the highest bioactivity

## 3.6 Four candidate proteins selected to investigate their effect on NHEK

In order to narrow down the search for candidate bioactive proteins secreted by *S. aureus,* the first step was to analyse mass spectrometry data to look for common proteins in all bioactive fractions from different separation approaches (Tables 3.1-3.3). Common proteins that were also identified in inactive fractions were excluded such as; Lipase, SpA, enolase and clumping factors. Also FnBPs were excluded as they were shown not to be essential for IL-33 and TSLP release from NHEK (Fig. 3.1). The second step was to study the proteins'

size and function. Experiments from our lab had shown that the release of IL-33 and TSLP from NHEK in response to FSA can be inhibited by protease inhibitors therefore proteins from bioactive fractions with known protease activity were considered as possible candidates. Four candidate proteins were selected to investigate their effect on NHEK (Fig. 3.10). Their molecular weight and known function summarised in Table 3.4**.**

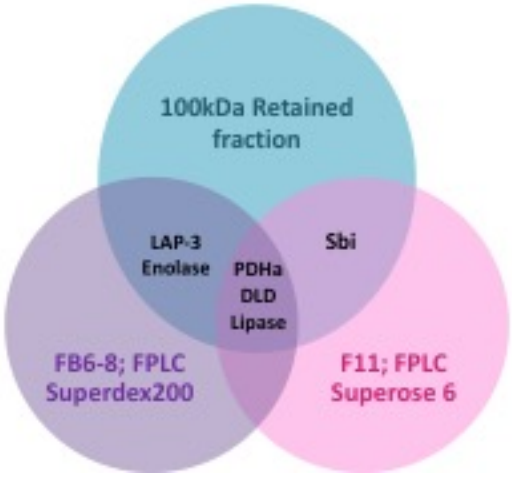


**Fig. 3.10 Summary of possible candidate proteins selected from bioactive fractions analysed by mass spectrometry.**
Analysis of common proteins in all bioactive fractions led to selection of four candidate proteins; DihydroLipoyl Dehydrogenase (DLD) and Pyruvate DeHydrogenase alpha subunit (PDHa) and lipase were identified in all bioactive fractions; Blue: 100 kDa retained fraction; Purple: fractions B6-8 obtained from FPLC Superdex 200 fractionation (F B6-8); Pink: fraction 11 from FPLC Superose 6 fractionation (F 11). *S. aureus* second IgG-binding protein (Sbi) was identified in 100 kDa retained fraction and F11 fractions. Leucine amino peptidase-3 (LAP-3) and enolase were identified in 100 kDa retained fraction and FB6-8 fractions.

**Table 3.4 List of candidate proteins selected based on analysis of common proteins identified in all bioactive fractions from different fractionation approaches. Known functions and molecular weights were obtained from www.uniprot.org.**

| Protein | Function | MW kDa |
|---|---|---|
| **Leucine aminopeptidase (LAP-3)** | **intracellular protease** | **54** |
| **Dihydrolipoyl dehydrogenase (DLD)** | **moonlight protein can function as serine protease** | **54** |
| ***S. aureus* second IgG-binding protein (Sbi)** | **immunoglobulin binding protein** | **50** |
| **Pyruvate dehydrogenase (PDHa)** | **catalyses conversion of pyruvate to acetyl-CoA + CO2** | **41** |

## 3.7 Summary

Results in this chapter show that *S. aureus* and its filtered supernatant (FSA) induced the release of IL-33 and TSLP from primary human keratinocytes after six hours stimulation. Unlike *S. epidermidis*, different clinical and lab strains of *S. aureus* induced the release of similar levels of IL-33 and TSLP. In order to isolate the bioactive factor/s, FSA was fractionated using size exclusion centrifuge columns which showed that the bioactive factor/s ≥ 50kDa. Further fractionation was done by FPLC using two size exclusion chromatography columns; Superdex 200 and Superose 6 which resulted in few fractions that induced the release of IL-33 and TSLP from NHEK. Fractionation of *S. aureus* supernatant has been a successful approach to study virulence factors in *S. aureus* secretome. It has been previously used in the identification of *S. aureus* extracellular adherence proteins (Eaps) as unique class of neutrophil serine protease inhibitors (Stapels *et al.*, 2014) that revealed another mechanisms of which this pathogen manipulate host immune system.

From collective analysis of common proteins identified by mass spectrometry of bioactive fractions obtained from different purification approaches, few candidate proteins were selected to investigate their effects on NHEK based on their size (≈ 50 kDa) and their known function either as protease or inducer of inflammatory cytokines. The bioactivity of FPLC fractions (Fig. 3.7, Fig. 3.9) imply that even if there are more than one factor involved in the bioactivity, they are similar in size as they were eluted in fractions with close proximity. Details on the rationale of candidate selection and their effect on NHEK will be discussed in chapter 4.

# Chapter 4 : Investigating the bioactivity of candidate proteins in the *S. aureus* secretome driving type-2 inflammation

## 4.1 Foreword

*S. aureus* has many cell-wall anchored and secreted factors that can modulate the host immune system either to induce inflammation or to mask the bacteria and allow immune evasion (Peetermans *et al.*, 2015; Thammavongsa *et al.*, 2015). Data from chapter 3 showed that *S. aureus* and its filtered supernatant induced the release of IL-33 and TSLP from NHEK. However, possible mechanisms cannot be determined based on published research as very little is known about the link between *S. aureus* secretome and IL-33 release from the skin. Therefore, the aim of this part of the study is to identify *S. aureus* secreted protein/s that caused the release of IL-33 and TSLP from human keratinocytes. As previous results from our laboratory had shown that IL-33 and TSLP release in response to *S. aureus* can be almost completely inhibited by serine, cysteine and metallo protease inhibitors (Alkahtani, 2016), proteases secreted by *S. aureus* are considered as possible bioactive candidates.

An interesting group of *S. aureus* Serine protease-like proteins (SplA-SplF) was recently shown to induce allergic airway inflammation in asthmatic patients (Stentzel *et al.*, 2017). SplD was then shown to induce IL-33 dependent type 2 inflammation in mouse lung (Teufelberger, et al 2018). Nevertheless, no direct interaction between the bacteria and the epithelium was shown. Therefore, SplD (25 kDa) selected as good candidate to investigate its effect on NHEK even if it was not picked by mass spectroscopy (data in Chapter 3). It is known that identification of proteins by mass spectrometry depends of their abundance in the sample. Therefore, some proteins might be missed out because of their presence in concentration lower than the threshold required for its identification. The bioactivity of potential candidate proteins identified by mass spectrometry (Table 3.4) with molecular weight around 50 kDa and either known protease activity, or a known unique virulence factor to *S. aureus* were also studied. These included:

- Staphylococcal leucine aminopeptidase 3 (LAP-3) (54 kDa) which is part of M17 metallo-peptidases. It was thought that the main substrate of this enzyme is leucine however studies have shown that it has a broad range of substrates which include Lysine, Methionine, Alanine and Arginine in addition to Leucine (Carroll *et al.*, 2013). LAP-3 is not essential in bacterial growth but is thought to have a role in *S. aureus* intracellular persistence and pathogenesis (Carroll *et al.*, 2012).
- DihydroLipoyl Dehydrogenase (DLD) (54 kDa), a moonlight protein that can act as serine protease (Huberts & van der Klei, 2010) and its complex protein partner, Pyruvate DeHydrogenase alpha subunit (PDHa) (41kDa).

- *S. aureus* Second IgG-binding protein (Sbi) is multifunctional protein that has a role in immune evasion (Atkins *et al.*, 2008; Burman *et al.*, 2008) and induction of inflammation through IL-6 trans signalling (Gonzalez *et al.*, 2015). In addition, IL-33 is known to activate mast cells, basophils and dendritic cells leading to IL-6 release (Liew *et al.*, 2010). TSLP was also shown to induce the release of IL-6 from human airway smooth muscles cells (Shan *et al.*, 2010) and mast cells (Allakhverdi *et al.*, 2007).

A flowchart (Fig. 4.1) highlights the steps taken to investigate the candidate proteins in terms of their ability to induce the release of Th2-promoting cytokines (IL-33 and TSLP) by NHEK.

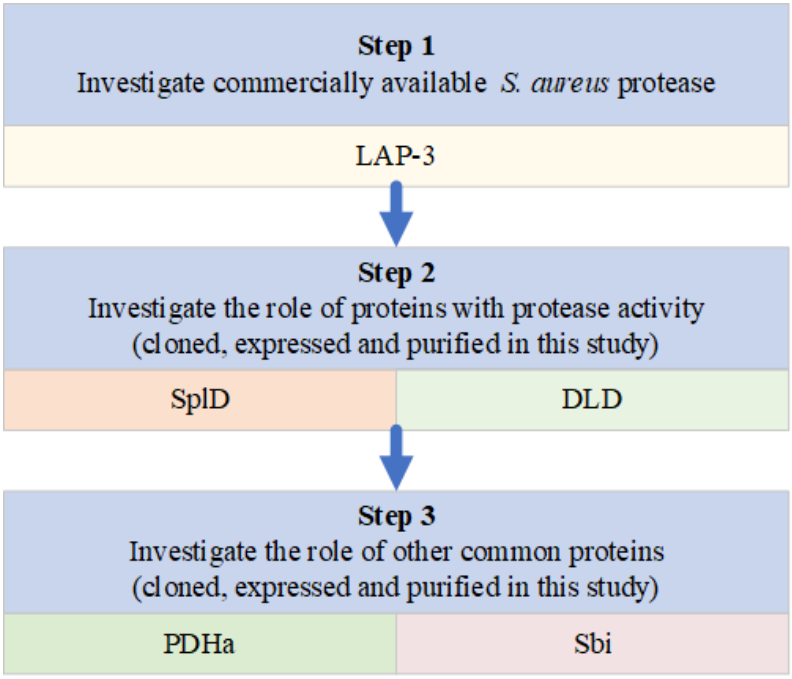


**Fig. 4.1 Steps taken to investigate the role of *S. aureus* secreted proteins in the release of Th2 promoting cytokines from NHEK.**
Leucine AminoPeptidase-3 (LAP-3), *S. aureus* Serine like protease D (SplD), DihydroLipoyl Dehydrogenase (DLD), Pyruvate DeHydrogenase alpha subunit (PDHa) and *S. aureus* Second IgG-binding protein (Sbi).

## 4.2 Stimulation of NHEK with commercially available LAP-3 does not induce IL-33 or TSLP release by NHEK

Leucine aminopeptidase 3 (LAP-3) is a metallopeptidase, known to have a role in *S. aureus* pathogenicity (Carroll et al, 2012). Five or 10 µg/ml of microsomal LAP-3 derived from porcine kidney (Sigma-Aldrich, UK) were added to NHEK pre-stimulated with $10^7$ CFU/ml LiSA. Pre-stimulation for 1 h with LiSA was to done in order to prime NHEK to allow enzymes or receptor activation. This was followed by washing and treatment with 2% penicillin/streptomycin to eliminate remaining bacteria from the cells. LAP-3 is known to require cofactors for its activation such as $Mn^{2+}$ , $Ni^{2+}$ and $Co^{2+}$ (Carroll *et al.*, 2013). Therefore LAP-3 was also added to FSA to see if it synergised with the supernatant. NHEK were stimulated with $10^7$ CFU/ml LiSA or FSA for 6 h as positive controls, and with LiSA for 1 h or growth media (GM) as a negative controls (Fig. 4.2). The results show that LAP-3 did not induce IL-33 or TSLP release from NHEK.

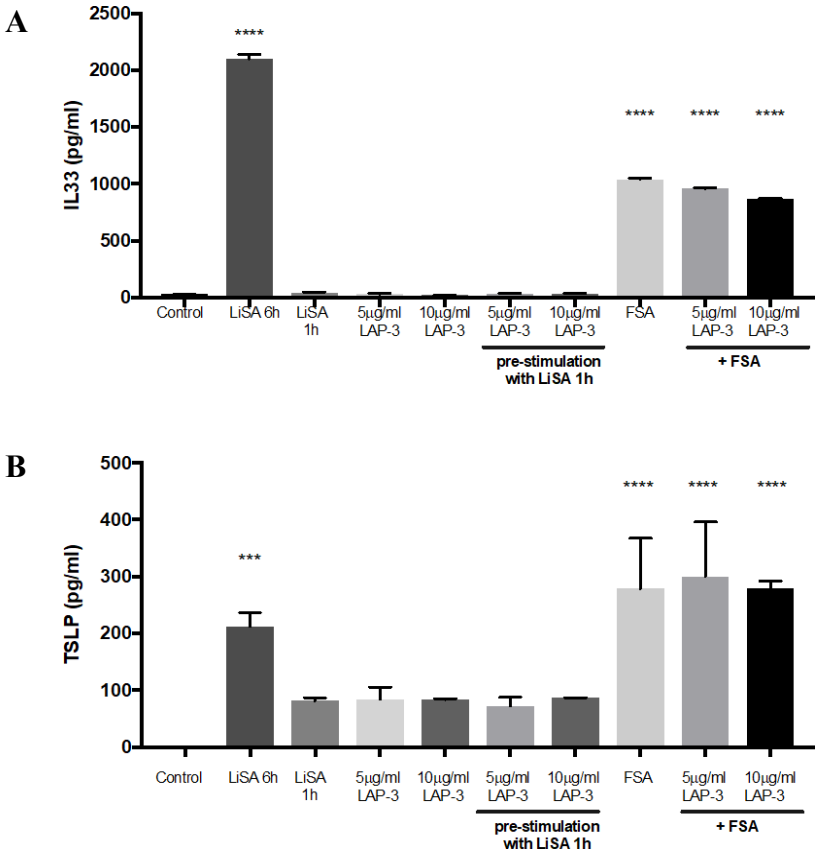


**Fig. 4.2 Leucine aminopeptidase 3 (LAP-3) did not induce IL-33 or TSLP release by NHEK.** A. IL-33, B. TSLP measured by ELISA. NHEK were stimulated with 5 or 10µg/ml of LAP3. Same concentration of LAP-3 was also added to FSA. LiSA; $10^7$ CFU/ml *S. aureus* and FSA 6 h stimulation used as positive controls. LiSA 1 h; NHEK pre-stimulated with $10^7$ CFU/ml as negative controls. Control is non infected NHEK. Supernatants were collected after 6 h. Data represent three independent experiments each performed in triplicate ± standard error of the mean. P values were determined by one way ANOVA with Dunnett's post hoc test.
***P=0.0002 **** P<0.0001.

## 4.3 Cloned *S. aureus* SplD does not induce the release of IL-33 from NHEK

*S. aureus* serine like protease protein SplD can induce IL-33 dependent type 2 inflammation in mouse lung (Teufelberger et al, 2018), although the precise mechanism hasn't been shown. We postulated that even though SplD had not been identified through our mass spectrometry studies, it could be involved in the IL-33 release by keratinocytes. The effect of SplD on NHEK was therefore investigated. SplD was not available commercially and therefore was expressed in *E. coli* to be studied.

### 4.3.1 Cloning and Expression of *SplD* and protein purification

*SplD* DNA manipulation and protein purification was done in collaboration with Professor Ian Roberts, University of Manchester as detailed in the Methods section. The procedure is summarised in Fig. 4.3.

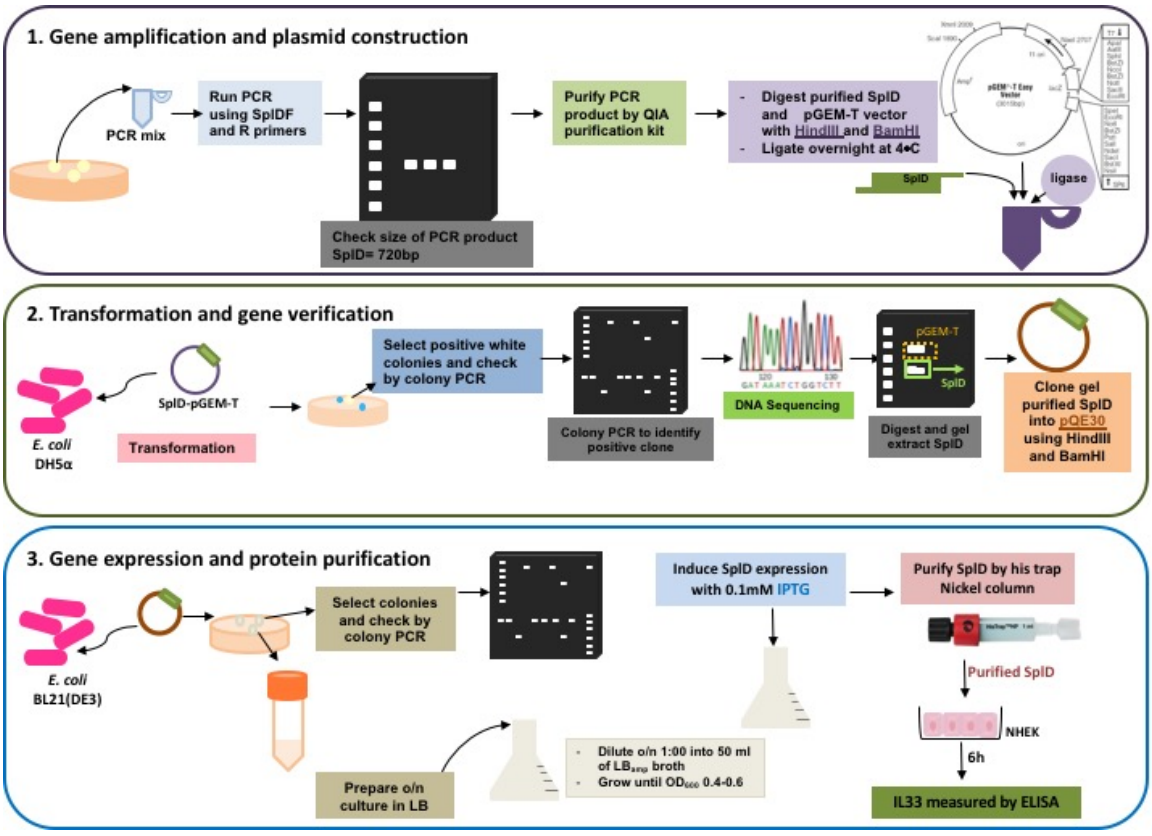


**Fig. 4.3 Summary of *SplD* cloning into pQE30 vector and subsequent protein purification.** *SplD* gene was amplified by colony PCR and cloned into pGEM-T. pGMT-T;*SplD* was transformed into *E-coli* and the gene was verified by sequencing to ensure correct insertion. The insert was then sub-cloned into expression vector pQE30. pQE30;*SplD* was transformed into *E-coli* DH5α and *SplD* was expressed by IPTG. The protein was then purified by Nickel column and then used to stimulate NHEK. IL-33 release in the supernatant after 6 h was measured by ELISA.

The *SplD* gene was amplified by colony PCR (Fig. 4.4, A), then PCR product was cleaned up by QIA quick PCR purification kit and ligated to pGEM-T easy vector system (Fig. 4.4, B). The ligation mix was then transformed into chemically competent *E. coli* cells DH5α and cultured on LB-ampicillin+X-gel agar plates. Positive white colonies were screened by PCR using M13 primers to check the presence of *SplD* fragment (720bp) (Fig. 4.4, C).

Few clones with the correct fragment size were inoculated in LB-ampicillin broth and grown overnight for plasmid extraction and verification by DNA digest by HindIII and BamHI (New England BioLabs, UK) (Fig. 4.4, D**)** and sequencing by the Genomic Technologies Core Facility, University of Manchester.

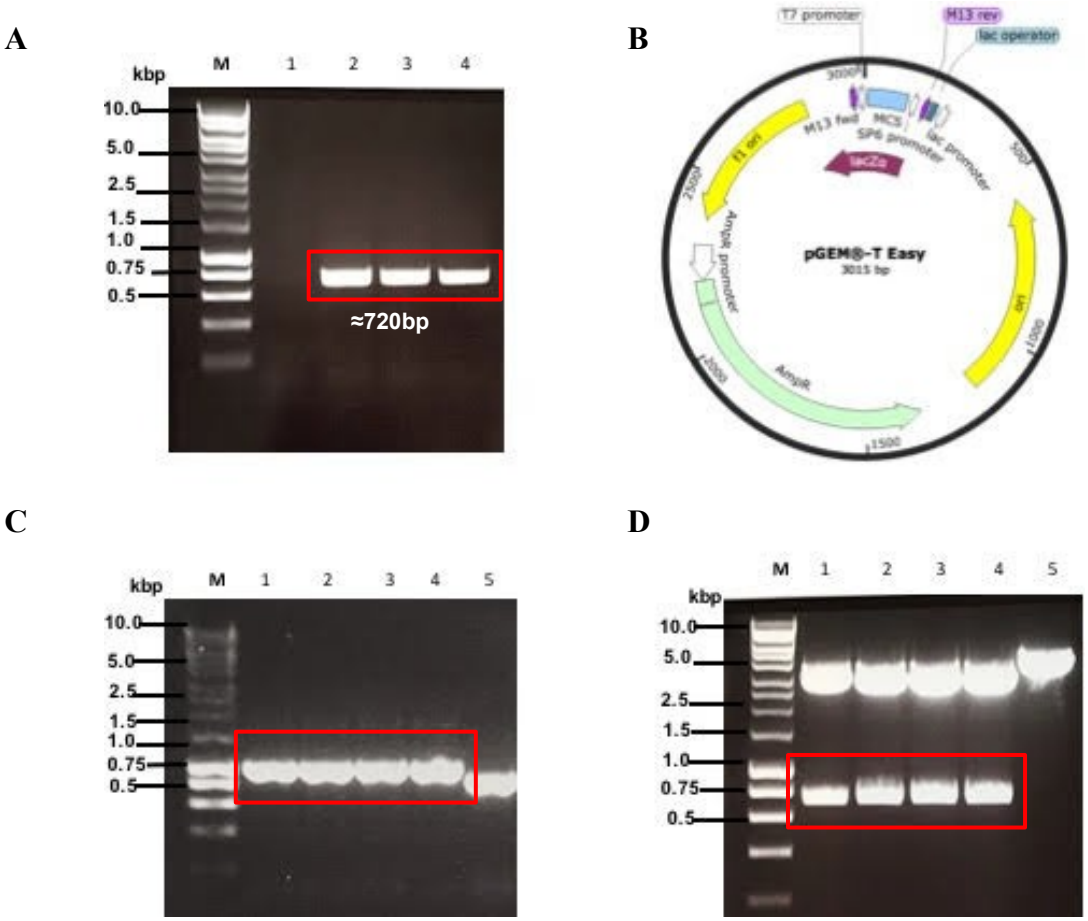


**Fig. 4.4 *SplD* cloning and verification.**
A. Colony PCR to amplify *SplD* (720bp) from Clin1-SA. B. pGEM-T map C. representative gel image of colony PCR for pGEM-T;*SplD*. D. verification of pGEM-T;*SplD* clones by DNA digest (HindIII and BamHI).Vector (pGEM-T) ≈ 3000bp (top bands) and insert (*SplD*) ≈720bp highlighted by red box.

From DNA sequences, the protein sequence was predicted by translate tool Expasy (https://web.expasy.org/translate/) and alignment of protein sequences was done by BLAST tool (https://blast.ncbi.nlm.nih.gov/) (Appendix A) to ensure no missense mutation present before the expression. A positive clone was selected for sub-cloning of the *SplD* into an expression vector pQE30 as discussed in details in the methods (2.13) . A positive clone with pQE30; *SplD* was used for protein expression which was purified by HisTrap™–HP nickel column (GE healthcare life sciences) following the manufacture instructions. The purified SplD protein was used to investigate its effect on NHEK.

### 4.3.2 SplD does not induce the release of IL-33 from NHEK

NHEK were stimulated with 5 or 10 µg/ml of the purified SplD protein for 6h and IL-33 release was measured in the supernatant by ELISA. No significant release of IL-33 from NHEK was detected in response to SplD compared to FSA stimulation (Fig. 4.5**)**

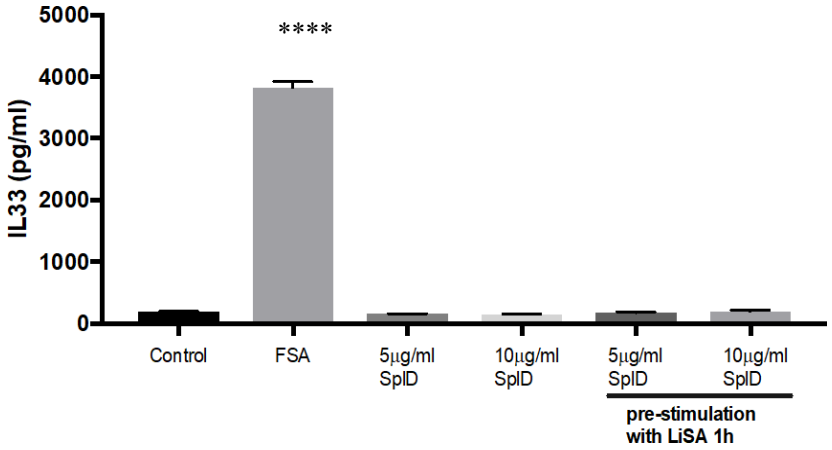


**Fig. 4.5 SplD did not induce the release of IL-33 from NHEK after 6 h stimulation.**
NHEK were stimulated with 5 or 10 µg/ml of SplD diluted in growth media. FSA was used as a positive control. NHEK were also pre-stimulated with LiSA for 1 h and cells washed with 2% penicillin/streptomycin for 30 min before adding the SplD. Supernatants were collected after 6 h and IL-33 measured by ELISA. Data represent three independent experiments each performed in triplicate. P values were determined by one-way ANOVA with Dunnett's post hoc test. Mean ± standard error of the mean. **** P<0.0001.

## 4.4 Investigating role of DLD, PDHa and Sbi in inducing release of IL-33 and TSLP from NHEK

The pyruvate dehydrogenase complex is a multi-enzyme complex that form an important link between glycolysis and tricarboxylic acid (TCA) cycle. It consists of three enzymes; pyruvate dehydrogenase E1 subunit (PDH), dihydrolipoamide acetyltransferase E2 subunit and Dihydrolipoyl dehydrogenase E3 subunit (DLD) (Gao *et al.*, 2002).

In the mass spectrometry data of bioactive fractions obtained from different fractionation procedures (Chapter 3), two enzymes of the pyruvate dehydrogenase complex; PDH alpha subunit (PDHa) and DLD were identified.

No clear evidence of PDHa protease activity or involvement in inflammation was found in the current literature. However, DLD is known as a moonlight protein that can act as serine protease at specific conditions (Babady *et al.*, 2007; Huberts & van der Klei, 2010).

Another interesting protein, the *S. aureus* second IgG binding protein (Sbi), was identified in bioactive fractions by mass spectrometry. Sbi is well known for its role in immune evasion to facilitate *S. aureus* presence in host (Atkins *et al.*, 2008; Burman *et al.*, 2008). Recently, Sbi was shown to induce inflammation through IL-6 trans signalling (Gonzalez *et al.*, 2015). Therefore, these proteins were selected to investigate their effect on NHEK after 6 h stimulation. The proteins were not available commercially so they were cloned, expressed and purified in this study.

### 4.4.1 Cloning and expression of *pdhD*, *pdhA* and *Sbi* and protein purification

*pdhD* (DLD), *pdhA* (PDHa) and *Sbi* genes were synthesised by GeneArt, Thermofisher, UK and cloned into expression vector pHis (provided kindly by Dr. Edward Mckenzie, Protein Expression Unit, Manchester Institute of Biotechnology, University of Manchester).

Expression of the genes using this vector did not work; trouble shooting is shown in details in Appendix B.

Therefore, in collaboration with Dr Hayley Bennett, Gene Editing Unit, University of Manchester, *pdhD*, *pdhA*, *Sbi* genes were sub-cloned into a pGEX plasmid as detailed in the methods (2.15). Constructed plasmid maps are shown in Appendix B.

pGEX; *pdhD* was then transformed into BL21 (DE3) competent cells (New England BioLabs, UK) and the gene was expressed at 37 °C for 3 h by 0.5 mM IPTG (Fig. 4.6). Clear protein band (≈ 70kDa), represents the DLD-GST tagged protein, appeared after induction with IPTG.

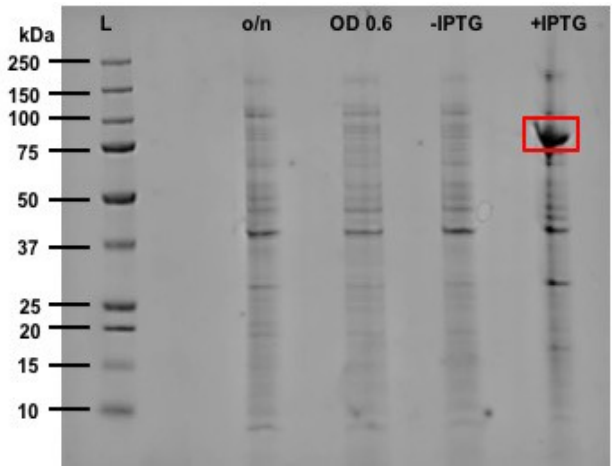


**Fig. 4.6 *pdhD* expression in BL21(DE3).**
o/n: Overnight culture of single BL21 (DE3) colony with pGEX; *pdhD*, OD0.6: diluted 1:100 and grown until OD 0.6. –IPTG: non induced culture. +IPTG: Expression of *pdhD* was induced with 0.5mM of IPTG. Red box represents the DLD- GST tagged protein. 4-12% Bis-Tris protein gradient gels was used and stained with Instant Blue Coomassie-based gel stain.

The same procedure was used to express *pdhA* and *Sbi* in BL21(DE3) competent cells (New England BioLabs, UK) (data not shown).Then DLD, PDHa and Sbi proteins were purified from the cell pellet by Glutathione Sepharose 4B beads (GE healthcare life sciences, USA) as mentioned in details in the methods (2.16) (Fig. 4.7**,** Fig. 4.8**,** Fig. 4.9**)**

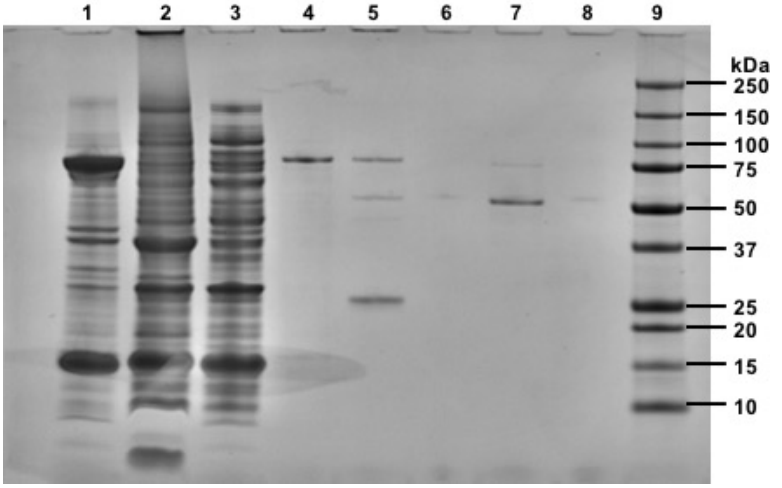


**Fig. 4.7 DLD purification from BL21(DE3) cell pellet.**
Lanes are as follows: 1) insoluble fraction which is the cell pellet after lysis diluted in 1ml wash buffer; 2) soluble fraction is the lysate; 3) flow through from first step of washing; 4) GST beads before elution which contain the DLD protein bound to the GST tag and attached to the beads; 5) beads after elution once the DLD was released by PreScission™ protease from the beads; 6) empty well; 7) purified DLD protein (54kDa) 8) empty well; 9) precision plus all blue pre-stained protein ladder. 4-12% Bis-Tris protein gradient gels was used and stained with Instant Blue Coomassie-based gel stain.

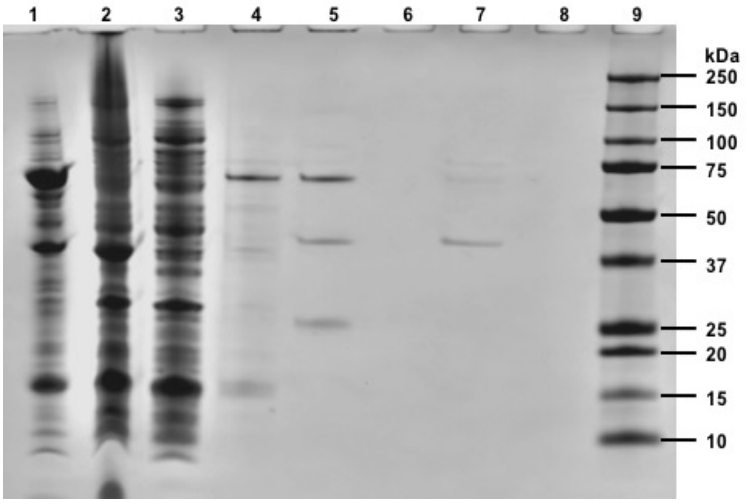


**Fig. 4.8 PDHa purification from BL21(DE3) cell pellet.**
Lanes as follows: 1) cell pellet 1ml wash buffer; 2) soluble fraction is the lysate; 3) flow through from first step of washing; 4) GST beads before elution which contain the PDHa-GST tagged protein and attached to the beads; 5) beads after elution once the PDHa is released by PreScission™ protease from the beads; 6) empty well; 7) purified PDHa protein (48kDa); 8) empty well; 9) precision plus all blue pre-stained protein ladder. 4-12% Bis-Tris protein gradient gels was used and stained with Instant Blue Coomassie-based gel stain.

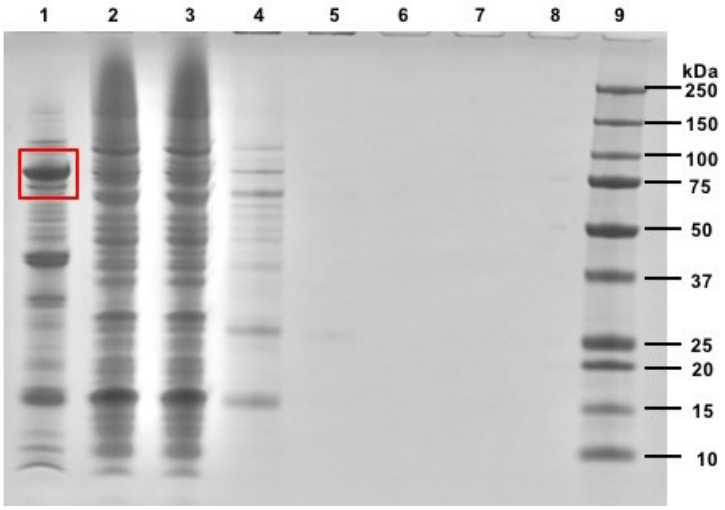


**Fig. 4.9 Sbi purification from BL21(DE3) cell pellet.**
Lanes as follows: 1) insoluble fraction which is the cell pellet after lysis diluted in 1 ml wash buffer; 2) soluble fraction is the lysate; 3) flow through from first step of washing; 4) GST beads before elution which contain the Sbi-GST tagged protein and attached to the beads; 5) beads after elution once the Sbi is released by PreScission™ protease from the beads; 6) empty well; 7) purified Sbi protein ; 8) empty well; 9) precision plus all blue pre-stained protein ladder.4 - 12% Bis-Tris protein gradient gels was used and stained with Instant Blue Coomassie-based gel stain.

Sbi protein could not be purified from the BL21(DE3) cell pellet, because of its poor solubility, as the protein was present in the insoluble fraction only (red box around 70 kDa in Fig. 4.9).

Expression of *Sbi* was therefore performed at a lower temperature using Arctic express cells (Agilent Technologies, USA) which allows better folding of the expressed protein and enhances its solubility. pGEX; *Sbi* was transformed into Arctic Express *E-coli* following manufacture protocol. 24 h protein expression was induced with 0.5 mM IPTG at 12 °C. The protein was then purified using Sepharose 4B beads (GE healthcare life sciences, USA) (Fig. 4.10) as described in the methods (2.16). The bands around 70 kDa (lanes 1-7 in Fig. 4.10) represent the Sbi- GST tagged protein. After elution, the band of purified Sbi on the gel was not clear which is more likely due to its low concentration and small volume loaded (5 µl). However, since the insert (Sbi) sequence was verified before expression and the expressed protein resembled the expected Sbi protein size, the purified Sbi sample concentration was measured by Nanodop™ (ThermoFisher Scientific) and was used to investigate it effect on NHEK.

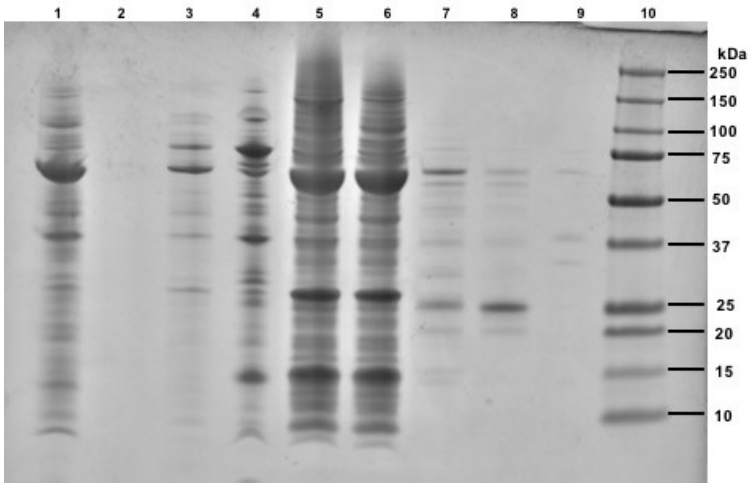


**Fig. 4.10 Sbi expression and purification in Arctic express cell pellet.**
Lanes as follows: 1) overnight culture of single Arctic cell express colony with pGEX;*Sbi* 2) non induced cell culture of (1) diluted 1:100 and grown until OD 0.6; 3) then expression of *Sbi* was induced with 0.5 mM of IPTG; 4) insoluble fraction which is the cell pellet after lysis diluted in 1ml wash buffer; 5) soluble fraction is the lysate; 6) flow through from first step of washing; 7) GST beads before elution which contain the Sbi-GST tagged protein and attached to the beads; 8) beads after elution once the Sbi is released by PreScission™ protease from the beads; 9) purified Sbi protein (50 kDa) not clear due to low concentration; 10) precision plus all blue pre-stained protein ladder. 4 -12% Bis-Tris protein gradient gels was used and stained with Instant Blue Coomassie-based gel stain.

All purified proteins were then tested for their effect on NHEK as summarised in the flowchart below (Fig. 4.11)

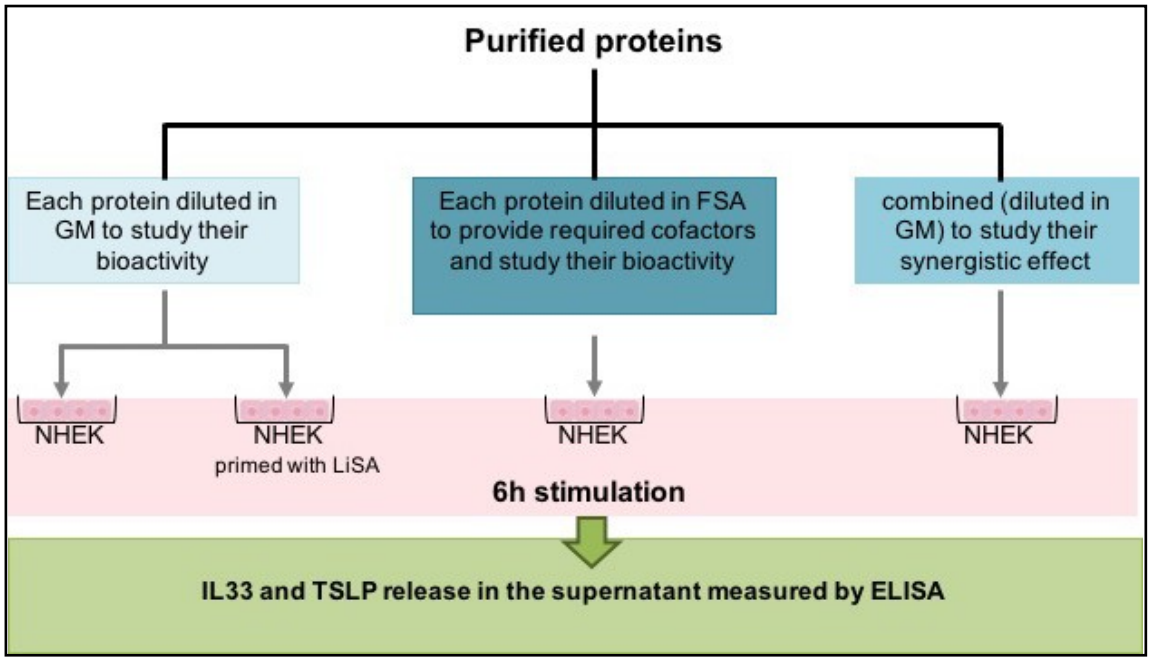


**Fig. 4.11 Summary of experimental design to evaluate the effect of purified protein candidates (DLD, PDHa and Sbi) on NHEK**

### 4.4.2 DLD and PDHa did not induce the release of IL-33 or TSLP from NHEK

Five or 10 µg/ml of DLD and PDHa were each used for 6 h stimulation of NHEK alongside NHEK pre-stimulated with $10^7$ CFU/ml LiSA for 1 h. Stimulation with LiSA $10^7$ CFU/ml for 6 h was used as positive control. No IL-33 or TSLP were released in response to DLD stimulation or PDHa (Fig. 4.12, Fig. 4.13). In order to investigate if DLD or PDHa needed co-factors in FSA to induce IL-33 and TSLP, proteins were diluted into 5 or 10 µg/ ml in FSA. No increase in IL-33 or TSLP release was detected (Fig. 4.12, Fig.4.13).

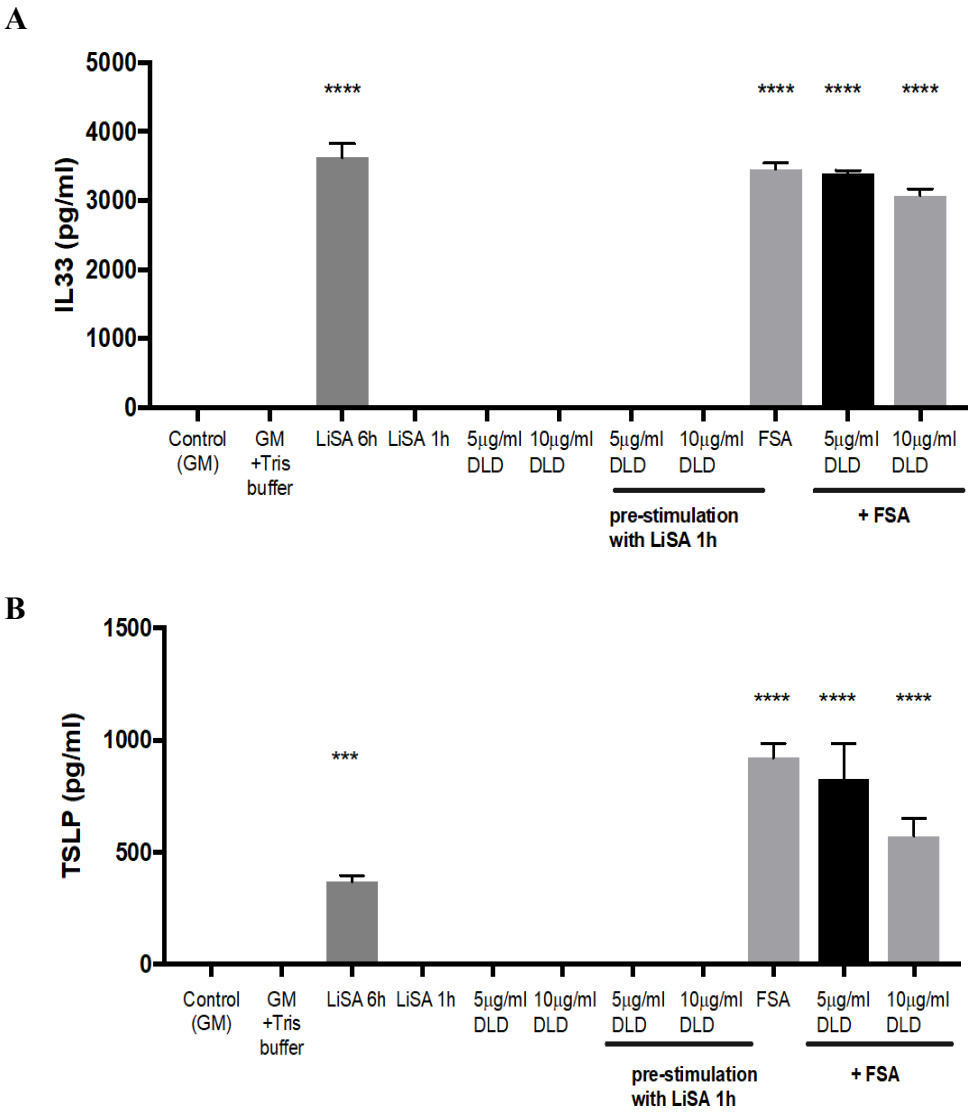


**Fig. 4.12 DLD did not induce the release of IL-33 or TSLP by NHEK.**
A. IL-33 and B. TSLP measured by ELISA. NHEK were stimulated with growth media (GM) as negative control; GM+ Tris buffer used during process of protein purification; $10^7$ CFU/ml (LiSA) 6 h as positive control; LiSA 1 h refer to NHEK stimulated with LiSA for 1 h washed and treated with 2% penicillin/streptomycin then incubated in GM for 6 h; 5 or 10µg/ml of DLD diluted in GM. Same concentrations of DLD used to stimulate NHEK that was pre-stimulated with LiSA. NHEK was also stimulated with FSA as positive control, 5 and 10 µg/ml of DLD diluted in FSA. Supernatants were collected after 6 h. Data represent three independent experiments each performed in triplicate. P values were determined by one-way ANOVA with Dunnett's post hoc test. Mean ± standard error of the mean. 4-12% Bis-Tris protein gradient gels was used and stained with Instant Blue Coomassie-based gel stain. ***P=0.0009 **** P<0.0001.

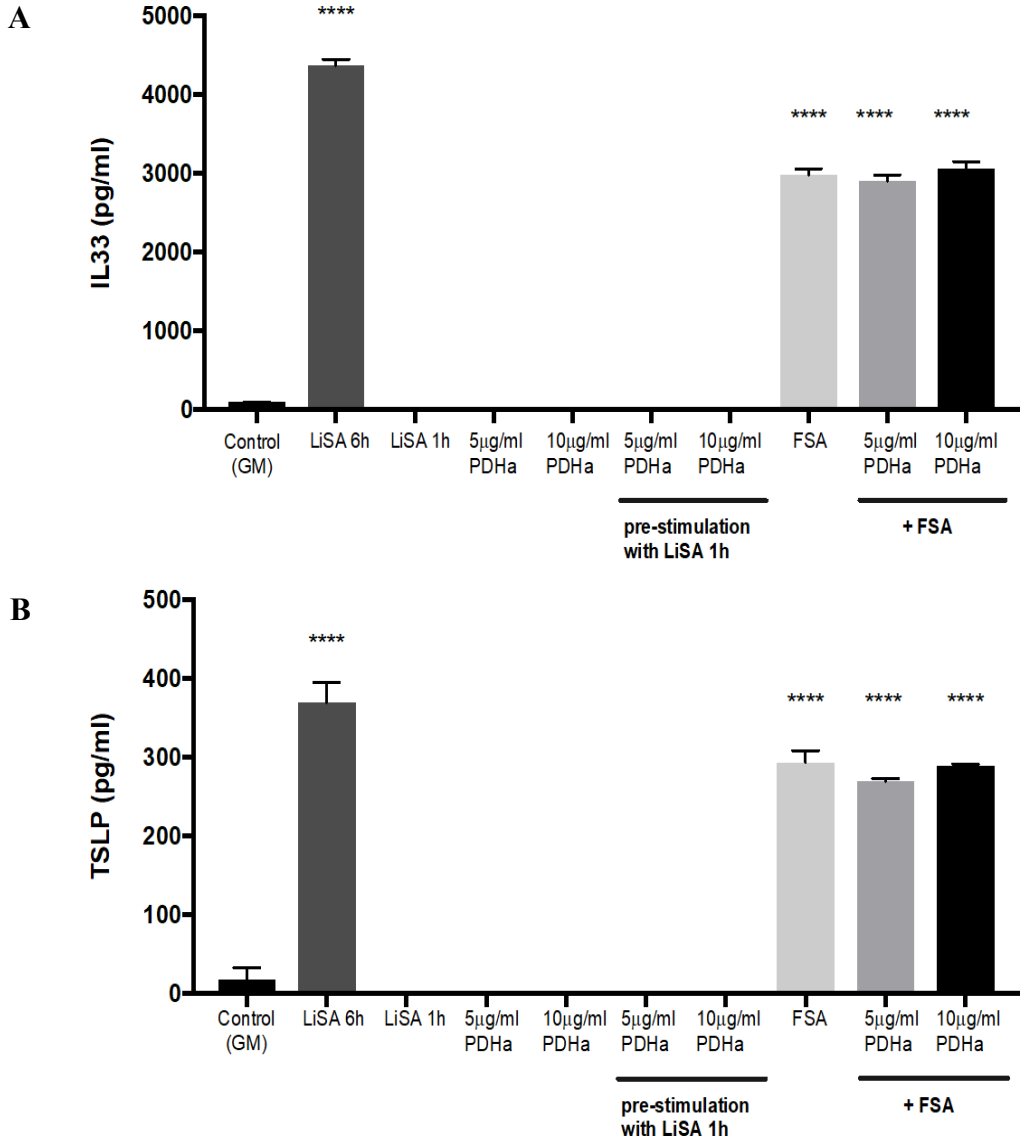


**Fig. 4.13 PDHa did not induce the release of IL-33 or TSLP by NHEK.**
A. IL-33 and B. TSLP measured by ELISA. NHEK were stimulated with growth media (GM) as negative control; $10^7$ CFU/ml (LiSA) 6 h as positive control; LiSA 1h refer to NHEK stimulated with LiSA for 1h washed and treated with 2% penicillin/streptomycin then incubated in GM for 6h; 5 or 10 µg/ml of PDHa diluted in GM. Same concentrations of PDHa used to stimulate NHEK that was pre-stimulated with LiSA. NHEK was also stimulated with FSA as positive control, 5 or 10 µg/ml of PDHa diluted in FSA. Supernatants were collected after 6 h. Data represent three independent experiments each performed in triplicate. P values were determined by one-way ANOVA with Dunnett's post hoc test. Mean ± standard error of the mean. 4-12% Bis-Tris protein gradient gels was used and stained with Instant Blue Coomassie-based gel stain. **** P<0.0001.

### 4.4.3 Sbi induced IL-33 and TSLP release by NHEK

NHEK and pre-stimulated NHEK were stimulated for 6 h with Sbi (5,10 or 20 µg/ml). Sbi was also added to FSA to study its ability to synergise with FSA to release IL-33 and TSLP. Both 10 and 20 µg/ml of Sbi induced significant release of IL-33 (≈276 pg/ml) from NHEK but the TSLP levels released were not significant (Fig. 4.14). No significant increase in IL-33 or TSLP release by FSA was seen after addition of Sbi (Fig. 4.14)

### 4.4.4 Addition of DLD and PDHa to Sbi did not enhance its bioactivity

Since both PDHa and DLD are part of pyruvate dehydrogenase complex (PDHC) which converts pyruvate into acetyl-CoA, these two enzymes were added together to evaluate their effect on NHEK. No IL-33 or TSLP were release in response to combination of DLD and PDHa, and these two enzymes were not able to enhance the bioactivity of Sbi. Investigating the effect of the proteins together was done because of the fact that the bioactivity of FSA was retained in the 100 kDa column (3.4). This suggested that the bioactive factor/s might be part of a complex. From FPLC fractionation the bioactivity appeared in fractions in close proximity suggesting similar sizes of the proteins. As PDHa, DLD and Sbi were identified in the bioactive fractions it was important to check if there any synergetic effect of these proteins on NHEK.

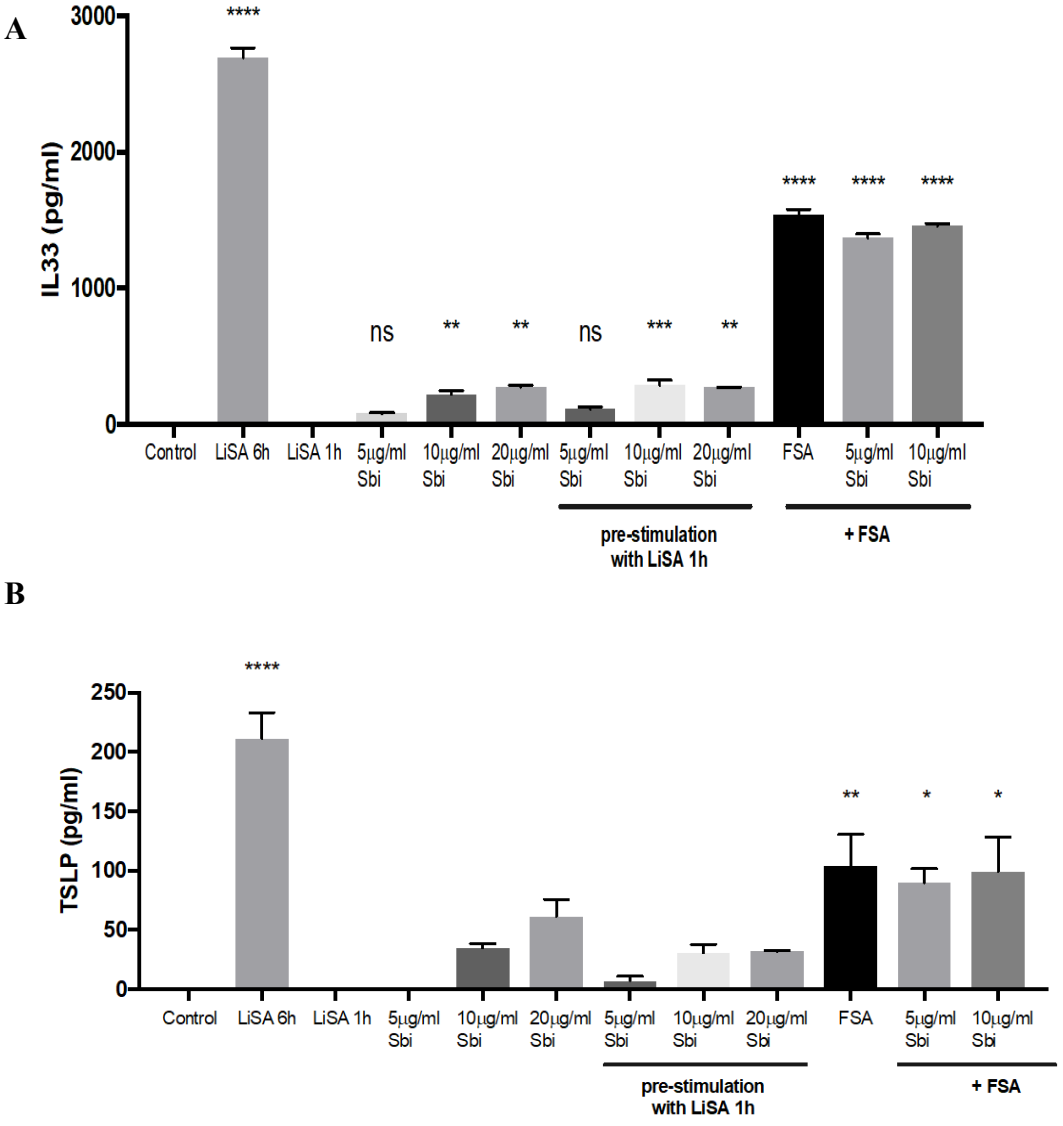


**Fig. 4.14 Sbi induced release of IL-33 and TSLP from NHEK.**
NHEK were stimulated with GM growth media as negative control; $10^7$ CFU/ml (LiSA) 6h as positive control; LiSA 1h refer to pre-stimulated NHEK for 1 h with LiSA washed and treated with 2% penicillin/streptomycin then incubated in GM for 6 h; 5, 10 or 20 µg/ml of Sbi diluted in GM; same concentrations of Sbi used to stimulate NHEK that was pre-stimulated with LiSA. NHEK were also stimulated with FSA as positive control, 5 or 10 µg/ml of Sbi diluted in FSA. Supernatants were collected after 6 h. A. IL-33 and B. TSLP measured by ELISA. Data represent three independent experiments each performed in triplicate. P values were determined by one-way ANOVA with Dunnett's post hoc test. Mean ± standard error of the mean. *P < 0.028, **P <0.006, ***P< 0.0009 ****P<0.0001.

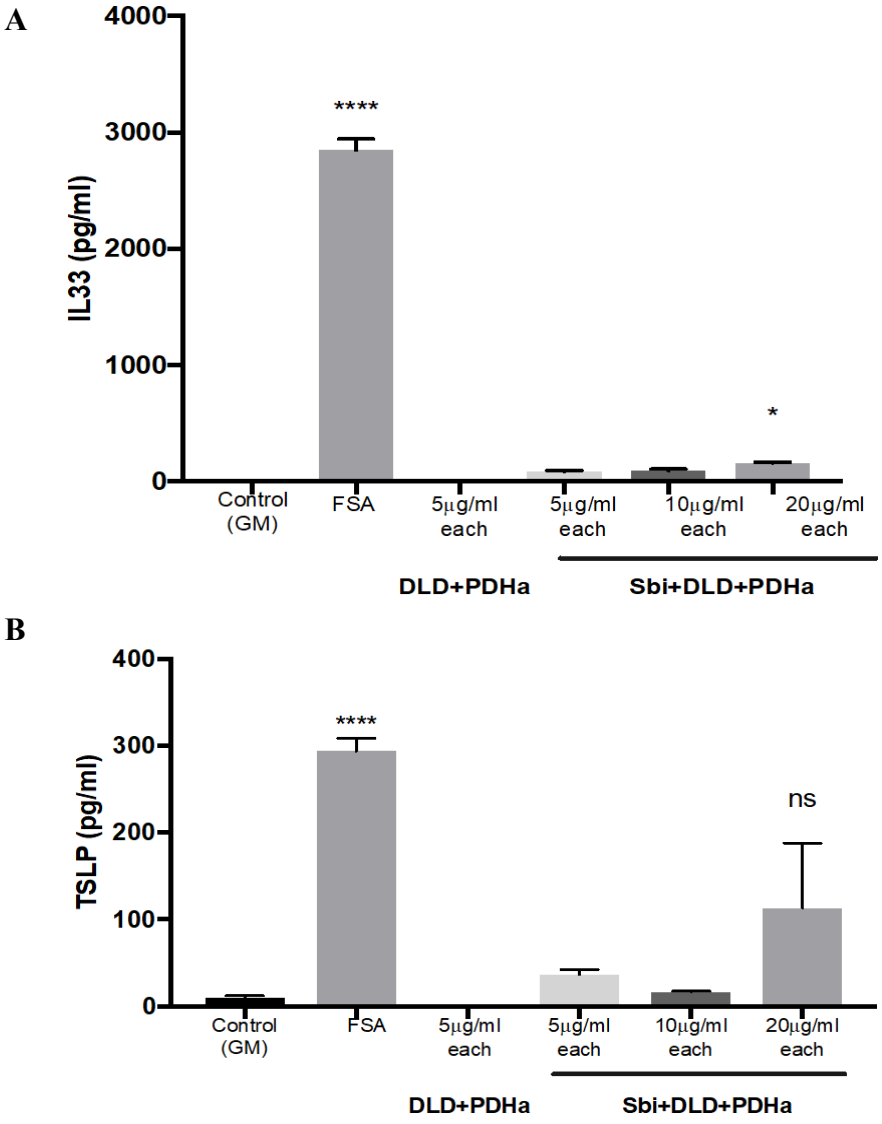


**Fig. 4.15 Addition of DLD and PDHa to Sbi did not enhance its bioactivity.**
A. IL-33 and B. TSLP measured by ELISA. NHEK were stimulated with growth media (GM) as negative control; FSA 6 h as positive control; combination of 5 µg/ml of DLD and PDHa. DLD and PDHa were also combined with Sbi at 5, 10 or 20µg/ml. Supernatants were collected after 6h. Data represent three independent experiments each performed in triplicate. P-values were determined by one-way ANOVA with Dunnett's post hoc test. Mean ± standard error of the mean. *P <0.04, ****P<0.0001.

## 4.5 Summary

Although previous laboratory results suggested that IL-33 and TSLP release in response to *S. aureus* can be inhibited by protease inhibitors (Alkahtani, 2016), results from this chapter demonstrate that *S. aureus* secreted proteases; Leucine aminopeptidase 3 (LAP-3) and Serine-like protease D (SplD) are not involved in the release of Th2-promoting cytokines (IL-33 and TSLP) by NHEK. Moreover, known *S. aureus* protease V8 (36 kDa) was also previously shown not essential for the release of IL-33 and TSLP from mouse fibroblast and human adult keratinocytes (Alkahtani, 2016).

Furthermore, Dihydrolipoyl dehydrogenase (DLD), which can act as serine protease (Huberts & van der Klei, 2010), did not induce any release of these cytokines either. Interestingly, 10 and 20 µg/ml of the *S. aureus* second IgG-binding protein Sbi was able to induce significant release of IL-33 by NHEK. There is no known association between Sbi and IL-33 induction. However, it has been recently shown that Sbi can induce IL-6 dependent inflammatory responses (Gonzalez *et al.*, 2015).

# Chapter 5 *: Staphylococcus aureus* internalised by skin keratinocytes evade antibiotic killing

## 5.1 Foreword

*S. aureus* colonises the skin of patients with atopic dermatitis (AD) and is one of the most common triggers for eczema flares (Kobayashi *et al.*, 2015;Tauber *et al.*, 2016). Many patients suffer from recurrent infections, reported to be as high as 39 - 51% within 3 to 6 months of initial infection (Miller *et al.*, 2015). The main cause of recurrence is thought to be cross infection from family members, healthcare providers and fomites (Montgomery *et al.*, 2015). Moreover, it has been found that most patients with recurrent infections are caused by the same strain of *S. aureus* (Byrd *et al.*, 2017).

As *S. aureus* is known to be internalised by epidermal keratinocytes (Mempel *et al.*, 2002; Kintarak *et al.*, 2004; Bur *et al.*, 2013), we hypothesised that internalised *S. aureus* may evade host immunity and killing by anti-staphylococcal antibiotics. In this chapter, *S. aureus* internalisation into NHEK is studied by flow cytometry, Amnis® and confocal microscopy. Potential cytotoxicity after internalisation was then assessed by flow cytometry and IL-33 release. Finally, the antimicrobial activity of five anti-staphylococcal antibiotics routinelyused in clinical practice to treat methicillin-sensitive *S. aureus* infections and their ability to kill *S. aureus* that had been internalised into human keratinocytes were examined. This part of the study has now been published in the open-access peer-reviewed journal *Frontiers in Microbiology* (Al Kindi *et al.*, 2019).

## 5.2 *S. aureus* but not *S. epidermidis* are internalised by Human Skin Keratinocytes (NHEK)

The ability of *S. aureus* to be internalised by NHEK was assessed by FiTC labeled and GFP-expressing *S. aureus* using flow cytometry, Amnis® and confocal microscopy. For flow cytometry analysis, NHEK was co-cultured with $10^7$ CFU bacteria for 1 h followed by 1 h treatment with 2% penicillin/streptomycin to eliminate extracellular bacteria. Cells were then either analysed by flow cytometry immediately or after 24 h incubation at 37 ˚C. To overcome autofluorescent false positive cells we used the gating strategy described in detail in the methods (2.17.2) to exclude FiTC and PerCp-Cy5 double positives of non-infected keratinocytes. Flow plots showed that FITC-labelled Clin1-SA ($^{FiTC}$LiSA) but not FITC- *S. epidermidis* ($^{FiTC}$LiSE) co-localised with NHEK (Fig. 5.1).

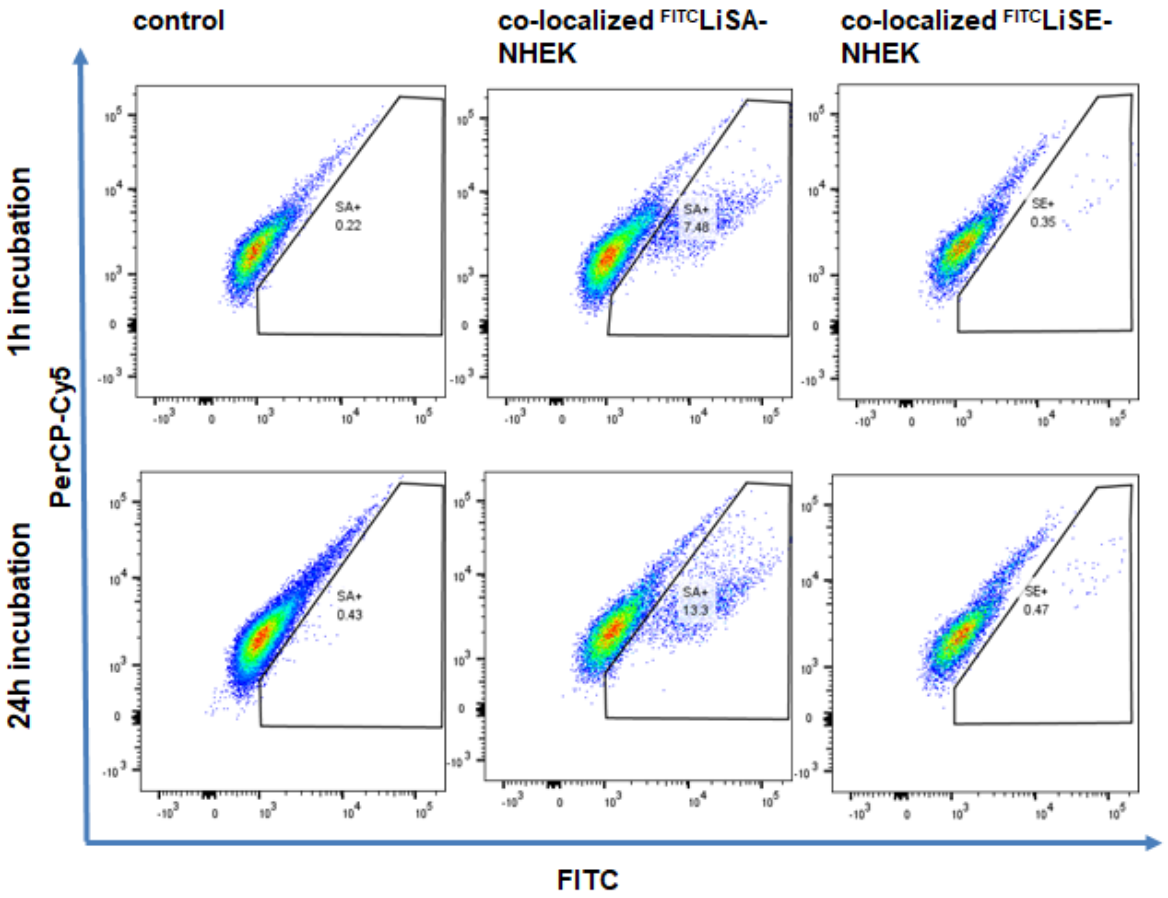


**Fig. 5.1 Live *S. aureus* but not live *S. epidermidis* is internalised into NHEK.**

NHEK were co-cultured with FITC-labeled live *S. aureus* (Clin1-SA) ( $^{FITC}$LiSA) or live *S. epidermidis* ($^{FITC}$LiSE) at 37 ˚C for 1 h, followed by washing with 2% penicillin/streptomycin to kill extracellular bacteria. Cells were either analysed directly (1 h incubation) or cultured for a further 24 h and co-localisation determined by flow cytometry. Autofluorescence is shown on PerCp-Cy5/FITC double positive population. Controls represent NHEK without bacterial co-culture. Flow cytometry scatter plots are representative of three independent experiments with technical triplicates .

To confirm co-localisation, Amnis® imaging and confocal microscopy were used, analysing GFP-expressing *S. aureus* (Lab2-SA-GFP ) co-localisation with NHEK (Fig. 5.2 A,B).

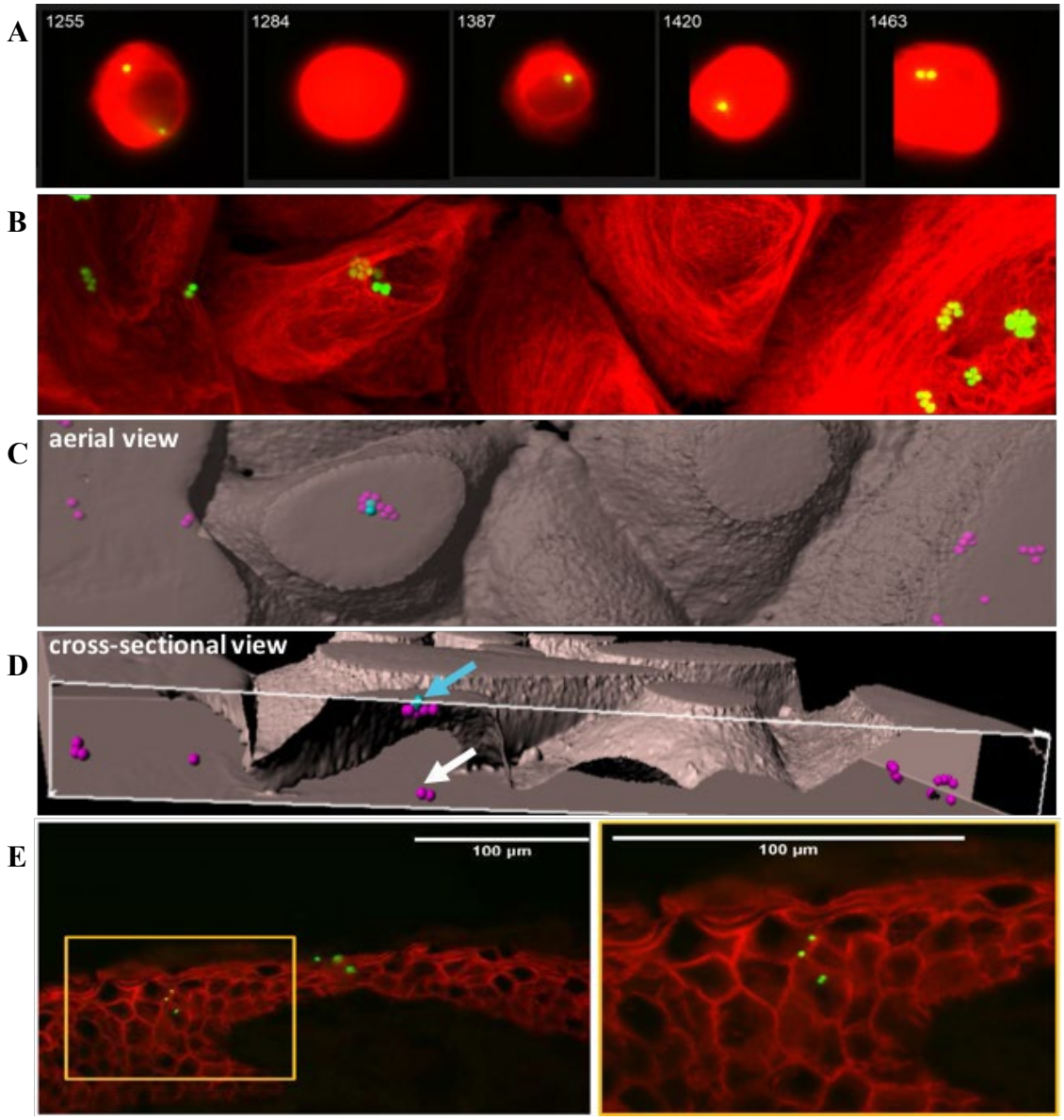


**Fig. 5.2 Internalisation of $^{GFP}$*S. aureus* by NHEK.**
A. Representative Amnis® Image of NHEK co-cultured with $10^7$ CFU/ml Lab2-SA-GFP for 1 h at 37°C, then treated for 30 min with 2% penicillin/streptomycin to eliminate extracellular bacteria and cultured for a further 4 h prior to staining and analysis. Red stain: Alexa Fluor® 647 mouse anti-human cytokeratin 14/15/16/19. Green stain: Lab2-SA-GFP. B. Representative confocal 2D image of NHEK after co-culture with $10^7$ CFU/ml Lab2-SA-GFP for 1 h at 37°C. 3D representative. C. aerial and D. cross-sectional views of extracellular (blue spots) and intracellular (pink spots) *S. aureus*. E. Representative immunofluorescent staining of healthy human skin explant after 3h infection with Lab2-SA-GFP ($10^7$ CFU/ml) at 37°C. Red: anti-rabbit claudin-1 antibody. Green: Lab2-SA-GFP. Yellow box (left panel) highlights area magnified in right hand panel. All data are representative of three independent experiments. Images in E taken at 40X magnification. Scale bars represents100 µm.

Amnis® results confirms co-localisation of *S. aureus* with NHEK. Most of the cells images showed the co-localisation of one or two *S. aureus* with each cell. 3D-analysis of confocal images showed the presence of intracellular Lab2-SA-GFP (Fig. 5.2 C,D and the supplementary video in the published journal paper (link in Appendix C)). Some Lab2-SA-GFP can be seen across the cell membrane in their way to get inside the cell. Using *ex-vivo* human skin explants, we confirmed that Lab2-SA-GFP can be found deep within the epidermis after 3 h incubation (Fig. 5.2 E) but their presence within the cells could not be concluded from these 2D images.

## 5.3 Internalisation of live *S. aureus* into NHEK via α5β1-integrin

To demonstrate that internalisation of *S. aureus* is not unique to a particular strain, two clinical (Clin1-SA and Clin2-SA) and two laboratory *S. aureus* (Lab1-SA-SH1000 and Lab2-SA-GFP) strains were studied for their ability to be internalised by NHEK (Fig. 5.3 A). All *S. aureus* strains were internalised by NHEK, unlike *S. epidermidis* (SE) which was not. Internalisation of *S. aureus* is thought to be mediated by FnBP-α5β1-integrin interaction as described in (1.6.3.1). To confirm that internalisation was an active process, internalisation of Lab1-SA isogenic fibronectin binding protein mutant (FnBP A and B) and Clin2-SA in the presence of anti α5β1-integrin antibody was examined (Fig. 5.3 B). Internalisation of FnBP mutant strain was reduced by almost 50% compared to its wild type strain (Lab1-SA-SH1000). Furthermore, internalisation of Clin2-SA was reduced by 80% in the presence of an anti-α5β1-integrin antibody. These results confirmed that internalisation of *S. aureus* is mediated by FnBP-α5β1-integrin pathway but its inhibition did not abrogate internalisation suggesting other pathways involved.

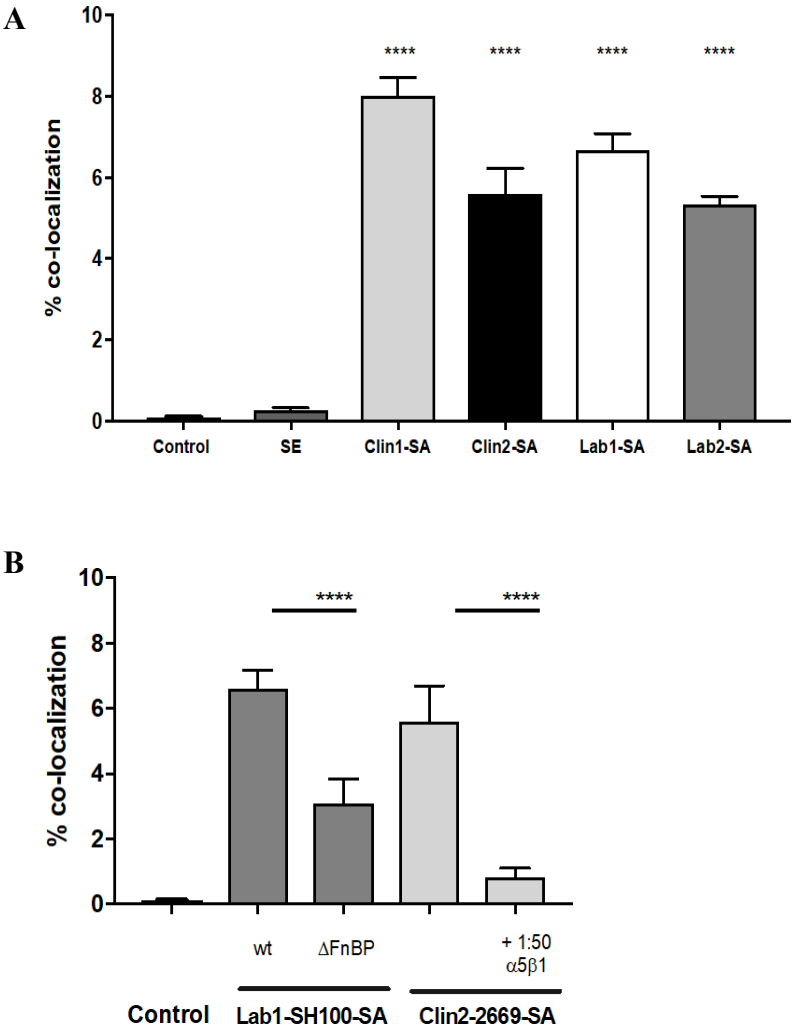


**Fig. 5.3 Clinical and laboratory strains of *S. auerus* were able to internalise into NHEK.**

Internalisation of *S. aureus* strains into NHEK was assessed by flow cytometry. FITC- *S. epidermidis* (SE) was used as negative control. (A) FITC-labeled clinical (Clin1-SA and Clin2- NCTC2669-SA) and laboratory (Lab1- SH1000- SA and Lab2-SA-GFP) isolates of *S. aureus* were internalized to a similar extent by NHEK. B. Fibronectin binding protein *S. aureus* mutant strain (Lab1- SH1000-SA;ΔFnBP) was less effectively internalised than the wild-type. Internalisation of FITC-labeled Clin2 -NCTC2669-SA was inhibited by anti-α5β1-integrin antibody (diluted to1:50). All experiments were performed in triplicate. P-values were determined by (A)one-way ANOVA with Dunnett's post hoc test. (B)Statistical comparison performed in comparison to WT using unpaired t-test. Mean ± standard error of the mean. **P =0.002, ****P<0.0001

## 5.4 Internalisation of *S. aureus* by NHEK does not induce cytotoxicity or release of the IL-33 danger signal

To assess cytotoxicity of NHEK after internalisation of *S. aureus,* cells were stained with Annexin V and DAPI as described in methods (2.17.2) after 1 h or 24 h co-culture. There was no evidence of increased cytotoxicity in the NHEK population that co-localised with

*S. aureus* compared with the total cell population in the control, which had not been co-cultured with *S. aureus*, even after 24 h (Fig. 5.4).

IL-33 release from NHEK harboring *S. aureus* was measured and compared with constant 6 h live *S. aureus* stimulation, known from experiments shown in Chapter 3 to induce high levels of IL-33 release. No significant release of IL-33 from NHEK harboring internalised *S. aureus* was seen (Fig. 5.5).

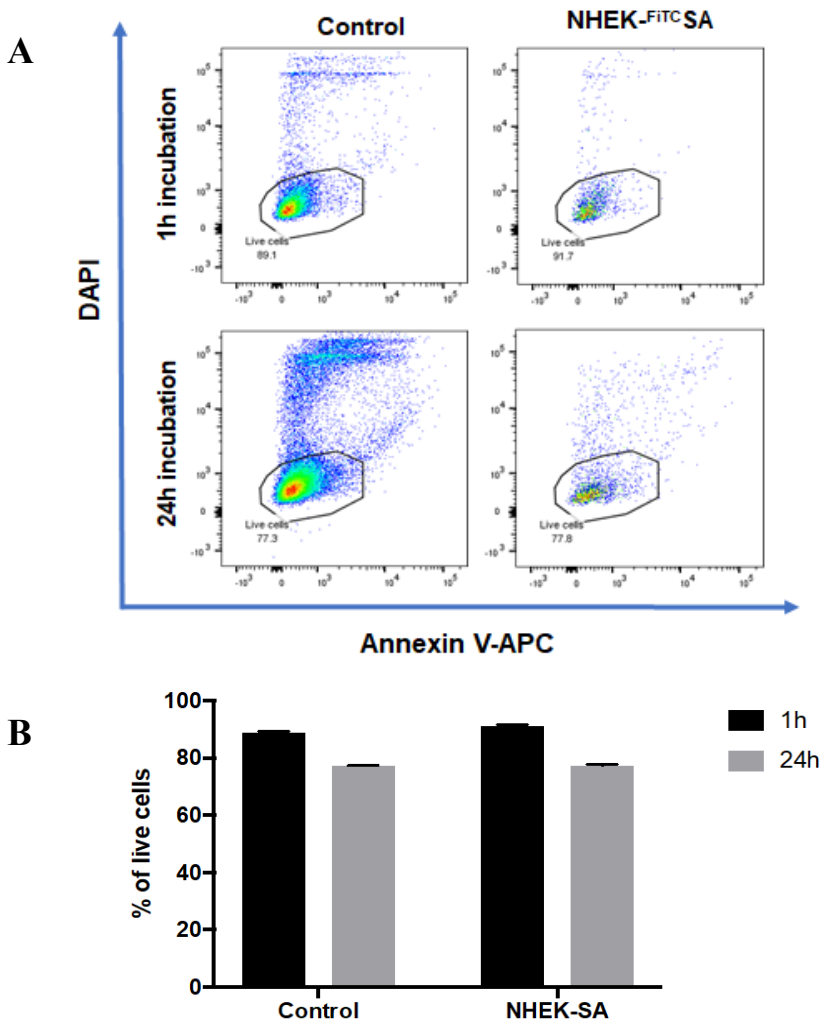


**Fig. 5.4 Internalisation of *S. aureus* into NHEK does not induce cytotoxicity.** A. NHEK co-cultured with *S. aureus* for 1 h before removing extra-cellular bacteria did not lead to increased apoptosis (Annexin V) or necrosis (DAPI) staining. Representative flow cytometry plots showing Control: non infected NHEK, and keratinocytes incubated with *S. aureus* for 1 h, treated with penicillin/streptomycin and then either analysed directly (1 h) or incubated in media alone for a further 24 h. Gate shows DAPI−/Annexin V− cells. B. Bar graph collating data from three independent experiments each done in triplicate. Black bars: 1 h, gray bars: 24 h incubation of internalised *S. aureus* and NHEK. There was no significant difference between control (non infected NHEK) and NHEK-*S. aureus* (SA+) groups.

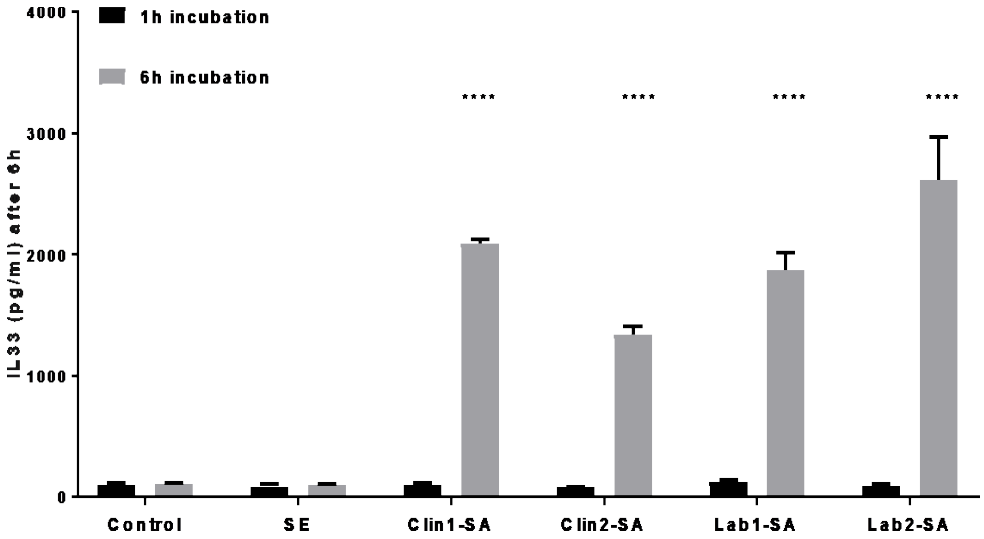


**Fig. 5.5 Internalisation of *S. aureus* does not induce IL-33 release by NHEK.**
IL-33 release by NHEK was induced by extracellular, but not intracellular clinical and laboratory *S. aureus*. FITC-labeled clinical (Clin1-SA and Clin2- NCTC2669-SA) and laboratory (Lab1- SH1000-SA and Lab2-SA-GFP) isolates of *S. aureus* Gray bars: 6 h co-culture of *S. aureus* and NHEK. Black bars: 1 h co-culture followed by penicillin/streptomycin treatment. Six-hour supernatants were collected and analysed by ELISA. Data are representative of three independent experiments each performed in triplicate. Mean ± standard error of the mean. *P*-values were determined by two-way ANOVA. **** $P < 0.0001$.

## 5.5 Ability of common anti-staphylococcal antibiotics to eradicate *S. aureus* internalised into NHEK

As the internalisation of *S. aureus* into NHEK was not associated with keratinocyte cytotoxicity, the ability of five anti-staphylococcal antibiotics; flucoxacillin, clindamycin, teicoplanin, linezolid and rifampicin, that are routinely used clinically to treat *S. aureus* infection, were assessed for their ability to eliminate intracellular methicillin-sensitive *S. aureus*. Firstly, the minimum inhibitory concentration (MIC) of each antibiotic on medium cultured *S. aureus* was measured by Etest and Microtitre Broth Dilution (Table 5.1). Then the viability of NHEK in the presence of antibiotics were assessed by trypan blue after 24 h treatment with 10X or 20X MIC of each antibiotic used in the assay (Fig. 5.6). No significant difference in trypan blue negative cells (% live cell) percentages was seen between control (incubated in growth media) and cells incubated with antibiotics. After that, the ability of these antibiotics to kill NHEK-internalised *S. aureus* (Clin1-SA) was studied.

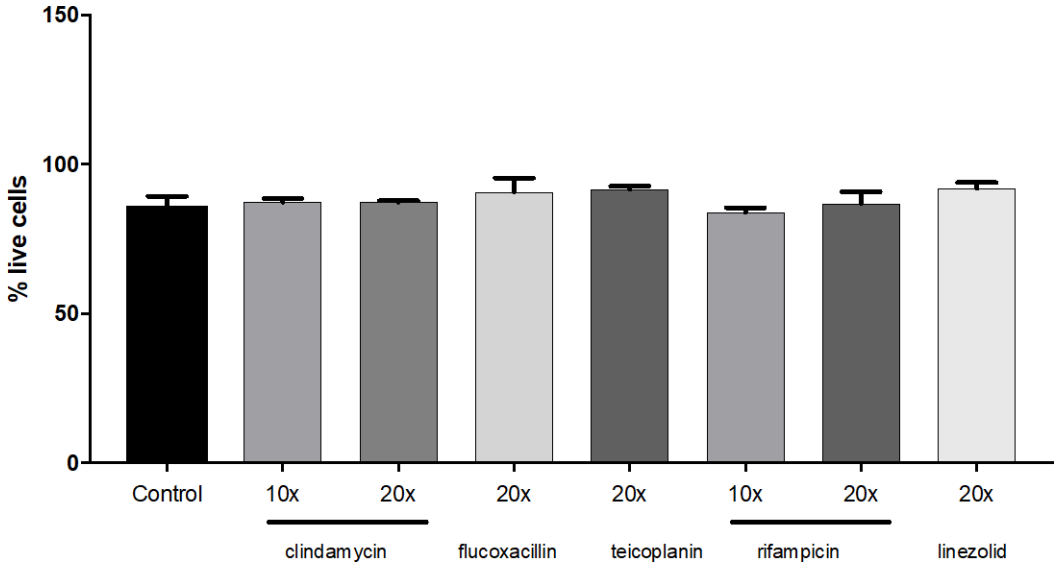


**Fig. 5.6 Anti-staphylococcal antibiotics are not cytotoxic to NHEK even when used at concentrations a log fold higher than the MIC.**
Trypan blue assay was used to calculate the percentage of live NHEK cells incubated in growth media (control) or 10X, 20X of anti-staphylococcal antibiotics for 24 h.

To perform the assay, NHEK was infected with *S. aureus* for 1 h to allow internalisation, then extracellular *S. aureus* eliminated using 2% penicillin/streptomycin treatment for 1h followed by 24 h incubation in either growth media (GM) or 2% penicillin/streptomycin (Fig. 5.7 A). Lysis of cells after 24 h released live *S. aureus* that were able to grow on nutrient agar plates. Their morphology was no different to extracellular *S. aureus* (Fig. 5.7 B).

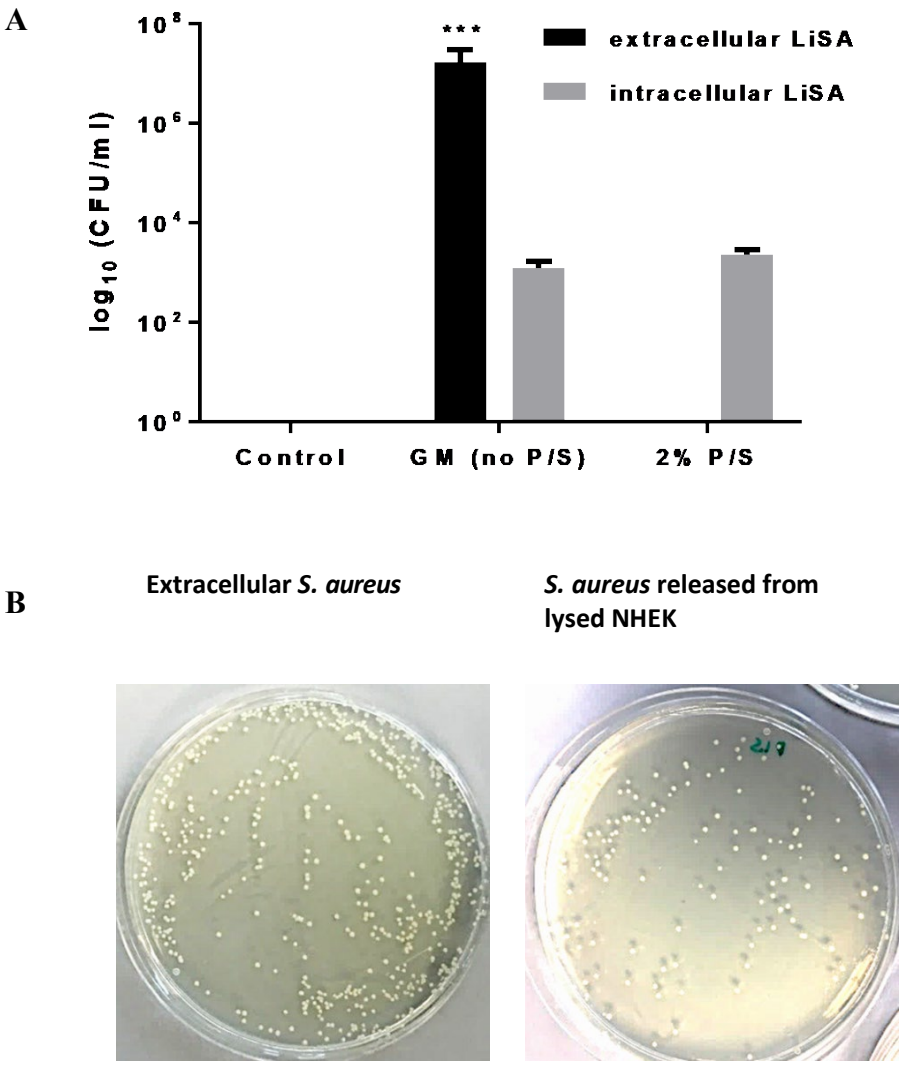


**Fig. 5.7 Intracellular *S. aureus* released from NHEK after 24 h are viable.**

A. NHEK were co-cultured with $10^7$ CFU/ml Clin1-SA for 1h at 37 °C. Cells were then washed and treated with 2% penicillin/streptomycin for 1 h to eliminate extracellular bacteria, before further culture for 24 h. The number of CFU of bacteria from supernatant (black bars) or lysed NHEK (gray bars) was quantified on nutrient agar. B. Representative *S. aureus* growth on nutrient agar plate from supernatant (left panel) and lysed NHEK (right panel).

After optimising the experiment, the antibiotics were evaluated for their effectiveness in eliminating intracellular *S. aureus* using three concentrations of each (MIC, 10X MIC and 20X MIC) (Fig. 5.8) after 24 h incubation. For each antibiotic three technical repeat per concentration and at least three biological repeats were performed. Although all antibiotics were bactericidal for extracellular methicillin-sensitive *S. aureus* in concentration ranging from 0.1 to 4 µg/ml (table 5.1), only rifampicin was effective in eliminating intracellular *S. aureus*. Flucloxacillin, teicoplanin, clindamycin, and linezolid had little effect on the intracellular *S. aureus* even at 20X the MIC.

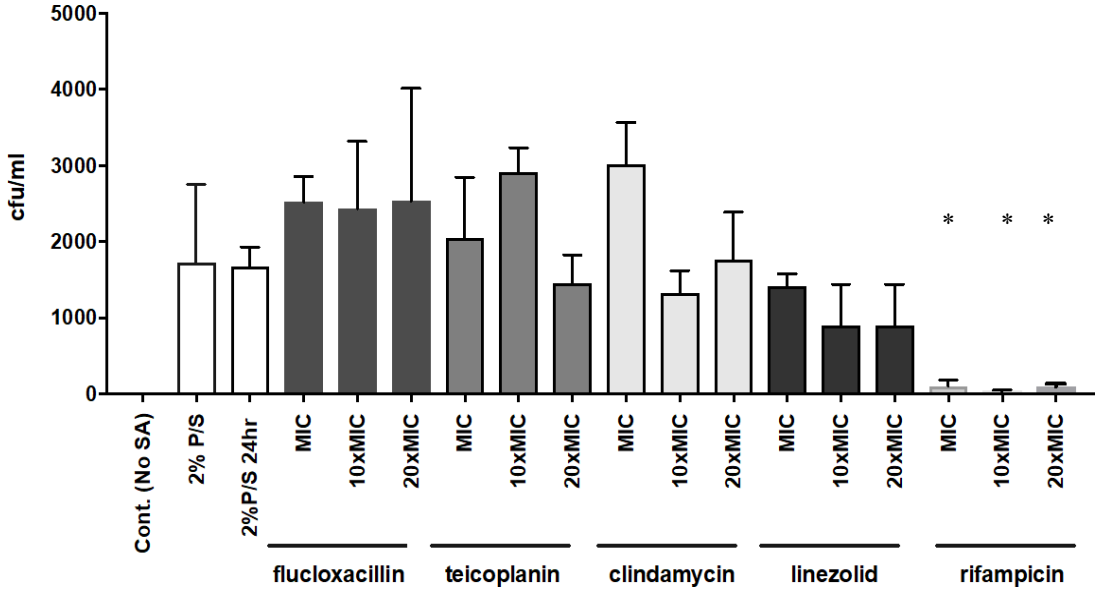


**Fig. 5.8 Antibiotic sensitivity of *S. aureus* internalised by NHEK.**
Quantitative analysis of bactericidal effects of anti-staphylococcal antibiotics (flucloxacillin, teicoplanin, clindamycin, linezolid, and rifampicin) on internalised *S. aureus* after 24 h of antibiotic treatment. Data are representative of at least three independent experiments performed in triplicate for each concentration. Mean ± standard error of the mean. P-values were determined by one-way ANOVA with Dunnett's post hoc test. $^{**}P < 0.001$ compared with 2% penicillin/streptomycin at 24 h.

**Table 5.1 Comparative killing of extracellular and intracellular *S. aureus* by anti-staphylococcal antibiotics**

| Antibiotic | Bacterial killing | |
|---|---|---|
| | MIC (μg/ml) [a] | MIC (μg/ml) for intracellular *S. aureus* [b] |
| flucloxacillin | 0.12 | >20 fold higher |
| clindamycin | 0.25 | >20 fold higher |
| linezolid | 4.00 | >20 fold higher |
| teicoplanin | 4.00 | >20 fold higher |
| rifampicin | 0.5 | 5 |

Minimum Inhibitory Concentration (MIC) of antibiotics that prevented visible bacterial growth. [a]Microtitre broth dilution method, [b]Miles & Misra method for intracellular *S. aureus.* The outcome of treatment will depend on maintaining effective antibiotic concentrations at the site of infection.

## 5.6 Summary

Results presented in this chapter demonstrate that *S. aureus* are internalised by primary human keratinocytes, confirming the finding in previously published studies that *S. aureus* can be internalised into non phagocytic cells (Mempel *et al.*, 2002; Kintarak *et al.*, 2004; Bur *et al.*, 2013). Nevertheless, this study provide visual evidence of internalisation from flow cytometry, Amnis® and confocal microscopy. Additionally, in this chapter it is shown that *S. aureus* internalisation is not strain dependent. Internalisation involves the FnBP-α1β5-integrin pathway and does not induce cytotoxicity or IL-33 release even after 24 h. Moreover, assessment of five anti-staphylococcal antibiotics has showen that only rifampicin effectively inhibited the growth of *S. aureus* internalised by NHEK. Therefore implementation of rifampicin in combination with other antibiotics in the treatment of patients with recurrent infection may improve their recovery.

# Chapter 6 : Discussion

*S. aureus* is a major cause of infection in AD and is readily isolated from skin. Acute AD pathogenesis is related to Th2 immune responses (Peng & Novak, 2015b). AD skin has higher IL-33 and TSLP expression levels (Brandt & Sivaprasad, 2011). Both IL-33 and TSLP can be sensors of protease activity (Cayrol *et al.*, 2018; Frateschi *et al.*, 2011) and inducers of Th2 immune response that are released form non hematopoietic cells such as keratinocytes (Li *et al.*, 2008; Brandt & Sivaprasad, 2011; Meephansan *et al.*, 2013; Ryu *et al.*, 2015). The role of keratinocyte in mediating Th2 immune responses in the presence of *S. aureus* is not fully understood. One aim of this study was to purify and identify the *S. aureus* factors responsible for causing the initiation of Th2 mediated inflammation in human keratinocytes. The second was to understand why *S. aureus* often persists on the skin of patients despite seemingly adequate courses of antibiotics. In this regard, the ability of keratinocytes to internalise *S. aureus* and protect the bacteria from antimicrobial action was also explored.

As demonstrated in chapter 3, this study showed that *S. aureus* and its sterile filtered supernatant (FSA) induced the release of IL-33 and TSLP from human primary keratinocytes (NHEK). Cell wall proteins are not required for this effect as HKSA did not induce release of IL-33 or TSLP from NHEK. Fractionation of FSA by size exclusion centrifuge column indicated that the bioactive factor/s ≥ 50 kDa. Further fractionation of FSA by FPLC and analysis of bioactive fractions by mass spectrometry was done to purify the bioactive *S. aureus* factor/s.

Based on results from our lab, the release of IL-33 and TSLP from NHEK in response to *S. aureus* is reduced by protease inhibitors. Therefore, identified proteins from bioactive fraction with protease activity were investigated for their effect on NHEK as shown in chapter 4. Three proteases were studied:

- Leucine aminopeptidase (LAP) 54 kDa a metallopeptidases;
- DihydroLipoyl Dehydrogenase (DLD) 54 kDa, a moonlight protein that can act as serine protease (Huberts & van der Klei, 2010); and
- Serine-like protease D (SplD) 25 kDa, as it had previously been shown to induce IL-33 dependent type 2 inflammation in mouse lung (Teufelberger, et al 2018).

Conversely, none of these proteases induced release of IL-33 or TSLP from NHEK either alone or in combination with FSA.

Interestingly, the secreted *S. aureus* Second IgG-Binding Protein (Sbi) was identified as the unique type 2 promoting factor in NHEK. Sbi consists of 436 amino acids and was first discovered in 1998 (Zhang *et al.*, 1998). Unlike the cell wall-anchored IgG-Binding Protein A (SpA), Sbi lacks the cell wall-binding LPXTG motif and is therefore found in the

secretome, rather than anchored to the cell wall (Burman *et al.*, 2008). Sbi does however have a proline-rich domain, which allows it to bind to the cell wall via electrostatic interaction (Smith *et al.*, 2011). Sbi has four domains, two IgG binding domains (Sbi- I, II) that has sequence similarity to protein A (SpA) domains E, D, A, B, C (Fig. 6.1). Sbi-IV can bind to plasma protein and a coagulation factor β2-glycoprotein I (β2-GPI), while Sbi- III-IV binds to complement component C3 (Zhang *et al.*, 1999; Smith *et al.*, 2011).

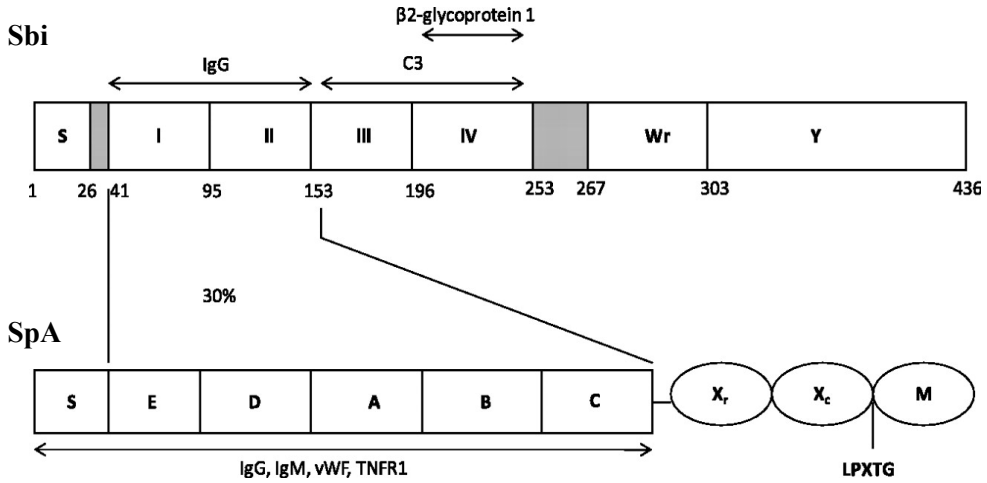


**Fig. 6.1 Schematic diagram of Sbi domain structure compared to SpA (Adapted from Smith *et al*, 2011).**
The upper panel represents Sbi and the lower SpA. The S domain in both proteins represent the signal peptide sequence, followed by the binding domains (Sbi: I and II, III and VI; SpA: E, D, A, B, and C) with their binding partners shown. Sbi I, II share similarity with SpA binding domains and binding to IgG. Sbi III-VI bind to complement component C3. Sbi VI bind to β2-glycoprotein I. Wr and Xr are proline-rich C-terminal domains of Sbi and Protein A respectively. The Y tyrosine-rich domain of Sbi is involved in cell wall interaction via electrostatic forces. In contrast, it is the C-terminal domain; LPXTG; M, transmembrane domain of Protein A which allows anchoring of this protein into the cell wall.

Sbi was been thought to be an immune evasion factor that *S. aureus* secreted to allow its survival in the host (Burman *et al.*, 2008; Haupt *et al.*, 2008; Smith *et al.*, 2011). Like SpA, Sbi binding to the Fc fragment on IgG can inhibit the proper binding of IgG to phagocytes and therefore inhibit bacterial clearance (Atkins *et al.*, 2008). Both secreted and cell wall associated Sbi can interact with IgG but only the secreted Sbi (Sbi-E) can interfere with the complement system by binding to C3 (Burman *et al.*, 2008). The structure of Sbi-VI domain was found to be similar to the C-terminus of the extracellular fibrinogen binding protein (Efb) suggesting a similar mechanism of action to inhibit the alternative complement pathway. Sbi forms a tripartite complex with iC3b and factor H which recruit plasminogen that is degraded by staphylokinase to plasmin which degrade

iC3b and therefore inhibit the alternative complement pathway activation against *S. aureus* (Haupt *et al.,* 2008*;* Burman *et al.*, 2008; Merle *et al.*, 2015). It is also thought that binding of Sbi to iC3b on the opsonised bacteria will inhibit its interaction with complement receptors 3 and 4 (CR3, CR4) on neutrophils and macrophages and therefore inhibit phagocytosis and bacterial clearance (Burman *et al.*, 2008). Sbi-E activates complement consumption of C3, which reduces complement activity (Burman *et al.*, 2008; Upadhyay *et al.*, 2008). Moreover Sbi binding to other C3 cleavage products such as C3a and C3dg will inhibit their interaction with B and T cells and therefore inhibit adaptive response to invading *S. aureus* (Burman *et al.*, 2008). However, in this study, NHEK were cultured in a serum free media suggesting that Sbi anti-inflammatory mechanisms by interference with complement system is not relevant. Recently Sbi has been associated with the induction of proinflammatory responses in macrophage *in vitro* culture and in a *in vivo* mouse model (Gonzalez *et al.*, 2015). In this study, Sbi induced epidermal growth factor receptor (EGFR) (Gonzalez *et al.*, 2015). As activation of EGFR is known to be involved in the induction of IL-33 and TSLP in keratinocytes (Meephansan *et al.*, 2013; Segawa *et al.*, 2018) and intestinal epithelial cells (Islam *et al.*, 2016), it is possible that Sbi induction of EGFR is the key step in inducing the release of IL-33 and TSLP from NHEK. However, there is no conclusive evidence that Sbi interacts directly with EGFR, but it was suggested by Gonzalez *et al* that Sbi interacts with EGFR in a similar pattern to SpA through a conserved region in the IgG binding domain which was shown to activate tumor necrosis factor- α (TNF α)- converting enzyme (TACE) (Gómez *et al.*, 2007). Therefore, further studies should be done to investigate the involvement of EGFR in mediating Sbi activity which may help in the development of new therapies targeting Sbi to suppress atopic march and improve the treatment of atopic dermatitis.

The other main finding of this thesis was that *S. aureus* is uniquely internalised into human keratinocytes, other staphylococcal species such as *S. epidermidis* are not. The concept of *S. aureus* internalisation into keratinocytes and other non- professional phagocytes had been previously studied and this could form a nidus for recurrent infections (Mempel *et al.*, 2002b; Kubica *et al.*, 2008; Sayedyahossein *et al.*, 2015; Nakatsuji *et al.*, 2017; Marbach *et al.*, 2019). Most importantly, the novel finding of this thesis is that most anti-staphylococcal antibiotics were not effective in eliminating intracellular *S. aureus* except rifampicin. These findings have recently been published in the journal *Frontiers of Microbiology* (Al Kindi *et al.*, 2019). Internalisation into human primary keratinocytes was unique to *S. aureus,* when compared to other staphylococcal species. Importantly, *S. epidermidis* the common commensal bacteria on the skin fails to be internalised by

keratinocyte.

This is contradictory to previous studies that showed that *S. epidermidis* can be internalised into HaCaT, immortalised keratinocytes, and endothelial cells (Hirschhausen et al., 2010; N'Diaye et al., 2016). Internalisation of *S. aureus* into NHEK was not associated with the induction of significant release of IL-33 or cell death even after 24 h post-internalisation. Again, this is contrary to what was previously shown when *S. epidermidis* was internalised by HaCaT keratinocytes (Strobel et al., 2016). This suggests that immortalised keratinocytes are not a suitable model to represent anti-pathogen responses by keratinocytes. In support of this conclusion, it was also shown separately that HaCaT are not a good model to study innate immune responses of keratinocytes and that NHEK is more reliable model as their response to *Propionibacterium acnes* are different in terms of cytokines release (Akaza *et al.*, 2011).

Other pathogens such as *Mycobacteria tuberculosis* have also been also shown to persist and grow in macrophages, which protects the pathogen from being eradicated by antibiotics (Jindani et al., 2003). This and our study clearly show that determination of MIC based on eliminating extracellular bacteria is not enough to eradicate intracellular bacteria. A major factor to consider here, to explain why even 20 times MIC of most antibiotics included in this study fail to eliminate intracellular bacteria, is the variation in the ability of antibiotics to penetrate the cell membrane. Development of antimicrobial nano-emulsions might be promising in eradication of intracellular bacteria and treatment of skin infections because of its relatively high kinetic stability and increased solubility and delivery of poorly soluble drugs (Yang et al., 2018).

Rifampicin is a powerful antibiotic that has been used for treatment of meningococcal carriage because of its high efficacy against intracellular mycobacteria (Deal and Sanders, 1969). However, rifampicin is known to cause rapid antibiotic resistance (Riedel et al., 2008; Thwaites et al., 2018) and therefore always used in combination with other antibiotics as is done in the treatment of tuberculosis. From the data of this study here, rifampicin had high efficiency in targeting intracellular *S. aureus* and maybe can be a good choice to use in combination with other antibiotics in treating recurrent skin infection.

## Limitation of this study and future work

The experiments presented in this thesis were mainly conducted *in vitro* using a monolayer of normal human keratinocytes which lacks the complexity of interactions between keratinocytes layers in their different differentiation stage and resident immune cells. This might not provide a complete picture of immune responses against the bacteria or their filtered supernatant as would be seen in an *in vivo* model. Parallel experiments have been conducted by colleagues in the laboratory using FSA and human skin explants. Alongside, collaborators in Japan have used the AD-like NC/Tnd mouse model and both models reassuringly show similar results to *in vitro* data in this thesis. The effects of Sbi on these two models has not yet been investigated. It will be a priority to investigate the effect of purified Sbi as well as a *S. aureus* mutant strain deficient in Sbi on the induction of Th2 promoting cytokines in human explants and *in vivo*.

IL-33 and TSLP were the main readouts of the induction of type 2 proinflammatory response, as these two cytokines are considered to be biomarkers of AD and are both secreted by keratinocytes. Other cytokines such as IL-6, IL-5 and IL-13, and chemokines such as CXCL9 and CXCL10 might also be worth investigating in the future as this might help in better understanding the mechanism of inflammation, especially after purifying Sbi as a secreted bioactive factor released by *S. aureus*.

In the *S. aureus* internalisation experiments, intracellular bacteria were visualised by confocal microscopy and percentage of internalisation was calculated by flow cytometry. However, the antibiotic effectiveness assay was done manually, counting the number of colonies on agar plates. Although this was essential to confirm the viability of intracellular bacteria, it was time consuming and lots of optimisation procedures were done to minimise variation between replicates. Using flow cytometry or Amnis® might work but viability markers for the bacterial as well as cell viability markers are required.

Skin explants used in this study to investigate internalisation of *S. aureus* showed that the bacteria is present deep in the epidermis but the technique could not identify bacterial internalisation into keratinocytes, probably because of the fact that multi-layering of this tissue system made visualisation of bacteria within single cells difficult, and the images are only 2D. Several attempts were made to visualise 5-30 μm sections of the explant by confocal microscopy, but these failed. More work on this approach would clarify these observations.

## Conclusions

This study, for the first time, shows that Sbi secreted by *S. aureus* is a key inducer of type 2 proinflammatory cytokines IL-33 and TSLP release by primary human keratinocytes. It is not yet clear if this is a direct effect or if secreted Sbi interacts with other factors, possibly on the skin, to induce the release of these two cytokines. Although most published studies have discussed Sbi as an anti-inflammatory factor that *S. aureus* uses to mask its presence and evade the host immune system, little is known about Sbi as an inducer of inflammation. Further studies are required to investigate the pathway through which secreted Sbi mediates inflammation in staphylococcal skin infections.

The second key finding is that *S. aureus* has mastered an important immune evasion strategy by internalisation into human keratinocytes without inducing danger signals, allowing a hideout from antibiotic treatment. The antibiotic assay performed here using five staphylococcal antibiotics used clinically to treat *S. aureus* infection, showed that all except rifampicin, had poor bactericidal efficacy on intracellular *S. aureus* even at concentrations 20X MIC. This suggests that MIC determination to eradicate extracellular bacteria is not accurate indicative of efficacy against intracellular bacteria. The ability of antibiotics to penetrate through the cell membrane should also be studied. Treatment of skin infection with rifampicin in combination with other antibiotics might be beneficial to minimise intracellular *S. aureus* persistence and avoid recurrent infections.

# References


Abel, J., Goldmann, O., Ziegler, C., Höltje, C., et al. (2011) *Staphylococcus aureus* evades the extracellular antimicrobial activity of mast cells by promoting its own uptake. *J Innate Immunity*. 3 (5), 495–507.

Adams, M.N., Ramachandran, R., Yau, M.K., Suen, J.Y., et al. (2011) Structure, function and pathophysiology of protease activated receptors. *Pharmacol Therap*. 130 (3), 248–282.

Akaza, N., Akamatsu, H., Kishi, M., Mizutani, H., et al. (2011) Normal human epidermal keratinocytes react differently than HaCaT keratinocyte cell line on exposure to Propionibacterium acnes. *J Dermatology*. 38 (5), 499–502.

Alkahtani, A.M. (2016) Mechanisms by which *Staphylococcus aureus* induces cytokines and cell death in human keratinocytes and mouse fibroblasts.PhD thesis, University of Manchester.

Allakhverdi, Z., Comeau, M.R., Jessup, H.K., Yoon, B.R.P., et al. (2007) Thymic stromal lymphopoietin is released by human epithelial cells in response to microbes, trauma, or inflammation and potently activates mast cells. *J Exp Med*. 204 (2), 253–258.

Atkins, K.L., Burman, J.D., Chamberlain, E.S., Cooper, J.E., et al. (2008) S. aureus IgG-binding proteins SpA and Sbi: Host specificity and mechanisms of immune complex formation. *Mol Immunol*. 45 (6), 1600–1611.

Babady, N.E., Pang, Y.P., Elpeleg, O. & Isaya, G. (2007) Cryptic proteolytic activity of dihydrolipoamide dehydrogenase. *PNAS*. 104 (15), 6158–6163.

Baird-Parker, A.C. (1990) The staphylococci: an introduction. *J Appl Microbiol.* 191-8.

Behne, M.J., Meyer, J.W., Hanson, K.M., Barry, N.P., et al. (2002) NHE1 regulates the stratum corneum permeability barrier homeostasis. Microenvironment acidification assessed with fluorescence lifetime imaging. *Journal Biol Chem*. 277 (49), 47399–47406.

Benenson, S., Zimhony, O., Dahan, D., Solomon, M., et al. (2005) Atopic dermatitis; a risk factor for invasive *Staphylococcus aureus* infections: two cases and review. *Am.J.Med.* 118 (9), 1048–1051.

Bjerketorp, J., Jacobsson, K. & Frykberg, L. (2004) The von Willebrand factor-binding protein (vWbp) of *Staphylococcus aureus* is a coagulase. *FEMS Lett*. 234 (2), 309–314.

Bjerketorp, J., Nilsson, M., Ljungh, A., Flock, J.-I., et al. (2002) A novel von Willebrand

factor binding protein expressed by *Staphylococcus aureus*. *Microbiology*. 148, 2037–2044.

Blake, K.J., Baral, P., Voisin, T., Lubkin, A., et al. (2018) *Staphylococcus aureus* produces pain through pore-forming toxins and neuronal TRPV1 that is silenced by QX-314. *Nature Commun*. 9 (1), 37.

Bleem, A., Francisco, R., Bryers, J.D. & Daggett, V. (2017) Designed α-sheet peptides suppress amyloid formation in *Staphylococcus aureus* biofilms. *NPJ Biofilms Microbiomes*. 3 (1), 16.

Borisova, M., Shi, Y., Buntru, A., Worner, S., et al. (2013) Integrin-mediated internalization of *Staphylococcus aureus* does not require vinculin. *BMC Cell Biol*. 14 (2), 1471–2121.

Brandt, E.B. & Sivaprasad, U. (2011) Th2 Cytokines and Atopic Dermatitis. *J Clin Cell Immunol*. 2 (3).

Brown, L., Wolf, J.M., Prados-Rosales, R. & Casadevall, A. (2015) Through the wall: extracellular vesicles in Gram-positive bacteria, mycobacteria and fungi. *Nature*. 13.

Brüggemann, H., Henne, A., Hoster, F., Liesegang, H., et al. (2004) The complete genome sequence of Propionibacterium acnes, a commensal of human skin. *Science*. 305 (5684), 671–673.

Bur, S., Preissner, K.T., Herrmann, M. & Bischoff, M. (2013) The *Staphylococcus aureus* Extracellular Adherence Protein Promotes Bacterial Internalization by Keratinocytes Independent of Fibronectin-Binding Proteins. *J Invest Dermatol*. 133 (8), 2004–2012.

Burman, J.D., Leung, E., Atkins, K.L., O'Seaghdha, M.N., et al. (2008) Interaction of human complement with Sbi, a staphylococcal immunoglobulin-binding protein: Indications of a novel mechanism of complement evasion by *Staphylococcus aureus*. *J Biol Chem*. 283 (25), 17579–17593.

Byrd, A.L., Deming, C., Cassidy, S.K.B., Harrison, O.J., et al. (2017) *Staphylococcus aureus* and Staphylococcus epidermidis strain diversity underlying pediatric atopic dermatitis. *Sci Transl Med*. 9 (397).

Carroll, R.K., Robison, T.M., Rivera, F.E., Davenport, J.E., et al. (2012) Identification of an intracellular M17 family leucine aminopeptidase that is required for virulence in Staphylococcus aureus. *Microb Infect*. 14 (11), 989–999.

Carroll, R.K., Veillard, F., Gagne, D.T., Lindenmuth, J.M., et al. (2013) The *Staphylococcus aureus* leucine aminopeptidase is localized to the bacterial cytosol and demonstrates a broad substrate range that extends beyond leucine. *Biol Chem*. 394 (6), 791–803.

Cayrol, C., Duval, A., Schmitt, P., Roga, S., et al. (2018) Environmental allergens induce allergic inflammation through proteolytic maturation of IL-33. *Nature Immunol* 19 (4), 375–385.

Cevikbas, F. & Steinhoff, M. (2012) IL-33: a novel danger signal system in atopic dermatitis. *J Invest Dermatol*. 132 (5), 1326–1329.

Chua, K.Y.L., Stinear, T.P. & Howden, B.P. (2013) Functional genomics of staphylococcus aureus. *Brief Funct Genom*. 12 (4), 305–315.

Classen, A., Kalali, B.N., Schnopp, C., Andres, C., et al. (2011) TNF receptor I on human keratinocytes is a binding partner for staphylococcal protein A resulting in the activation of NF kappa B, AP-1, and downstream gene transcription. *Exp Dermatol*. 20 (1), 48–52.

Cogen, A.L., Yamasaki, K., Sanchez, K.M., Dorschner, R.A., et al. (2010) Selective antimicrobial action is provided by phenol-soluble modulins derived from Staphylococcus epidermidis, a normal resident of the skin. *J Invest Dermatol*. 130 (1), 192–200.

Dominguez-Bello, M.G., Costello, E.K., Contreras, M., Magris, M., et al. (2010) Delivery mode shapes the acquisition and structure of the initial microbiota across multiple body habitats in newborns. *PNAS*. 107 (26), 11971–11975.

Dunkelberger, J.R. & Song, W.C. (2010) Complement and its role in innate and adaptive immune responses. *Cell Research*. 20 (1), 34–50.

von Eiff, C., Becker, K., Machka, K., Stammer, H., et al. (2001) Nasal Carriage As a Sourc E of *Staphylococcus aureus* Bacteremia Nasal Carriage As a Source of *Staphylococcus aureus* Bacteremia. *NEJM*. 344 (1), 11–16.

Flick, M.J., Du, X., Prasad, J.M., Raghu, H., et al. (2013) Genetic elimination of the binding motif on fibrinogen for the S. aureus virulence factor ClfA improves host survival in septicemia. *Blood*. 121 (10), 1783–1794.

Foster, T.J., Geoghegan, J.A., Ganesh, V.K. & Höök, M. (2014) Adhesion, invasion and evasion: the many functions of the surface proteins of Staphylococcus aureus. *Nat Rev Microbiol.* 12 (1), 49–62.

Frateschi, S., Camerer, E., Crisante, G., Rieser, S., et al. (2011) PAR2 absence completely rescues inflammation and ichthyosis caused by altered CAP1/Prss8 expression in mouse skin. *Nat Commun*. 2 (1), 161.

Gao, H., Jiang, X., Pogliano, K. & Aronson, A.I. (2002) The E1β and E2 subunits of the Bacillus subtilis pyruvate dehydrogenase complex are involved in regulation of sporulation. *J Bacteriol*. 184 (10), 2780–2788.

Garzoni, C., Francois, P., Huyghe, A., Couzinet, S., et al. (2007) A global view of *Staphylococcus aureus* whole genome expression upon internalization in human epithelial cells. *BMC Genomics*. 8 (171) 1471-2164.

Geoghegan, J.A., Irvine, A.D. & Foster, T.J. (2018) *Staphylococcus aureus* and Atopic Dermatitis: A Complex and Evolving Relationship. *Trends Microbiol*. 26 (6) 484–497.

Giese, B., Glowinski, F., Paprotka, K., Dittmann, S., et al. (2011) Expression of δ-toxin by *Staphylococcus aureus* mediates escape from phago-endosomes of human epithelial and endothelial cells in the presence of β-toxin. *Cell Microbiol*. 13 (2), 316–329.

Gómez, M.I., Seaghdha, M.O. & Prince, A.S. (2007) *Staphylococcus aureus* protein a activates TACE through EGFR-dependent signaling. *EMBO*. 26 (3), 701–709.

Gonzalez, C.D., Ledo, C., Giai, C., Garófalo, A., et al. (2015) The Sbi protein contributes to *Staphylococcus aureus* inflammatory response during systemic infection Bernhard Ryffel. *PLoS ONE*. 10 (6), e0131879.

Goodyear, C.S. & Silverman, G.J. (2003) Death by a B cell superantigen: In vivo VH-targeted apoptotic supraclonal B cell deletion by a Staphylococcal Toxin. *J Exp Med*. 197 (9), 1125–1139.

Götz, F., Bannerman, T. & Schleifer, K. (2006) *The Genera Staphylococcus and Macrococcus*.*Prokaryotes*.(4), 5-75.

Grice, E.A. & Segre, J.A. (2011) The skin microbiome. *Nat Rev Microbiol*. 9 (4), 244–253.

Haupt, K., Reuter, M., Van Den Elsen, J., Burman, J., et al. (2008) The *Staphylococcus aureus* protein Sbi acts as a complement inhibitor and forms a tripartite complex with host complement factor H and C3b Ambrose Cheung. *PLoS Pathogens*. 4 (12), e1000250.

Hersh, A.L., Chambers, H.F., Maselli, J.H. & Gonzales, R. (2008) National trends in ambulatory visits and antibiotic prescribing for skin and soft-tissue infections. *Arch Intern Med*. 168 (14), 1585–1591.

Herz, U., Schnoy, N., Borelli, S., Weigl, L., et al. (1998) A human-SCID mouse model for allergic immune responses: Bacterial superantigen enhances skin inflammation and suppresses IgE production. *J Invest Dermatol*. 110 (3), 224–231.

Higgins, J., Loughman, A., van Kessel, K.P.M., van Strijp, J.A.G., et al. (2006) Clumping factor A of *Staphylococcus aureu*s inhibits phagocytosis by human polymorphonuclear leucocytes. *FEMS Microbiol lett*. 258 (2), 290–296.

Hirasawa, Y., Takai, T., Nakamura, T., Mitsuishi, K., et al. (2010) *Staphylococcus aureus* extracellular protease causes epidermal barrier dysfunction. *J Invest Dermatol.* 130

(2), 614–617.

Hirschhausen, N., Schlesier, T., Schmidt, M.A., Götz, F., et al. (2010) A novel staphylococcal internalization mechanism involves the major autolysin Atl and heat shock cognate protein Hsc70 as host cell receptor. *Cell Microbiol*. 12 (12), 1746–1764.

Huberts, D.H.E.W. & van der Klei, I.J. (2010) Moonlighting proteins: An intriguing mode of multitasking. *Mol Cell Res*. 1803 (4), 520–525.

Huebner, J. & Goldmann, D.A. (1999) Coagulase-negative staphylococci: role as pathogens. *Annu Rev Med*. 50223–236.

Hvid, M., Vestergaard, C., Kemp, K., Christensen, G.B., et al. (2011) IL-25 in atopic dermatitis: A possible link between inflammation and skin barrier dysfunction. *J Invest Dermatol*. 131 (1), 150–157.

Islam, M.S., Horiguchi, K., Iino, S., Kaji, N., et al. (2016) Epidermal growth factor is a critical regulator of the cytokine IL-33 in intestinal epithelial cells. *Br J Pharmacol*. 2532–2542.

Jang, H., Matsuda, A., Jung, K., Karasawa, K., et al. (2015) Skin pH is the Master Switch of Kallikrein 5-Mediated Skin Barrier Destruction in a Murine Atopic Dermatitis Model. *J Invest Dermatol*. 136, 1–32.

Jean-Baptiste, N., Benjamin, D.K., Cohen-Wolkowiez, M., Fowler, V.G., et al. (2011) Coagulase-negative staphylococcal infections in the neonatal intensive care unit. *Infect Control Hosp Epidemiol*. 32 (7), 679–686.

Jenkins, A., An Diep, B., Mai, T.T., Vo, N.H., et al. (2015) Differential expression and roles of *Staphylococcus aureus* virulence determinants during colonization and disease. *mBio*. 6 (1), 1–10.

Kabashima, K., Honda, T., Ginhoux, F. & Egawa, G. (2019) The immunological anatomy of the skin. *Nature Reviews Immunology*.19 (1) pp.19–30.

Kim, B.S., Siracusa, M.C., Saenz, S.A., Noti, M., et al. (2013) TSLP elicits IL-33-independent innate lymphoid cell responses to promote skin inflammation. *Sci Transl Med*. 5 (170)

Al Kindi, A., Alkahtani, A.M., Nalubega, M., El-Chami, C., et al. (2019) *Staphylococcus aureus* internalized by skin keratinocytes evade antibiotic killing. *Front Microbiol*. 10, 1–10.

Kintarak, S., Whawell, S.A., Speight, P.M., Packer, S., et al. (2004a) Internalization of *Staphylococcus aureus* by human keratinocytes. *Infect Immun*. 72 (10), 5668–5675.

Kintarak, S., Whawell, S.A., Speight, P.M., Packer, S., et al. (2004b) Internalization of *Staphylococcus aureus* by Human Keratinocytes. *Infect Immun.* 72 (10), 5668–5675.

Kloos, W.E. & Schleifer, K.H. (1975) Simplified scheme for routine identification of human Staphylococcus species. *J Clin Microbiol*. 1 (1), 82–88.

Knox, K.W., Vesk, M. & Work, E. (1966) Relation between excreted lipopolysaccharide complexes and surface structures of a lysine-limited culture of *Escherichia coli*. *J Bacteriol*. 92 (4), 1206–1217.

Kobayashi, T., Glatz, M., Horiuchi, K., Kawasaki, H., et al. (2015) Dysbiosis and *Staphylococcus aureus* Colonization Drives Inflammation in Atopic Dermatitis. *Immunity*. 42 (4), 756–766.

Kong, H.H., Oh, J., Deming, C., Conlan, S., et al. (2012) Temporal shifts in the skin microbiome associated with disease flares and treatment in children with atopic dermatitis. *Genome Research*. 22 (5), 850–859.

Krishna, S. & Miller, L.S. (2012) Host-pathogen interactions between the skin and *Staphylococcus aureus*. *Curr Opin Microbiol*.15: 28–35.

Krut, O., Sommer, H. & Krönke, M. (2004) Antibiotic-induced persistence of cytotoxic *Staphylococcus aureus* in non-phagocytic cells. *J Antimicrob Chemothe*. 53 (2), 167–173.

Kubica, M., Guzik, K., Koziel, J., Zarebski, M., et al. (2008) A potential new pathway for *Staphylococcus aureus* dissemination: The silent survival of S. aureus phagocytosed by human monocyte-derived macrophages. *PLoS ONE*. 3 (1), e1409.

Kupper, T. & Fuhlbrigge, R. (2004) Immune surveillance in the skin: mechanisms and clinical consequences. *Nat Rev Immunol*. 4 (3), 211–222.

Kuroda, M., Kuroda, H., Oshima, T., Takeuchi, F., et al. (2003) Two-component system VraSR positively modulates the regulation of cell-wall biosynthesis pathway in *Staphylococcus aureus*. *Mol Microbiol*. 49 (3), 807–821.

Kusch, H. & Engelmann, S. (2014) Secrets of the secretome in *Staphylococcus aureus*. *Int J Med Microbiol*.304 (2) pp.133–141.

Kwiecinski, J., Jin, T. & Josefsson, E. (2014) Surface proteins of *Staphylococcus aureus* play an important role in experimental skin infection. *APMIS*. 122 (12), 1240–1250.

Laarman, A.J., Ruyken, M., Malone, C.L., van Strijp, J.A.G., et al. (2011) *Staphylococcus aureus* Metalloprotease Aureolysin Cleaves Complement C3 To Mediate Immune Evasion. *J Immunol*. 186 (11), 6445–6453.

Lacey, K.A., Geoghegan, J.A. & McLoughlin, R.M. (2016) The Role of *Staphylococcus aureus* Virulence Factors in Skin Infection and Their Potential as Vaccine Antigens.

*Pathogens*. 5 (1).

Lee, S.E., Jeong, S.K. & Lee, S.H. (2010) Protease and Protease-activated Receptor-2 signaling in the pathogenesis of atopic dermatitis. *Yonsei Med J*. 51 (6) 808–822.

Lehar, S.M., Pillow, T., Xu, M., Staben, L., et al. (2015) Novel antibody–antibiotic conjugate eliminates intracellular S. aureus. *Nature*. 527 (7578), 323–328.

Li, M., Hener, P., Zhang, Z., Ganti, K.P., et al. (2008) Induction of Thymic Stromal Lymphopoietin Expression in Keratinocytes Is Necessary for Generating an Atopic Dermatitis upon Application of the Active Vitamin D3 Analogue MC903 on Mouse Skin. *J Invest Dermatol.* 129 (2), 498–502.

Liew, F.Y., Pitman, N.I. & McInnes, I.B. (2010) Disease-associated functions of IL-33: The new kid in the IL-1 family. *Nat Rev Immunol*.10 (2) 103–110.

Liu, D. (2014) Enterotoxin-Producing *Staphylococcus aureus. Mol Med Microbiol.* 979–995.

Liu, F.T., Goodarzi, H. & Chen, H.Y. (2011) IgE, mast cells, and eosinophils in atopic dermatitis. *Clin Rev Allergy Immunol*. 41 (3), 298–310.

Lund, S., Walford, H.H. & Doherty, T.A. (2013) Type 2 Innate Lymphoid Cells in Allergic Disease. *Curr Immunol Rev*. 9214–221.

Malachowa, N., Kobayashi, S.D., Braughton, K.R., Whitney, A.R., et al. (2012) *Staphylococcus aureus* leukotoxin GH promotes inflammation. *J Infect Dis*. 206 (8), 1185–1193.

Marbach, H., Vizcay-Barrena, G., Memarzadeh, K., Otter, J.A., et al. (2019) Tolerance of MRSA ST239-TW to chlorhexidine-based decolonization: Evidence for keratinocyte invasion as a mechanism of biocide evasion. *J Infect*. 78 (2), 119–126.

Meephansan, J., Komine, M., Tsuda, H., Karakawa, M., et al. (2013) Expression of IL-33 in the epidermis: The mechanism of induction by IL-17. *J Dermatol Sci*. 71 (2), 107–114.

Mempel, M., Schnopp, C., Hojka, M., Fesq, H., et al. (2002a) Invasion of human keratinocytes by *Staphylococcus aureus* and intracellular bacterial persistence represent haemolysin-independent virulence mechanisms that are followed by features of necrotic and apoptotic keratinocyte cell death. *Br J Dermatol*. 146 (6), 943–951.

Mempel, M., Schnopp, C., Hojka, M., Fesq, H., et al. (2002b) Invasion of human keratinocytes by *Staphylococcus aureus* and intracellular bacterial persistence represent haemolysin-independent virulence mechanisms that are followed by features of necrotic and apoptotic keratinocyte cell death. *Br J Dermatol*. 146 (6), 943–951.

Merle, N.S., Noe, R., Halbwachs-Mecarelli, L., Fremeaux-Bacchi, V., et al. (2015) Complement system part II: Role in immunity. *Front Immunol*.(6) 257.

Miller, L.G., Eells, S.J., David, M.Z., Ortiz, N., et al. (2015) *Staphylococcus aureus* skin infection recurrences among household members: an examination of host, behavioral, and pathogen-level predictors. *Clin Infect Dis.* 60 (5), 753–763.

Montgomery, C.P., David, M.Z. & Daum, R.S. (2015) Host factors that contribute to recurrent staphylococcal skin infection. *Curr Opin Infect Dis*. 28 (3), 253–258.

Mootz, J.M., Malone, C.L., Shaw, L.N. & Horswill, A.R. (2013) Staphopains Modulate *Staphylococcus aureus* Biofilm Integrity. *Infect Immun.* (9): 3227–3238

Mulcahy, M.E. & McLoughlin, R.M. (2016) Host–Bacterial Crosstalk Determines *Staphylococcus aureus* Nasal Colonization. *Trends Microbiol* .24 (11) 872–886.

N'Diaye, A.R., Leclerc, C., Kentache, T., Hardouin, J., et al. (2016) Skin-bacteria communication: Involvement of the neurohormone Calcitonin Gene Related Peptide (CGRP) in the regulation of Staphylococcus epidermidis virulence. *Sci Rep*. 6 (1), 35379.

Nakatsuji, T., Chen, T.H., Narala, S., Chun, K.A., et al. (2017) Antimicrobials from human skin commensal bacteria protect against *Staphylococcus aureus* and are deficient in atopic dermatitis. *Sci Transl Med*. 9 (378).

Nishifuji, K., Sugai, M. & Amagai, M. (2008) Staphylococcal exfoliative toxins: 'Molecular scissors' of bacteria that attack the cutaneous defense barrier in mammals. *J Dermatol Sci.* 49 (1) 21–31.

Olaru, F. & Jensen, L.E. (2010) *Staphylococcus aureus* stimulates neutrophil targeting chemokine expression in keratinocytes through an autocrine IL-1α signaling loop. *J Invest Dermatol*. 130 (7), 1866–1876.

Olaya-Abril, A., Prados-Rosales, R., McConnell, M.J., Martín-Peña, R., et al. (2014) Characterization of protective extracellular membrane-derived vesicles produced by *Streptococcus pneumoniae*. *J Proteomics*. 10646–60.

Oliveira, D., Borges, A. & Simões, M. (2018) *Staphylococcus aureus* toxins and their molecular activity in infectious diseases. *Toxins*.10 (6).

Omori, M. & Ziegler, S. (2007) Induction of IL-4 Expression in CD4+ T Cells by Thymic Stromal Lymphopoietin. *J Immunol*. 178 (3), 1396–1404.

Peetermans, M., Vanassche, T., Liesenborghs, L., Lijnen, R.H., et al. (2015a) Bacterial pathogens activate plasminogen to breach tissue barriers and escape from innate immunity. *Crit Rev Microbiol*. 7828 , 1–17.

Peetermans, M., Verhamme, P. & Vanassche, T. (2015b) Coagulase Activity by *Staphylococcus aureus*: A Potential Target for Therapy? *Semin Thromb Hemost*. 41433–444.

Peng, W. & Novak, N. (2015a) Pathogenesis of atopic dermatitis. *Clin Exp Allergy*. 45 (3), 566–574.

Peng, W. & Novak, N. (2015b) Pathogenesis of atopic dermatitis. *Clin Exp Allergy*. 45 (3), 566–574.

Powers, C.E., Mcshane, D.B., Gilligan, P.H., Burkhart, C.N., et al. (2015) Microbiome and pediatric atopic dermatitis. *J Dermatol*. 42 (12), 1137–1142.

Proft, T. & Fraser, J.D. (2003) Bacterial superantigens. *Clin Exp Immunol*. 133 (3), 299–306.

Ramachandran, R., Noorbakhsh, F., Defea, K. & Hollenberg, M.D. (2012) Targeting proteinase-activated receptors: therapeutic potential and challenges. *Nat Rev Drug Discov*. 11 (1), 69–86.

Resch, U., Tsatsaronis, J.A., Le Rhun, A., Stübiger, G., et al. (2016) A Two-Component Regulatory System Impacts Extracellular Membrane-Derived Vesicle Production in Group A Streptococcus. *mBio*. 7(6). e00207-16

Rivera, J., Cordero, R.J.B., Nakouzi, A.S., Frases, S., et al. (2010) *Bacillus anthracis* produces membrane-derived vesicles containing biologically active toxins. *PNAS*. 107 (44), 19002–19007.

Rocha-de-Souza, C.M., Berent-Maoz, B., Mankuta, D., Moses, A.E., et al. (2008) Human mast cell activation by *Staphylococcus aureus*: Interleukin-8 and tumor necrosis factor alpha release and the role of toll-like receptor 2 and CD48 molecules. *Infect Immun*. 76 (10), 4489–4497.

Rothmeier, A.S. & Ruf, W. (2012) Protease-activated receptor 2 signaling in inflammation. *Sem Immunopath.* 34 (1), 133–149.

Ryu, S., Song, P.I., Seo, C.H., Cheong, H., et al. (2014) Colonization and infection of the skin by *S. aureus*: immune system evasion and the response to cationic antimicrobial peptides. *Int J Mol Sci*. 15 (5), 8753–8772.

Ryu, W.I., Lee, H., Kim, J.H., Bae, H.C., et al. (2015) IL-33 induces Egr-1-dependent TSLP expression via the MAPK pathways in human keratinocytes. *Exp Dermatol.* 24 (11), 857–863.

Sandberg, A., Hessler, J.H.R., Skov, R.L., Blom, J., et al. (2009) Intracellular activity of antibiotics against *Staphylococcus aureus* in a mouse peritonitis model. *Antimicrob Agents Chemother*. 53 (5), 1874–1883.

Savinko, T., Matikainen, S., Saarialho-Kere, U., Lehto, M., et al. (2012) IL-33 and ST2 in atopic dermatitis: Expression profiles and modulation by triggering factors. *J Invest Dermatol*. 132 (5), 1392–1400.

Sayedyahossein, S., Nini, L., Irvine, T.S. & Dagnino, L. (2012) Essential role of integrin-linked kinase in regulation of phagocytosis in keratinocytes. *FASEB*. 26 (10), 4218–4229.

Sayedyahossein, S., Xu, S.X., Rudkouskaya, A., McGavin, M.J., et al. (2015) *Staphylococcus aureus* keratinocyte invasion is mediated by integrin-linked kinase and Rac1. *FASEB*. 29 (2), 711–723.

Segawa, R., Shigeeda, K., Hatayama, T., Dong, J., et al. (2018) EGFR transactivation is involved in TNF-α-induced expression of thymic stromal lymphopoietin in human keratinocyte cell line. *J Dermatol Sci*. 89 (3), 290–298.

Shan, L., Redhu, N.S., Saleh, A., Halayko, A.J., et al. (2010) Thymic Stromal Lymphopoietin Receptor-Mediated IL-6 and CC/CXC Chemokines Expression in Human Airway Smooth Muscle Cells: Role of MAPKs (ERK1/2, p38, and JNK) and STAT3 Pathways. *J Immunol*. 184 (12), 7134–7143.

Sharlow, E.R., Paine, C.S., Babiarz, L., Eisinger, M., et al. (2000) The protease-activated receptor-2 upregulates keratinocyte phagocytosis. *J Cell Sci.* 113 (17), 3093–3101.

Shukla, S.K., Rose, W. & Schrodi, S.J. (2015) Complex host genetic susceptibility to *Staphylococcus aureus* infections. *Trends Microbiol*. 23 (9), 529–536.

Smagur, J., Guzik, K., Magiera, L., Bzowska, M., et al. (2009) A new pathway of staphylococcal pathogenesis: Apoptosis-like death induced by staphopain B in human neutrophils and monocytes. *J Innate Immun*. 1 (2), 98–108.

Smith, E.J., Visai, L., Kerrigan, S.W., Speziale, P., et al. (2011) The Sbi Protein Is a Multifunctional Immune Evasion Factor of *Staphylococcus aureus* A. Camilli. *Infect Immun*. 79 (9), 3801–3809.

Somerville, D.A. (1969) The Normal Flora of the Skin in Different Age Groups. *Br J Derm*. 81 (1069), 248–258.

Spaan, A.N., Henry, T., van Rooijen, W.J.M., Perret, M., et al. (2013) The staphylococcal toxin Panton-Valentine Leukocidin targets human C5a receptors. *Cell host Microbe*. 13 (5), 584–594.

Stapels, D.A.C., Ramyar, K.X., Bischoff, M., Von Köckritz-Blickwede, M., et al. (2014) *Staphylococcus aureus* secretes a unique class of neutrophil serine protease inhibitors. *PNAS*. 111 (36), 13187–13192.

Stentzel, S., Teufelberger, A., Nordengrün, M., Kolata, J., et al. (2017) Staphylococcal serine protease–like proteins are pacemakers of allergic airway reactions to Staphylococcus aureus. *J Allergy Clin Immunol*. 139 (2), 492-500.

Surewaard, B.G.J., de Haas, C.J.C., Vervoort, F., Rigby, K.M., et al. (2013) Staphylococcal alpha-phenol soluble modulins contribute to neutrophil lysis after

phagocytosis. *Cell Microbiol*. 15 (8), 1427–1437.

Takai, T., Chen, X., Xie, Y., Vu, A.T., et al. (2014) TSLP expression induced via toll-like receptor pathways in human keratinocytes. *Methods Enzymol*. Academic Press. pp. 371–387.

Tauber, M., Balica, S., Hsu, C.-Y., Jean-Decoster, C., et al. (2016) *Staphylococcus aureus* density on lesional and nonlesional skin is strongly associated with disease severity in atopic dermatitis. *J Allergy Clin Immunol*. 137 (4), 1272-1274.

Teufelberger, A.R., Nordengrün, M., Braun, H., Maes, T., et al. (2018) The IL-33/ST2 axis is crucial in type 2 airway responses induced by *Staphylococcus aureus*–derived serine protease–like protein D. *J Allergy Clin Immunol*. 141 (2), 549-559.

Thammavongsa, V., Kim, H.K., Missiakas, D. & Schneewind, O. (2015) Staphylococcal manipulation of host immune responses. *Nat Rev Microbiol*.13 (9) 529–543.

Tong, S.Y.C., Chen, L.F. & Fowler, V.G. (2012) Colonization, pathogenicity, host susceptibility, and therapeutics for *Staphylococcus aureus*: What is the clinical relevance? *Sem Immunopath*. 34 (2), 185–200.

Upadhyay, A., Burman, J.D., Clark, E.A., Leung, E., et al. (2008) Structure-function analysis of the C3 binding region of *Staphylococcus aureus* immune subversion protein Sbi. *J Biol Chem*. 283 (32), 22113–22120.

Vanassche, T., Verhaegen, J., Peetermans, W.E., VAN Ryn, J., et al. (2011) Inhibition of staphylothrombin by dabigatran reduces *Staphylococcus aureus* virulence. *J Thromb haemost* .9 (12), 2436–2446.

Vu, A.T., Baba, T., Chen, X., Le, T.A., et al. (2010) *Staphylococcus aureus* membrane and diacylated lipopeptide induce thymic stromal lymphopoietin in keratinocytes through the Toll-like receptor 2-Toll-like receptor 6 pathway. *J Allergy Clin Immunol*. 126 (5), 985-993.

Walev, I., Martin, E., Jonas, D., Mohamadzadeh, M., et al. (1993) Staphylococcal alpha-toxin kills human keratinocytes by permeabilizing the plasma membrane for monovalent ions. *Infect Immun*. 61 (12), 4972–4979.

Wang, B., Mchugh, B.J., Qureshi, A., Campopiano, D.J., et al. (2016) IL-1beta-induced protection of keratinocytes against Staphylococcus aureus-secreted proteases is mediated by human beta defensin 2. *J Invest Dermatol*. 137(1), 95–105.

Wang, R., Braughton, K.R., Kretschmer, D., Bach, T.-H.L., et al. (2007) Identification of novel cytolytic peptides as key virulence determinants for community-associated MRSA. *Nat Med*. 13 (12), 1510–1514.

Wang, X., Thompson, C.D., Weidenmaier, C. & Lee, J.C. (2018) Release of

*Staphylococcus aureus* extracellular vesicles and their application as a vaccine platform. *Nat Commun*. 9 (1), 1379.

Wei, C.-F., Chang, S.-K., Shien, J.-H., Kuo, H.-C., et al. (2016) Synergism between two amphenicol of antibiotics, florfenicol and thiamphenicol, against Staphylococcus aureus. *Veterinary Record*. 178 (13), 319–319.

Alkahtani, A.M. (2016) *Mechanisms by which Staphylococcus aureus induces cytokines and cell death in human keratinocytes and mouse fibroblasts A thesis submitted to The University of Manchester for the the degree of Doctor of Philosophy ( PhD ) in the Faculty of Biology , Medic*. 1–182.

Kabashima, K., Honda, T., Ginhoux, F. & Egawa, G. (2019) The immunological anatomy of the skin. *Nature Reviews Immunology*.19 (1) pp.19–30.

Recker, M., Laabei, M., Toleman, M.S., Reuter, S., et al. (2017) Clonal differences in *Staphylococcus aureus* bacteraemia-associated mortality. *Nature Microbiology*. 2 (10), 1381–1388.

Weidinger, S., Beck, L.A., Bieber, T., Kabashima, K., et al. (2018) Atopic dermatitis. *Nature Reviews Disease Primers*.4 (1) p.1.

Wertheim, H.F., Vos, M.C., Ott, A., van Belkum, A., et al. (2004) Risk and outcome of nosocomial *Staphylococcus aureus* bacteraemia in nasal carriers versus non-carriers. *Lancet*. 364 (9435), 703–705.

Wilke, G.A. & Bubeck Wardenburg, J. (2010) Role of a disintegrin and metalloprotease 10 in *Staphylococcus aureus* alpha-hemolysin-mediated cellular injury. *PNAS*. 107 (30), 13473–13478.

Yamaguchi, T., Nishifuji, K., Sasaki, M., Fudaba, Y., et al. (2002) Identification of the *Staphylococcus aureus* etd pathogenicity island which encodes a novel exfoliative toxin, ETD, and EDIN-B. *Infect Immun*. 70 (10), 5835–5845.

Zecconi, A. & Scali, F. (2013) *Staphylococcus aureus* virulence factors in evasion from innate immune defenses in human and animal diseases. *Immunol lett*. 150 (1–2), 12–22.

Zhang, L., Jacobsson, K., Ström, K., Lindberg, M., et al. (1999) *Staphylococcus aureus* expresses a cell surface protein that binds both IgG and β2-glycoprotein I. *Microbiology*. 145 (1), 177–183.

Zhang, L., Jacobsson, K., Vasi, J., Lindberg, M., et al. (1998) A second IgG-binding protein in Staphylococcus aureus. *Microbiology*. 144 (4), 985–991.

Zipfel, P.F., Jokiranta, T.S., Hellwage, J., Koistinen, V., et al. (1999) The factor H protein family. *Immunopharmacology*. 53–60.

Zipperer, A., Konnerth, M.C., Laux, C., Berscheid, A., et al. (2016) Human commensals

producing a novel antibiotic impair pathogen colonization. *Nature*. 535 (7613), 511–516.

# Appendix A : SplD Amino Acid Sequence Verification

SplD DNA and amino acid sequences retrieved from https://www.ncbi.nlm.nih.gov/

>NC_007795.1:c1844909-1844190 *Staphylococcus aureus* subsp. aureus NCTC 8325 chromosome, complete genome
ATGAATAAAAATATAATCATCAAAAGTATTGCGGCATTGACGATTTTAACATCAATAACT
GGTGTCGGCA
CAACAGTGGTTGATGGTATTCAACAAACAGCCAAAGCAGAAAATAGTGTGAAATTAATT
ACCAACACGAA
TGTTGCACCATACAGTGGTGTTACATGGATGGGCGCTGGAACAGGATTTGTAGTTGGGA
ATCATACAATC
ATTACCAATAAACATGTTACTTATCACATGAAAGTCGGTGATGAAATCAAAGCACATCCT
AATGGTTTTT
ATAATAACGGTGGTGGACTTTATAAAGTTACTAAGATTGTAGATTATCCTGGTAAAGAAG
ATATTGCGGT
CGTACAAGTTGAAGAAAAATCAACGCAACCAAAAGGTAGAAAATTCAAAGATTTCACTA
GCAAATTTAAT
ATAGCATCAGAAGCTAAAGAAAATGAACCTATATCAGTCATTGGTTATCCAAATCCTAAT
GGAAATAAAC
TACAAATGTATGAATCAACTGGTAAAGTACTATCAGTGAATGGAAATATAGTGACATCTG
ATGCGGTTGT
CCAACCTGGCAGCTCTGGTTCACCTATATTAAATAGTAAGCGAGAAGCAATTGGTGTTAT
GTATGCTAGT
GATAAACCAACAGGTGAAAGTACAAGGTCATTTGCTGTTTATTTCTCTCCTGAAATTAAG
AAATTTATTG
CAGATAATTTAGATAAATAA

>YP_500439.1 serine protease SplD [*Staphylococcus aureus* subsp. aureus NCTC 8325]
MNKNIIIKSIAALTILTSITGVGTTVVDGIQQTAKAENSVKLITNTNVAPYSGVTWMGAGTGF
VVGNHTIITNKHVTYHMKVGDEIKAHPNGFYNNGGGLYKVTKIVDYPGKEDIAVVQVEEKST
QPKGRKFKDFTSKFNIASEAKENEPISVIGYPNPNGNKLQMYESTGKVLSVNGNIVTSDAVVQ
PGSSGSPILNSKREAIGVMYASDKPTGESTRSFAVYFSPEIKKFIADNLDK

After successful cloning of pQE30; *SplD* as shown in chapter 4, the plasmid DNA was purified from four clones to ensure no missense mutation present before the expression. DNA sequences were retrieved and then used to predict amino acid sequences by translation tool Expasy (https://web.expasy.org/translate/). After that, for each clone the amino acid sequence was aligned against the SplD sequence from https://www.ncbi.nlm.nih.gov/ by BLAST tool (https://blast.ncbi.nlm.nih.gov/) as shown here. The sequences from both forward and reverse primers were studied.

# Clone 1

## Sequenced using M13

**Sequence ID:** Query_49127 **Length:** 239 **Number of Matches:** 1

**Range 1: 1 to 239** Graphics ▼ Next Match ▲ Previous Match

| Score | Expect | Method | Identities | Positives | Gaps |
|---|---|---|---|---|---|
| 474 bits(1219) | 3e-177 | Compositional matrix adjust. | 236/239(99%) | 236/239(98%) | 0/239(0%) |

```
Query  1    MNKNIIIKSIAALTILTSITGVGTTVVDGIQQTAKAENSVKLITNTNVAPYSGVTWMGAG  60
            MNKNIIIKSIAALTILTSITGVGTTVVDGIQQTAKAENSVKLITNTNVAPYSGVTWMGAG
Sbjct  1    MNKNIIIKSIAALTILTSITGVGTTVVDGIQQTAKAENSVKLITNTNVAPYSGVTWMGAG  60

Query  61   TGFVVGNHTIITNKHVTYHMKVGDEIKAHPNGFYNNGGGLYKVTKIVDYPGKEDIAVVQV  120
            TGFVVGNHTIITNKHVTYHMKVGDEIKAHPNGFYNNGGGLYKVTKIVDYPGKEDIAVVQV
Sbjct  61   TGFVVGNHTIITNKHVTYHMKVGDEIKAHPNGFYNNGGGLYKVTKIVDYPGKEDIAVVQV  120

Query  121  EEKSTQPKGRKFKDFTSKFNIASEAKENEPISVIGYPNPNGNKLQMYESTGKVLSVNGNI  180
            EEKSTQPKGRKFKDFTSKFNIASEAKENEPISVIGYPNPNGNKLQMYESTGKVLSVNGNI
Sbjct  121  EEKSTQPKGRKFKDFTSKFNIASEAKENEPISVIGYPNPNGNKLQMYESTGKVLSVNGNI  180

Query  181  VTSDAVVQPGSSGSPILNSKREAIGVMYASDKPTGESTRSFAVYFSPEIKKFIADNLDK  239
            VTSDAVVQPGSSGSPILNSKREAIGVMYASDKPTGEST SFAVYFSPEI KFIADNI K
Sbjct  181  VTSDAVVQPGSSGSPILNSKREAIGVMYASDKPTGESTMSFAVYFSPEIXKFIADNLXK  239
```

## Sequenced using M13 R

**Sequence ID:** Query_67763 **Length:** 241 **Number of Matches:** 1

**Range 1: 1 to 241** Graphics ▼ Next Match ▲ Previous Match

| Score | Expect | Method | Identities | Positives | Gaps |
|---|---|---|---|---|---|
| 476 bits(1226) | 3e-178 | Compositional matrix adjust. | 239/241(99%) | 239/241(99%) | 2/241(0%) |

```
Query  1    MNKNIIIKSIAALTILTSITGVGTTVVDGIQQTAKAENSVKLITNTNVAPYSGVTWM-G  58
            MNKNIIIKSIAALTILTSITGVGTTVVDGIQQTAKAENSVKLITNTNVAPYSGVTWM G
Sbjct  1    MNKNIIIKSIAALTILTSITGVGTTVVDGIQQTAKAENSVKLITNTNVAPYSGVTWMETG  60

Query  59   AGTGFVVGNHTIITNKHVTYHMKVGDEIKAHPNGFYNNGGGLYKVTKIVDYPGKEDIAVV  118
            AGTGFVVGNHTIITNKHVTYHMKVGDEIKAHPNGFYNNGGGLYKVTKIVDYPGKEDIAVV
Sbjct  61   AGTGFVVGNHTIITNKHVTYHMKVGDEIKAHPNGFYNNGGGLYKVTKIVDYPGKEDIAVV  120

Query  119  QVEEKSTQPKGRKFKDFTSKFNIASEAKENEPISVIGYPNPNGNKLQMYESTGKVLSVNG  178
            QVEEKSTQPKGRKFKDFTSKFNIASEAKENEPISVIGYPNPNGNKLQMYESTGKVLSVNG
Sbjct  121  QVEEKSTQPKGRKFKDFTSKFNIASEAKENEPISVIGYPNPNGNKLQMYESTGKVLSVNG  180

Query  179  NIVTSDAVVQPGSSGSPILNSKREAIGVMYASDKPTGESTRSFAVYFSPEIKKFIADNLD  238
            NIVTSDAVVQPGSSGSPILNSKREAIGVMYASDKPTGESTRSFAVYFSPEIKKFIADNLD
Sbjct  181  NIVTSDAVVQPGSSGSPILNSKREAIGVMYASDKPTGESTRSFAVYFSPEIKKFIADNLD  240

Query  239  K  239
            K
Sbjct  241  K  241
```

Red boxes represent mismatch with the reference sequence.

# Clone 2

## Sequenced using M13 F

Sequence ID: Query_244507 Length: 229 Number of Matches: 1

Range 1: 1 to 227 Graphics ▼ Next Match ▲ Previous Match

| Score | Expect | Method | Identities | Positives | Gaps |
|---|---|---|---|---|---|
| 436 bits(1120) | 2e-162 | Compositional matrix adjust. | 219/227(96%) | 219/227(96%) | 2/227(0%) |

```
Query  1    MNKNIIIKSIAALTILTSITGVGTTVVDGIQQTAKAENSVKLITNTNVAPYSGVTWM-G  58
            MNKNIIIKSIAALTILTSITGVGTTVVDGIQQTAKAENSVKLITNTNVAPYSGVTWM G
Sbjct  1    MNKNIIIKSIAALTILTSITGVGTTVVDGIQQTAKAENSVKLITNTNVAPYSGVTWMETG  60

Query  59   AGTGFVVGNHTIITNKHVTYHMKVGDEIKAHPNGFYNNGGGLYKVTKIVDYPGKEDIAVV  118
            AGTGFVVGNHTIITNKHVTYHMKVGDEIKAHPNGFYNNGGGLYKVTKIVDYPGKEDIAVV
Sbjct  61   AGTGFVVGNHTIITNKHVTYHMKVGDEIKAHPNGFYNNGGGLYKVTKIVDYPGKEDIAVV  120

Query  119  QVEEKSTQPKGRKFKDFTSKFNIASEAKENEPISVIGYPNPNGNKLQMYESTGKVLSVNG  178
            QVEEKSTQPKGRKFKDFTSKFNIASEAKENEPISVIGYPNPNGNKLQMYESTGKVLSVNG
Sbjct  121  QVEEKSTQPKGRKFKDFTSKFNIASEAKENEPISVIGYPNPNGNKLQMYESTGKVLSVNG  180

Query  179  NIVTSDAVVQPGSSGSPILNSKREAIGVMYASDKPTGESTRSFAVYF  225
            NIVTSDAVVQPGSSGSPILNSKREAIGVMYASDKPTGEST     F
Sbjct  181  NIVTSDAVVQPGSSGSPILNSKREAIGVMYASDKPTGESTMVICCLF  227
```

## Sequenced using M13 R

Sequence ID: Query_244055 Length: 239 Number of Matches: 1

Range 1: 1 to 239 Graphics ▼ Next Match ▲ Previous Match

| Score | Expect | Method | Identities | Positives | Gaps |
|---|---|---|---|---|---|
| 481 bits(1238) | 3e-180 | Compositional matrix adjust. | 239/239(100%) | 239/239(100%) | 0/239(0%) |

```
Query  1    MNKNIIIKSIAALTILTSITGVGTTVVDGIQQTAKAENSVKLITNTNVAPYSGVTWMGAG  60
            MNKNIIIKSIAALTILTSITGVGTTVVDGIQQTAKAENSVKLITNTNVAPYSGVTWMGAG
Sbjct  1    MNKNIIIKSIAALTILTSITGVGTTVVDGIQQTAKAENSVKLITNTNVAPYSGVTWMGAG  60

Query  61   TGFVVGNHTIITNKHVTYHMKVGDEIKAHPNGFYNNGGGLYKVTKIVDYPGKEDIAVVQV  120
            TGFVVGNHTIITNKHVTYHMKVGDEIKAHPNGFYNNGGGLYKVTKIVDYPGKEDIAVVQV
Sbjct  61   TGFVVGNHTIITNKHVTYHMKVGDEIKAHPNGFYNNGGGLYKVTKIVDYPGKEDIAVVQV  120

Query  121  EEKSTQPKGRKFKDFTSKFNIASEAKENEPISVIGYPNPNGNKLQMYESTGKVLSVNGNI  180
            EEKSTQPKGRKFKDFTSKFNIASEAKENEPISVIGYPNPNGNKLQMYESTGKVLSVNGNI
Sbjct  121  EEKSTQPKGRKFKDFTSKFNIASEAKENEPISVIGYPNPNGNKLQMYESTGKVLSVNGNI  180

Query  181  VTSDAVVQPGSSGSPILNSKREAIGVMYASDKPTGESTRSFAVYFSPEIKKFIADNLDK  239
            VTSDAVVQPGSSGSPILNSKREAIGVMYASDKPTGESTRSFAVYFSPEIKKFIADNLDK
Sbjct  181  VTSDAVVQPGSSGSPILNSKREAIGVMYASDKPTGESTRSFAVYFSPEIKKFIADNLDK  239
```

Red boxes represent mismatch with the reference sequence.

# Clone 3

## Sequenced using M13 F

Sequence ID: Query_100039 Length: 239 Number of Matches: 1

Range 1: 1 to 239 Graphics ▼ Next Match ▲ Previous Match

| Score | Expect | Method | Identities | Positives | Gaps |
|---|---|---|---|---|---|
| 474 bits(1219) | 3e-177 | Compositional matrix adjust. | 236/239(99%) | 236/239(98%) | 0/239(0%) |

```
Query  1    MNKNIIIKSIAALTILTSITGVGTTVVDGIQQTAKAENSVKLITNTNVAPYSGVTWMGAG  60
            MNKNIIIKSIAALTILTSITGVGTTVVDGIQQTAKAENSVKLITNTNVAPYSGVTWMGAG
Sbjct  1    MNKNIIIKSIAALTILTSITGVGTTVVDGIQQTAKAENSVKLITNTNVAPYSGVTWMGAG  60

Query  61   TGFVVGNHTIITNKHVTYHMKVGDEIKAHPNGFYNNGGGLYKVTKIVDYPGKEDIAVVQV  120
            TGFVVGNHTIITNKHVTYHMKVGDEIKAHPNGFYNNGGGLYKVTKIVDYPGKEDIAVVQV
Sbjct  61   TGFVVGNHTIITNKHVTYHMKVGDEIKAHPNGFYNNGGGLYKVTKIVDYPGKEDIAVVQV  120

Query  121  EEKSTQPKGRKFKDFTSKFNIASEAKENEPISVIGYPNPNGNKLQMYESTGKVLSVNGNI  180
            EEKSTQPKGRKFKDFTSKFNIASEAKENEPISVIGYPNPNGNKLQMYESTGKVLSVNGNI
Sbjct  121  EEKSTQPKGRKFKDFTSKFNIASEAKENEPISVIGYPNPNGNKLQMYESTGKVLSVNGNI  180

Query  181  VTSDAVVQPGSSGSPILNSKREAIGVMYASDKPTGESTRSFAVYFSPEIKKFIADNLDK  239
            VTSDAVVQPGSSGSPILNSKREAIGVMYASDKPTGESTRSFAVYFSPEI KFIA NL K
Sbjct  181  VTSDAVVQPGSSGSPILNSKREAIGVMYASDKPTGESTRSFAVYFSPEIXKFIAXNLXK  239
```

## Sequenced using M13 R

Sequence ID: Query_236271 Length: 239 Number of Matches: 1

Range 1: 1 to 239 Graphics ▼ Next Match ▲ Previous Match

| Score | Expect | Method | Identities | Positives | Gaps |
|---|---|---|---|---|---|
| 481 bits(1238) | 3e-180 | Compositional matrix adjust. | 239/239(100%) | 239/239(100%) | 0/239(0%) |

```
Query  1    MNKNIIIKSIAALTILTSITGVGTTVVDGIQQTAKAENSVKLITNTNVAPYSGVTWMGAG  60
            MNKNIIIKSIAALTILTSITGVGTTVVDGIQQTAKAENSVKLITNTNVAPYSGVTWMGAG
Sbjct  1    MNKNIIIKSIAALTILTSITGVGTTVVDGIQQTAKAENSVKLITNTNVAPYSGVTWMGAG  60

Query  61   TGFVVGNHTIITNKHVTYHMKVGDEIKAHPNGFYNNGGGLYKVTKIVDYPGKEDIAVVQV  120
            TGFVVGNHTIITNKHVTYHMKVGDEIKAHPNGFYNNGGGLYKVTKIVDYPGKEDIAVVQV
Sbjct  61   TGFVVGNHTIITNKHVTYHMKVGDEIKAHPNGFYNNGGGLYKVTKIVDYPGKEDIAVVQV  120

Query  121  EEKSTQPKGRKFKDFTSKFNIASEAKENEPISVIGYPNPNGNKLQMYESTGKVLSVNGNI  180
            EEKSTQPKGRKFKDFTSKFNIASEAKENEPISVIGYPNPNGNKLQMYESTGKVLSVNGNI
Sbjct  121  EEKSTQPKGRKFKDFTSKFNIASEAKENEPISVIGYPNPNGNKLQMYESTGKVLSVNGNI  180

Query  181  VTSDAVVQPGSSGSPILNSKREAIGVMYASDKPTGESTRSFAVYFSPEIKKFIADNLDK  239
            VTSDAVVQPGSSGSPILNSKREAIGVMYASDKPTGESTRSFAVYFSPEIKKFIADNLDK
Sbjct  181  VTSDAVVQPGSSGSPILNSKREAIGVMYASDKPTGESTRSFAVYFSPEIKKFIADNLDK  239
```

Red boxes represent mismatch with the reference sequence.

# Clone 4

## Sequenced using M13 F

Sequence ID: Query_223653 Length: 239 Number of Matches: 1

Range 1: 1 to 239 Graphics ▼ Next Match ▲ Previous Match

| Score | Expect | Method | Identities | Positives | Gaps |
|---|---|---|---|---|---|
| 475 bits(1223) | 6e-178 | Compositional matrix adjust. | 237/239(99%) | 237/239(99%) | 0/239(0%) |

```
Query  1    MNKNIIIKSIAALTILTSITGVGTTVVDGIQQTAKAENSVKLITNTNVAPYSGVTWMGAG  60
            MNKNIIIKSIAALTILTSITGVGTTVVDGIQQTAKAENSVKLITNTNVAPYSGVTWMGAG
Sbjct  1    MNKNIIIKSIAALTILTSITGVGTTVVDGIQQTAKAENSVKLITNTNVAPYSGVTWMGAG  60

Query  61   TGFVVGNHTIITNKHVTYHMKVGDEIKAHPNGFYNNGGGLYKVTKIVDYPGKEDIAVVQV  120
            TGFVVGNHTIITNKHVTYHMKVGDEIKAHPNGFYNNGGGLYKVTKIVDYPGKEDIAVVQV
Sbjct  61   TGFVVGNHTIITNKHVTYHMKVGDEIKAHPNGFYNNGGGLYKVTKIVDYPGKEDIAVVQV  120

Query  121  EEKSTQPKGRKFKDFTSKFNIASEAKENEPISVIGYPNPNGNKLQMYESTGKVLSVNGNI  180
            EEKSTQPKGRKFKDFTSKFNIASEAKENEPISVIGYPNPNGNKLQMYESTGKVLSVNGNI
Sbjct  121  EEKSTQPKGRKFKDFTSKFNIASEAKENEPISVIGYPNPNGNKLQMYESTGKVLSVNGNI  180

Query  181  VTSDAVVQPGSSGSPILNSKREAIGVMYASDKPTGESTRSFAVYFSPEIKKFIADNLDK  239
            VTSDAVVQPGSSGSPILNSKREAIGVMYASDKPTGEST SFAVYFSPEIKKFIADNI K
Sbjct  181  VTSDAVVQPGSSGSPILNSKREAIGVMYASDKPTGESTXSFAVYFSPEIKKFIADNLXK  239
```

## Sequenced using M13 R

Range 1: 1 to 239 Graphics ▼ Next Match ▲ Previous Match

| Score | Expect | Method | Identities | Positives | Gaps |
|---|---|---|---|---|---|
| 481 bits(1238) | 3e-180 | Compositional matrix adjust. | 239/239(100%) | 239/239(100%) | 0/239(0%) |

```
Query  1    MNKNIIIKSIAALTILTSITGVGTTVVDGIQQTAKAENSVKLITNTNVAPYSGVTWMGAG  60
            MNKNIIIKSIAALTILTSITGVGTTVVDGIQQTAKAENSVKLITNTNVAPYSGVTWMGAG
Sbjct  1    MNKNIIIKSIAALTILTSITGVGTTVVDGIQQTAKAENSVKLITNTNVAPYSGVTWMGAG  60

Query  61   TGFVVGNHTIITNKHVTYHMKVGDEIKAHPNGFYNNGGGLYKVTKIVDYPGKEDIAVVQV  120
            TGFVVGNHTIITNKHVTYHMKVGDEIKAHPNGFYNNGGGLYKVTKIVDYPGKEDIAVVQV
Sbjct  61   TGFVVGNHTIITNKHVTYHMKVGDEIKAHPNGFYNNGGGLYKVTKIVDYPGKEDIAVVQV  120

Query  121  EEKSTQPKGRKFKDFTSKFNIASEAKENEPISVIGYPNPNGNKLQMYESTGKVLSVNGNI  180
            EEKSTQPKGRKFKDFTSKFNIASEAKENEPISVIGYPNPNGNKLQMYESTGKVLSVNGNI
Sbjct  121  EEKSTQPKGRKFKDFTSKFNIASEAKENEPISVIGYPNPNGNKLQMYESTGKVLSVNGNI  180

Query  181  VTSDAVVQPGSSGSPILNSKREAIGVMYASDKPTGESTRSFAVYFSPEIKKFIADNLDK  239
            VTSDAVVQPGSSGSPILNSKREAIGVMYASDKPTGESTRSFAVYFSPEIKKFIADNLDK
Sbjct  181  VTSDAVVQPGSSGSPILNSKREAIGVMYASDKPTGESTRSFAVYFSPEIKKFIADNLDK  239
```

This clone was used for expression of *SplD*.

# Appendix B: Optimisation of expression using pHis plasmids

*S. aureus* DLD genes (*pdhD*), PDH (*pdhA*) and Sbi (*Sbi*) were cloned by GeneArt, Thermofisher, UK into the expression vector pHis (provided by Edward Mckenzie, Protein Expression Unit, Manchester Institute of Biotechnology, University of Manchester). Plasmids maps shown in **Figure 1**.

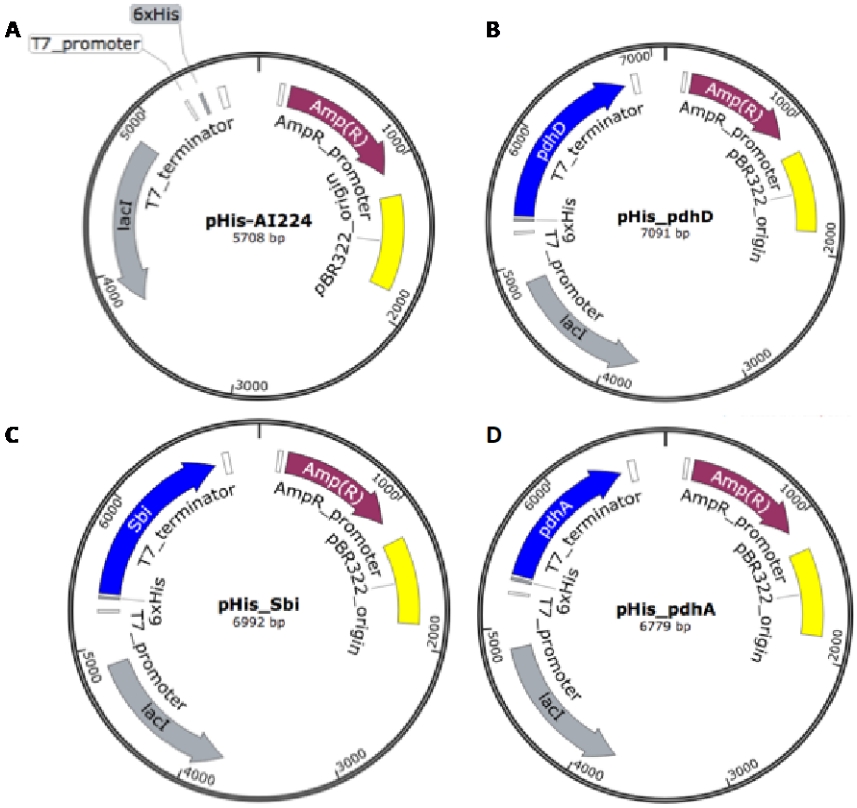


**Figure 1. pHis plasmids' maps.**

A. map of pHis-AI224 vector provided by Protein Expression unit, UoM. B. C & D maps of pHis;*pdhD* , pHis;*Sbi* and pHis;*pdhA* respectively cloned by GeneArt. All maps were created by SnapGene®

To express *pdhD* gene, pHis; *pdhD* was transformed into BL21(DE3) *E-coli* competent cells following supplier manual and cultured on LB ampicillin agar plates. One colony was used for an overnight culture preparation. Next day the overnight culture was diluted 1:100 in LB ampicillin broth and grown at 37°C until $OD_{600}$ reached 0.6. Then an overnight expression was induced by 0.5 mM IPTG at 30°C (**Figure 2**).

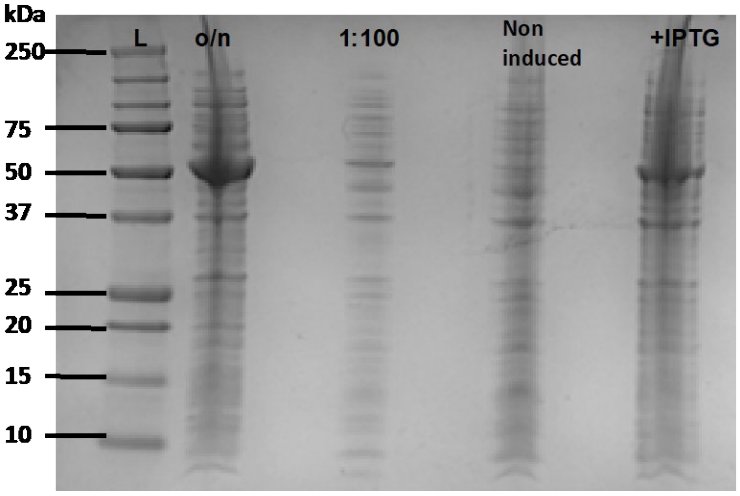


**Figure 2 *pdhD* was not expressed efficiently after induction in overnight expression at 30°C.**
SDS-PAGE stained with Instant Blue Coomassie-based stain of *pdhD* expression in BL21 (DE3). A single colony of BL21(DE3)- pHis*; pdhD* was inoculated in LB ampicillin and grown overnight at 30°C. Overnight culture (o/n) was diluted in LB ampicillin (1:100) and grown until $OD_{600}$ reached 0.6. Expression was induced by 0.5 mM IPTG and incubated overnight at 30°C. Protein band of ≈50kDa appeared in both o/n and +IPTG is consistent with the DLD protein.

The DLD protein was present in the overnight culture (≈50kDa) but no increase in the amount of protein produced after induction with IPTG was seen suggesting leaky expression of *pdhD* which means that the gene is expressed at a basal level without presence of inducer. This can affect the bacterial growth rate and therefore affect the amount protein produced. Another possible explanation is that the protein might be released under stress conditions, therefore a shorter expression period (3 h) was done at two temperatures 30°C and 37°C (**Figure 3.A**). However, no improvement in the *pdhD* expression was seen.

In order to confirm that protein bands ~50kD were the DLD protein (54kDa) and not an *E-coli* endogenous protein, western blotting using Dihydrolipoamide Dehydrogenase/DLD Antibody NBP1-31302 (NovusBiologicals, USA) was done. Western bolt confirmed the presence of DLD (**Figure 3.B**) in bacterial cultures before and after induction of expression with IPTG. Therefore, further optimisation of expression was required.

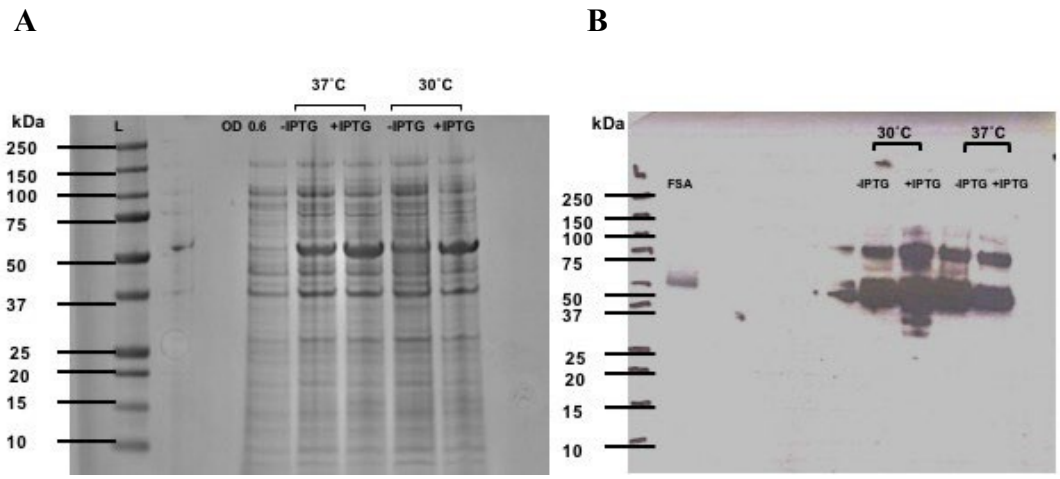


**Figure 3 *pdhD* expressed before induction and produced protein confirmed to be DLD.**

**A.** SDS-PAGE stained with Instant Blue Coomassie-based stain showing expression of *pdhD* from BL21(DE3)- pHis; *pdhD* colony. When cultures reached OD 0.6 they were incubated at 30 or 37°C, Induced (+IPTG) and non-induced (-IPTG) cultures were incubated for 3 h. **B.** Western blot of FSA, non-induced (-IPTG) and induced (+IPTG) cultures of BL21(DE3)-*pdhD*-pHis incubated for 3 h at 30°C or 37°C treated with DLD Antibody. DLD (54kDa).

An alternative broth for expression was used, Terrific broth (TB), which is known to reduce background. Also, instead of inducing the expression with IPTG, auto-induction was performed. One colony of BL21(DE3)- pHis;*pdhD*, pHis; *pdhA* and pHis;*Sbi* was inoculated in TB-ampicillin with 2% glucose and incubated overnight at 24°C or 37°C. Glucose in the broth provided a source of energy to enable bacterial growth. Once glucose was depleted, lactose used by the bacteria as source of energy which simultaneously induced the expression (**Figure 4).**

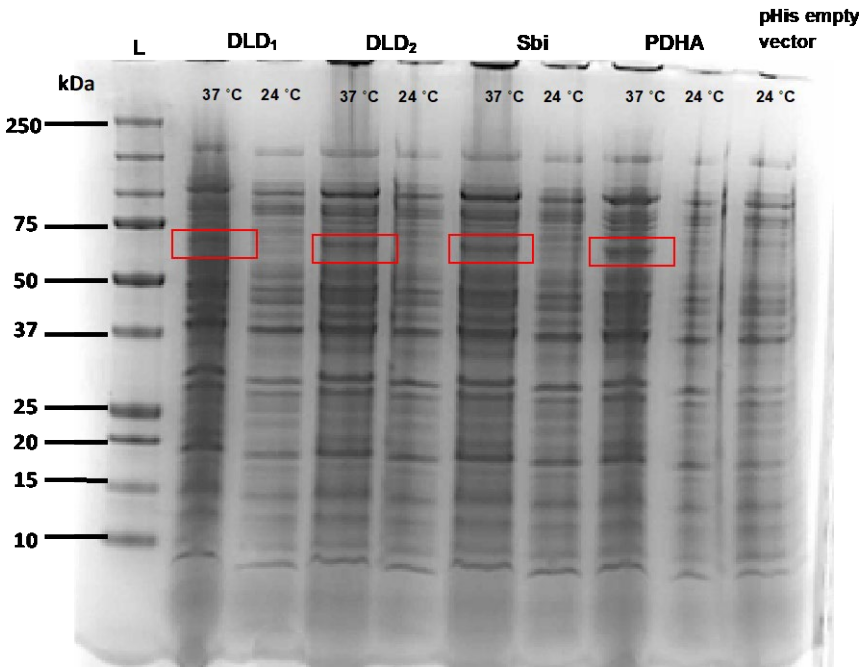


**Figure 4 Auto-induction of *pdhD, Sbi* and *pdhA* expression didn't produce efficient amounts of proteins.**

Auto-induction performed overnight in TB-ampicillin at 37°C and 24°C. A faint band~70kD (red box) present in cultures incubated at 37°C might show slight production of DLD, Sbi and PDH proteins.

Although a faint band of protein size around 70 kDa at 37 °C that was not present at 24°C or in the expression of an empty pHis vector as a control, no improvement in the expression was seen. pHis vector was therefore not deemed to be suitable for efficient expression of these proteins and therefore sub-cloning of the genes into pGEX vector was performed as discussed in chapter 4 in collaboration Dr Hayley Bennett from the Genome Editing Unit, University of Manchester. Maps of pGEX plasmid are shown in **Figure 5**.

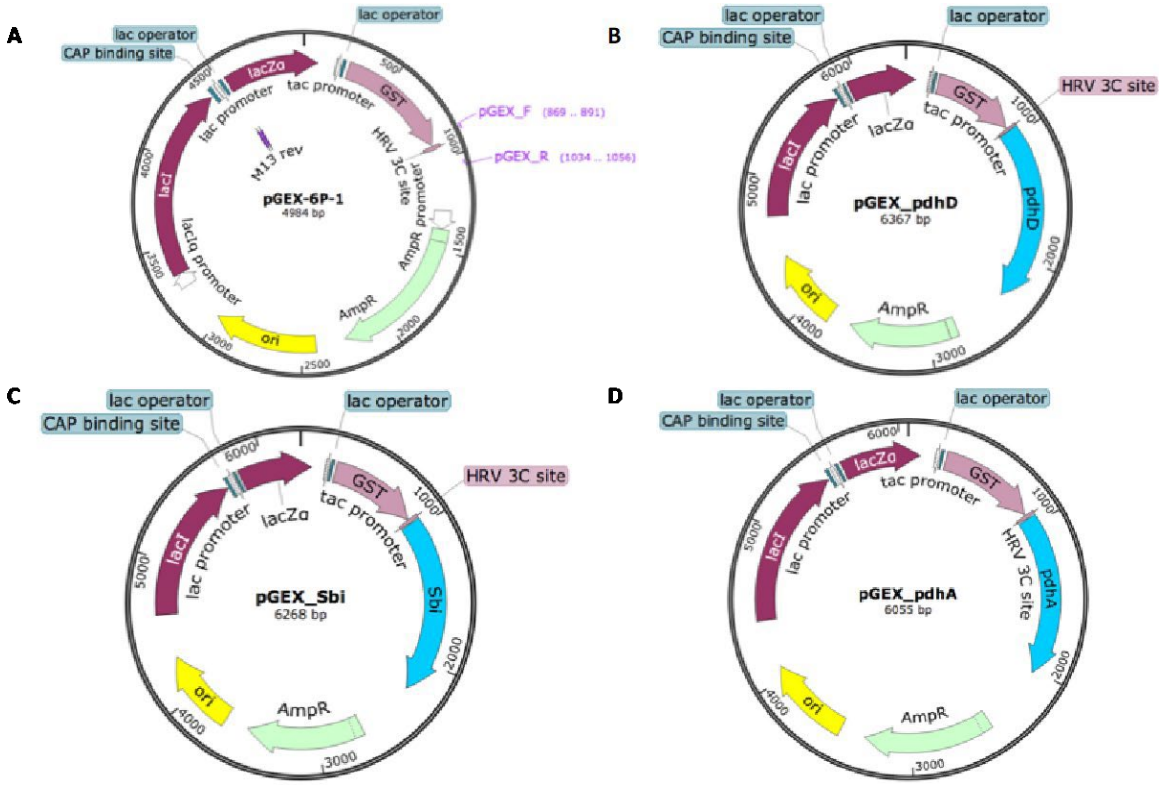


**Figure 5 pGEX plasmids' maps.**

A. map of pGEX-6P-1 vector provided by the genome Editing Unit, UoM. B. C & D maps of pGEX;*pdhD* , pGEX;*Sbi* and pGEX;*pdhA* respectively cloned by the Genome Editing unit, UoM. All maps were created by SnapGene®.

# Appendix C: Paper published in the journal

## *Frontiers of Microbiology*

Article is found online at :

https://doi.org/10.3389/fmicb.2019.02242

The Supplementary Material for this article can be found online at:

https://www.frontiersin.org/articles/10.3389/fmicb.2019.02242/full#supplementary-material